THE UNIVERSITY
of EDINBURGH

THE UNIVERSITY *of* EDINBURGH

THE UNIVERSITY *of* EDINBURGH
The Royal (Dick) School of Veterinary Studies

Design and validation of an *ex vivo*, whole organ joint model using *post mortem* specimens

Carola Riccarda Daniel

Thesis submitted for the degree of Doctor of Philosophy

Division of Clinical Veterinary Sciences

Royal (Dick) School of Veterinary Studies and The Roslin Institute
College of Medicine and Veterinary Medicine
University of Edinburgh

Table of contents

Declaration

The thesis presented is the work of the author except where stated otherwise by reference and/ or acknowledgment. Any work presented, which has been conducted by others is explicitly acknowledged at the beginning of each chapter. No part of this work has been submitted in candidature for any other degree or professional qualification.

Name:_____ Date:_____

Carola Daniel

Acknowledgements

I may not have gone where I intended to go,
but I think I have ended up where I needed to be.
-Douglas Adams-

This PhD was a truly life changing experience. It had its ups and downs, broadened my horizon, gave me new perspectives and influenced my future in so many ways. It was not always easy, but overall it was a memorable and enjoyable experience.

I would like to thank my initial supervisor Dr. Labens for having the idea for this project and his never ending stream of new thoughts. He introduced me into the world of research and was always willing to discuss my ideas. Furthermore without his hands-on support during experiments this project would not have been possible. I would also want to say a huge thank you to Raf, his family and Mel, who gave me a warm welcome when I moved to a foreign country.

My most profound thanks also go to Prof. Pirie, who took over the supervision of this project, despite the topic not necessarily being his own research interest. He provided incredible scientific support and practical guidance and gave valuable new input. He encouraged me to believe more in me and my work and always had an open door. He is also quite possibly the quickest proof-reader I have ever seen.

I would like to extend my gratitude to Prof. Argyle for his enormous support that I received throughout this PhD and his huge engagement when it comes to career development.

I am further indebted to my thesis committee, Prof. Rossi and Dr. MacRae for their guidance.

I am grateful for the mentorship of Prof. Licka, who pointed me towards this project and supported the development of the presented model with her expertise.

This thesis would not have been possible without the support of the team of the Whishaw Abattoir and the Dryden Farm team, for which I am very thankful.

Special thanks have to go to Bob Fleming, who patiently and tirelessly helped with bio imaging issues of all sorts and has an infectious passion for imaging.

Similarly I would like to thank my lab colleagues and especially Rhona for helping to transform a vet into a researcher, who does not feel too out of place in a lab anymore.

Vielen Dank an meine Mama und Oma, dafür, dass sie immer für mich da waren. Genauso wie mein Bruder Dominic, dessen wissenschaftliche Neugier für viele interessante Gespräche gesorgt hat. Außerdem danke an Dad und Conny, die mir mit dem Start und dem Leben hier in Schottland geholfen haben.

Thank you to my best friends Bine, Andrea and Tobi for being as crazy as me. Ihr seid spitze!

Also a big thank you to Kathleen (hiking, outdoor shopping, coffee breaks, Schleckeis in Roslin and a bit of science), Dewi and Bonnie (Clevaaa4life, gossip lane, Jacks, Joes and dog walks), Jule and Jari (Terrieristen and lots of banter), Zof (the pigs, honorary Collies and weird Terriers, Pentlands plods and keeping me sane towards the end), my TAM bams (runs, inappropriate conversations and cake) and last but not least Sally.

In the end I would like to thank Matt, for being the best!!!

Lay summary

Arthritis is a common disease which has a detrimental impact on the quality of life of both human and veterinary patients. Advances in the development of novel treatments can be facilitated by the use of live experimental animals, such as mice. However, the findings derived from such animals can, for various reasons, have questionable relevance for human disease. Although, the use of certain large animal models may represent an appropriate alternative translational approach, the associated loss of animal life remains a significant concern from an ethical viewpoint. Alternative approaches include the use of organ models, whereby the viability of the organ is temporarily maintained as an isolated unit following separation from the body. Such models have the potential to promote therapeutic advances without the drawbacks of cell culture and live animal models. Isolated limb perfusion (ILP) models, whereby appendices are separated from the body's blood circulation but maintained under physiologic conditions using an extracorporeal circuit, are well established in transplantation surgery and selected research applications. Extending this principle to the maintenance of joint viability through the use of pig cadaver limbs offers a significant opportunity, under almost natural conditions, to study short-term events following specific interventions relevant to arthritis. The body of work described in the thesis focuses on (a) the establishment, validation and attempted optimisation of this novel approach and (b) the potential applicability of the model to arthritis research.

Dissection of pig limbs revealed two arteries, which were suitable to link the specimen to a non-circulating ILP set-up. The model was perfused (low flow) with an oxygenated artificial solution (perfusate) warmed to body temperature. An intra-arterial pressure monitoring system allowed continuous perfusate pressure assessment. Any increase in weight of the perfused limb was measured, reflective of unwanted fluid movement out of the circulatory system (i.e. blood vessels) into surrounding tissues. Validation studies revealed good overall specimen viability over a period of six hours, as evidenced by oxygen consumption and glucose metabolism and further supported by microscopy of joint specific tissue stained for live and dead cells. Constant levels of markers for cell death within the perfusate further substantiated

functionality of the model. Specimen weight gain was in line with results reported in the scientific literature using comparable models.

Following optimisation, the model was used to investigate inflammatory cell migration to an inflammatory source within the dewclaw joint. This was assessed by microscopy of joint capsule samples following the incorporation of labelled inflammatory cells into the perfusion fluid; this revealed very limited cell migration. The presence of inflammation within the joint was confirmed by a measured trend towards an increased expression of inflammatory genes within the joint tissue. This trend was observed following the injection of inflammatory stimuli into the joint, but was not observed solely in response to perfusion of the limb.

The short term viability of the model, and the absence of any joint inflammation associated with perfusion *per se*, support the potential value of this system as an appropriate model for future arthritis research. Further refinements are required with respect to optimising the methodology used to study inflammatory cell migration into the joint tissues.

Publications

"Extracorporeal perfusion of isolated organs of large animals – review of the research method bridging the gap between in vitro and in vivo studies"

CR Daniel, R Labens, D Argyle, TF Licka; 2018; Alternatives to animal experimentation - ALTEX 35(1): 77-98

Abstract

Arthritis is a disease associated with high morbidity, affecting the quality of life of both human and veterinary patients. Therapeutic advances are aided by the use of *in vivo* rodent models however their translational value for human disease has been questioned. Therefore alternative models using large animals have come to the forefront of translational research. However despite the potentially greater applicability of experimental observations, the associated loss of animal life remains a concern. Availability of an *ex vivo* whole organ joint model has the potential to promote therapeutic advances without the drawbacks of *in vitro* and *in vivo* models. Isolated limb perfusion (ILP), a technique in which appendices are separated from the body's blood circulation but maintained under physiologic conditions using an extracorporeal circuit, is well established in transplantation surgery and selected research applications. Extending this principle to the maintenance of joint viability through the use of porcine cadaver limbs offers a significant opportunity to study post interventional short-term events relevant to arthritis in a relatively physiological environment. The body of work described in the thesis focused on (a) the establishment, validation and attempted optimisation of this novel approach and (b) the potential applicability of the model to arthritis research.

After dissection of porcine distal hind limb specimens, two arteries (*A. dorsalis pedis* and *Ramus caudalis* of the saphenous artery) were selected to link the specimen to a non-circulating ILP set-up. The model was perfused (low flow) with oxygenated adapted Tyrode solution warmed to body temperature. An intra-arterial pressure monitoring system allowed continuous perfusate pressure assessment, while scales recorded weight gain of the perfused limb. For cellular migration experiments, a second controlled fluid channel, formed by a syringe pump, was introduced into the circuit. Studies on the porcine cadaver limb model revealed good overall specimen viability over a period of six hours, as evidenced by oxygen consumption and glucose metabolism and further supported by multiphoton laser scanning microscopy (MLSM) of joint specific tissue stained for live and dead cells. Constant lactate, potassium, and LDH levels further substantiated functionality of the model. Weight gain as an indirect

measure of oedema formation was in line with results reported in the literature using comparable models. Inflammatory cell migration towards an intra-articular stimulus was assessed by MSLM of joint capsule samples following isolation and fluorescent labelling of porcine neutrophils and their incorporation into the perfusate; this revealed very limited neutrophil migration. Quantitative PCR analysis of synovium for inflammatory gene (TNF-α, IL-1β, IL-6, IFN-γ, and COX-1) expression revealed a trend towards an upregulation of some genes in response to joint injection; perfusion itself did not seem to induce inflammatory gene expression. Results of the presented work suggest that the model is applicable to arthritis research as a pharmaceutical tool for testing new drugs and delivery systems; however, further refinements are required to ensure its full potential value is achieved.

Table of figures

Table of tables

Table of abbreviations

°C	degrees celsius
µg	micrograms
2-ME	2-mercaptoethanol
A.	arteria
Aa.	arteriae
ACTB	beta actin
AR	arterial reservoir
ATP	adenosine triphosphate
aTS	adapted Tyrode solution
bp	base pairs
cDNA	complementary deoxyribonucleic acid
cm	centimetre
CMFDA	5-chloromethylfluorescein diacetate
CO_2	carbon dioxide
Con A	concanavalin A
COX-1	cyclooxygenase-1
COX-2	cyclooxygenase-2
CPB	cardiopulmonary bypass
Ct	cycle threshold
DIP	distal interphalangeal
DMEM	Dulbecco's Modified Eagle Medium
DMSO	dimethyl sulfoxide
DNA	deoxyribonucleic acid
DNase	deoxyribonuclease
e.g.	exempli gratia
et al.	et alia
GAPDH	glyceraldehyde-3-phosphate dehydrogenase
GOI	gene of interest
h	hour
HBSS	Hanks' Balanced Salt Solution

HKG	housekeeping gene
HPRT1	hypoxanthine phosphoribosyltransferase 1
IFN-γ	interferon gamma
IL-1β	interleukin 1 beta
IL-6	interleukin 6
ILP	isolated limb perfusion
K^+	potassium
LDH	lactate dehydrogenase
LPS	lipopolysaccharide
LTB4	leukotriene B four
mg	milligram
min	minute
mL	millilitre
mm	millimetre
MMP1	matrix metalloproteinase-1
MMP3	matrix metalloproteinase-3
MTP	metatarsophalangeal
Na^+	sodium
NAD	oxidized form of nicotinamide adenine dinucleotide
NADH	reduced form of nicotinamide adenine dinucleotide
ng	nanogram
O_2	oxygen
OA	osteoarthritis
PBMC	peripheral blood mononuclear cell
PBS	phosphate-buffered saline
PI	propidium iodide
qPCR	quantitative polymerase chain reaction
R.	ramus
RA	rheumatoid arthritis

rcf	relative centrifugal force
RNA	ribonucleic acid
RNase	ribonuclease
rpm	revolutions per minute
RPMI 1640	Roswell Park Memorial Institute 1640
Rr.	rami
RT	reverse transcriptase
s	second
SHG	second harmonic generation
SPIONs	superparamagnetic iron oxide nanoparticles
TNF-α	tumor necrosis factor alpha
V	volt
V.	vena
VR	venous return
Vv.	venae
λ	lambda (wavelength)

Chapter 1 Introduction

The joint (*Articulatio synovialis*) is a connection between two or more bones and permits motion of each relative to the other(s). It normally consists of the following components: cartilage (*Cartilago articularis*) covered bone ends of two or more bones, a joint cavity (*Cavum articulare*), joint ligaments (*Ligamentia articularia*), synovial fluid (*Synovia*) and the joint capsule (*Capsula articlularis*), the outer layer of which is termed the fibrous membrane (*Stratum fibrosum*) and the inner layer, the synovium (*Stratum synoviale*).

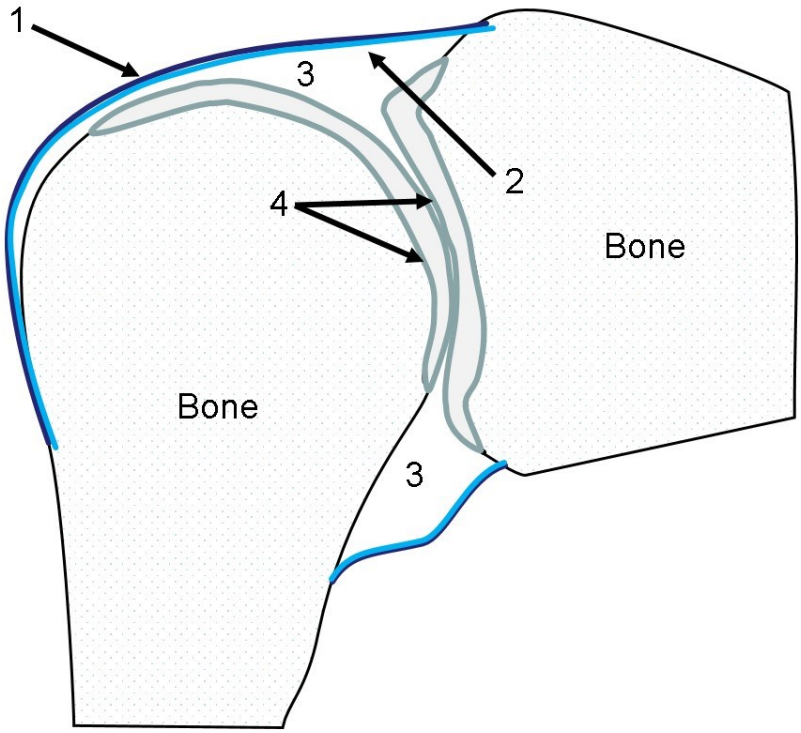

Figure 1-1: Schematic illustration of a synovial joint

Stratum fibrosum (**1**) and Stratum synovium (**2**) form the joint capsule. The joint cavity (**3**) is filled with synovial fluid to allow frictionless movement. A cartilage layer (**4**) covers the bone ends protecting against high impact stresses and likewise facilitating smooth movement.

1.1 Arthritis

Disorders affecting the joint are referred to as arthritis. They have a significant impact on the lives of both humans and animals and are generally divided into three main categories: osteoarthritis, rheumatoid arthritis and other conditions (gout, lupus, septic arthritis etc.). While often summarised under the general term "arthritis" the pathogenesis of the different disorders is very distinct and it has to be distinguished between inflammatory arthropathies, such as immune mediated (rheumatoid arthritis) or infectious (septic arthritis) conditions, and degenerative arthropathies (osteoarthritis).

Rheumatoid arthritis (RA) is a very prevalent chronic immune-mediated inflammatory joint disease which is often associated with more generalized symptoms affecting other anatomical sites/organs. The pathogenesis is still not fully understood; however, it is assumed that the disease requires both exposure to an arthritogenic antigen and genetic susceptibility of the affected individual (Kumar, Abbas et al. 2010). Currently there is no known cure with the majority of cases progressing to long-term disability (Anderson, Bradley et al. 1985, Choy and Panayi 2001).

Osteoarthritis (OA) is one of the most prevalent musculoskeletal conditions in mammals with historic evidence of its occurrence being traceable over centuries in skeletal collections (Pelletier, Martel-Pelletier et al. 2001, Weiss and Jurmain 2007). The aetiology of OA is still not fully understood; although currently, it is widely accepted that OA represents a multifactorial disease influenced by a variety of factors including age, sex, genetics, body condition, anatomical development and joint loading (Weiss and Jurmain 2007, Lotz and Loeser 2012). Despite these associated factors, inflammation plays a pivotal role in disease pathogenesis (Pelletier, Martel-Pelletier et al. 2001, Punzi, Oliviero et al. 2005).

Synovium from RA patients shows hypertrophy, hyperplasia and infiltration of the sub-lining tissue with inflammatory cells (pannus formation) (Firestein 2003). Inflammatory changes can also be found in severely affected OA joints (Pelletier,

Martel-Pelletier et al. 2001), however their nature is different from RA affected joints. Nevertheless, the main symptoms of synovial inflammation (swelling, effusion, stiffness) found in RA may also be found in clinical cases of OA (Pelletier, Martel-Pelletier et al. 2001).

1.2 Research models

With regard to arthritis research focussing on inflammation in large animal models, two broad categorical approaches might be considered; namely, *in vivo* and *in vitro* studies.

1.2.1 *In vitro* studies

In vitro models have the advantage of being convenient to handle. They allow experiments to be carried out relatively quickly (e.g. no waiting for animals to mature) and a high number of replicates is possible, without disproportional increase in costs and sacrifice of animal life. This also allows simultaneous investigation of a great number of experimental factors. Additionally only a small amount of initial tissue/ cells is required, which might be easy to source. Relatively low costs can generally be considered as an advantages of cell culture models (e.g. no costs for breeding/ housing, rarely need for specialty equipment). *In vitro* model have the potential to modify and design specific individual components and conditions. The complexity of a living organism and its potentially unknown interference with the research question being investigated can be ruled out to the highest possible degree and variability between animals and species do not have to be taken into consideration.

However there are obvious disadvantages associated with the study of cells isolated from their natural environment as cell to cell contact can have a significant influence on the behaviour and possibly the phenotype of the cell (Caron, Emans et al. 2012). Such drawbacks may be overcome by the use of tissue explants, whereby cartilage

samples can be harvested and cultured while retaining their physiological 3D structure. However, Gruber et al. (2004) did highlight the fact that explantation of porcine articular cartilage can induce inflammatory signalling pathways (Gruber, Vincent et al. 2004), thus potentially influencing the results of studies aimed at assessing the inflammatory response.

1.2.2 *In vivo* studies

Although *in vivo* models facilitate the study of organs and cells within their natural physiological environment, they are generally associated with long and costly experimental set-ups and the potential for significant loss of animal life. Live animal research on OA may involve the study of either spontaneously occurring or artificially induced disease (Bendele 2001). Clearly, study of the naturally affected joint represents the optimal investigatory environment as it most accurately reflects disease aetiology and progression; however, such studies are generally protracted, costly and often result in variability with respect to the conclusions drawn (McCoy 2015). Transgenic animals, predominantly mice, represent another extensively adopted means by which to study spontaneously developing OA. Although such models generally reflect the pathogenesis and time frame of the natural disease, the translational value of the results and the failure for such systems to recognise the polygenic nature of OA can be problematic (Helminen, Kiraly et al. 1993). Transgenic mice are also used in RA-related research, whereby genetic modifications in the inflammatory pathway can result in interesting and potentially beneficial data e.g. TNF-α expression (Keffer, Probert et al. 1991).

Yet another approach relies on the surgical or chemical induction of arthritis. Surgical techniques either aim to impair joint stability and/ or induce intra-articular lesions with the objective to change mechanical properties and induce inflammation relevant to OA (Colombo, Butler et al. 1983, Linhorst, Vail et al. 2000, Lampropoulou-Adamidou, Lelovas et al. 2014). Significant advantages of such models include the short experimental intervals and the potential they offer for greater standardization. A

significant disadvantage is the inevitable acute nature of disease induction which may not reflect the more insidious time-course typical of naturally occurring OA. The same considerations also apply to chemically induced OA (Bentley 1975, Guingamp, Gegout-Pottie et al. 1997). Collagenase induced arthritis is a frequently adopted model in RA related research, aiming to mimic similar inflammatory changes (Williams, Feldmann et al. 1992, Wooley, Dutcher et al. 1993).

Of note, approximately 77% of all *in vivo* experiments in the field of OA research involve small animal models (McCoy 2015), thus raising questions with respect to the appropriateness of the translational application of data derived from such studies to other species.

The ultimate decision of whether *in vitro* or *in vivo* techniques are applied is dependent on the research question. While the study of e.g. certain pathways can be conveniently done in cell culture models, the e.g. study of biomechanical aspects of diseases like OA requires the use of a live animal and its natural joint loading.

1.3 Methodologies used for extracorporeal perfusion of large animal organs and extremities

The following section has been published in the context of this project as part of a review article ("Extracorporeal perfusion of isolated organs of large animals – review of the research method bridging the gap between in vitro and in vivo studies"; CR Daniel, R Labens, D Argyle, TF Licka (2018); Alternatives to animal experimentation – ALTEX; **35**(1): 77-98) . The article was conceptualised and written by Carola R. Daniel. The co-authors Raphael Labens, David Argyle and Theresia F. Licka provided valuable guidance and support during this process. The article was distributed under the terms of the Creative Common Attribution 4.0 International license and the copyright is retained by the authors. For the purpose of this thesis the wording of the original article was slightly adapted where appropriate.

Begin article

In this section of the review, the following nomenclature will be used: the term "perfusion" is used for a technique in which organs are separated from the body's blood circulation but maintained under physiological conditions using an extracorporeal artificial circuit. Specimens used in these experiments are denoted as "organs" which includes internal organs as well as limbs, muscles, skin, and udder unless otherwise specified. The fluid serving as the blood equivalent in perfusions will be referred to as "perfusate" and the pressure, flow rate and temperature at which the perfusate is administered, are termed "perfusion pressure, - flow and – temperature" respectively.

In the field of organ perfusion, numerous set-ups have been designed and individually tailored to fit specific requirements. In addition to the hardware set-up, a multitude of different variables also have to be defined; these include perfusion flow and pressure, perfusate composition and oxygenation. As isolated organ perfusion represents a complex interaction between numerous different factors that cannot be fully assessed in isolation, it is difficult to compare findings derived from different species and different organs due to varying experimental techniques and differing scientific aims. However, an outline of commonly applied methods in extracorporeal perfusion of large animal organs (ECP LA) experiments may still serve to demonstrate the range of possibilities and inform decisions regarding future use of this methodology.

Within the presented project it was proposed that, as a minimum, the following information should be reported for extracorporeal perfusion experiments in order to allow other researchers to comprehend the conducted experiments and potentially replicate results: donor selection, organ collection and transport, perfusion fluid (oxygenation system, perfusion flow and pressure, temperature, type, additives) and viability measurements (e.g. oedema formation, oxygen uptake and glucose consumption). Parameters indicative of cell death, such as changes in the concentration of potassium and lactate dehydrogenase (LDH) in the perfusate, are also

recommended. Histology and organ specific parameters (e.g. milk synthesis for udders) are of additional benefit.

1.3.1 Donor selection

To date, as research has predominantly focused on physiological aspects or organ preservation techniques, specimens from healthy large animals have largely been used. Specimens of healthy individuals can be sourced from abattoirs, thus supporting the 3R principles. The collection of naturally diseased organs represents a promising future step, however it requires greater flexibility within the research team, as the availability of such organs is typically difficult to predict and diseased animals will generally not be presented to local abattoirs. Therefore, considering the uncertainty regarding the availability of samples (and potentially staff at the time of sample availability), this approach may prove challenging. Alternatively the use of organs from animals that have had disease induced in the course of (other) experiments, and have reached their study end-point may allow greater and more efficient use of available resources. In most terminal experiments, not all organs are used, and those which are not integral to the disease investigated are simply discarded, thus making these organs available for collection. This is certainly an avenue worth pursuing as such organs may allow modelling of advanced disease stages, when the original animal experiment *per se* has been concluded. However in order to effectively utilize this resource, close links between research groups are required. Finally, induction of disease in live animals for the sole purpose of using their organs post mortem could also be considered. While this would still reduce the burden on animal well-being and facilitate structured and controlled experiments it negates one of the core 3R principles; namely, replacement of animal use altogether.

The decision whether to use euthanized or slaughtered animals would depend on the perfusion set-up and the research questions being addressed. In euthanized animals, the available blood volume for perfusion is smaller, as animals are not routinely stunned and exsanguinated, thus rendering autologous blood perfusion difficult to

achieve. Moreover, potential drug interactions between the drugs used for euthanasia (typically barbiturates) and organ performance during perfusion remain a concern. To my knowledge, these questions have not, as yet, been addressed and further work would be required before the use of naturally diseased organs harvested after euthanasia could be advocated as an appropriate research tool.

1.3.2 Organ collection and transport

Organs should be harvested as soon as possible after death, to avoid excessive ischemia/ reperfusion injury (Blaisdell 2002). As tissues show variable susceptibility to ischemia, the critical time window varies depending on the organs harvested (Steinau 2013). Limbs represent a particular challenge, as due to the inclusion of skeletal muscle, specimens are particularly sensitive to ischemia with a critical time window of four hours only (Blaisdell 2002). Arteries used for perfusion have to be cannulated swiftly, and larger arteries not used for perfusion have to be occluded to reduce retrograde perfusate flow. If a closed system is intended, major veins also require cannulation with the remaining veins equally occluded. In open systems, veins remain open and the venous return can drip freely into a reservoir or sampling container. Once catheters have been placed, specimens should be either connected to the perfusion circuit or, if transportation of the specimen is required, flushed with cold preservation solution. Irrespective of which of the above scenarios apply, the first fluid used for perfusion should always contain an anticoagulant to prevent thrombus formation. If temporary storage or transport of the organ is necessary, the time of warm ischemia should be kept as short as possible. Therefore after the cold flush, specimens should also be cooled externally to further reduce cellular metabolism (Patan, Budras et al. 2009). This is best achieved either by wrapping specimens in swabs soaked in electrolyte solution or by complete immersion in electrolyte solution, with subsequent storage on ice (VanGiesen, Seaber et al. 1983). While this is suitable for many internal organs, it may not be applicable to limb preparations, particularly when bacterial skin contamination may be a concern.

The ischemic phase of the organ is a concern in perfusion experiments. The mechanism underlying anoxic cell injury of O_2-dependent cells during ischemia is a drop in adenosine triphosphate (ATP) synthesis and oxidative phosphorylation. This leads to detrimental intracellular changes (disruption of homeostasis, increased membrane permeability, activation of hydrolases) and ultimately cell death. While this process is basically the same in warm and cold ischemia, it is markedly slower if organs are maintained between four and zero degree Celsius (De Groot and Rauen 2007). Upon reperfusion of the organ, an inflammatory response is triggered by cell debris and/or altered tissue matrix as a result of anoxic cell injury; this may also be triggered by cold induced iron ion-dependent apoptosis (e.g. endothelial cells, renal tubular cells, hepatocytes). So despite showing the same ischemic injury (albeit at different rates), warm and cold ischemia are distinct with respect to the nature of the subsequent reperfusion injury and associated inflammatory response (De Groot and Rauen 2007). The use of complex preservation solutions aims to minimise the problems associated with reperfusion injury via the incorporation of protective compounds such as iron chelators (to reduce cold induced apoptosis) and/or the provision of low levels of sodium (to re-establish cell homeostasis) (De Groot and Rauen 2007). The preservation solution should also be formulated to the same specifications as the perfusate as inadequate oncotic pressure may lead to oedema formation even before ECP LA has been initiated (Drapanas, Zemel et al. 1966).

1.3.3 Initiation of perfusion following transport and data collection

The organ should be connected to the perfusion system as soon as possible following arrival in the laboratory, thus limiting the period of ischemia. An equilibration period, with a flow rate that is initially kept low and gradually increased, allows the specimen to warm up slowly; this has been shown to be advantageous as it reduces oedema formation (Wüstenberg 2006, Patan, Budras et al. 2009).

Organ viability should either be continuously or, at least, regularly monitored, to allow early detection and correction of any parameter deviations (e.g. potassium

concentration, blood pressure, and pH). Due to the nature of most experiments which adopt this approach, tissue samples are usually collected following conclusion of the perfusion period; however, careful sampling during the perfusion period may also be possible.

1.3.4 Perfusate

The choice of the most suitable perfusate is of particular importance and is largely determined by the specifics of the research study and the availability of resources. While autologous blood is obviously the most appropriate choice, availability, coagulation and the cellular damage induced by the mechanical perfusion system limit its use. Other isotonic and iso-oncotic solutions that adequately sustain physiological functions may be preferred.

1.3.4.1 Oxygenation

In order to meet the tissues' oxygen demand, most perfusion set-ups use gas enriched perfusates. A sufficient oxygen supply guarantees availability of ATP as an aerobic energy source, thereby protecting and sustaining mitochondrial function. As these cell organelles are known to be involved in signaling pathways responsible for apoptosis and necrosis, their protection leads to a reduction in cellular damage and therefore better preservation and (re)transplantation outcomes (Fuller and Lee 2007). Early experiments in isolated perfused caprine, canine and feline udders incorporated isolated perfused lungs in the circulatory system. In such a system, the trachea is connected to a gas source and the perfusate flow is directed via the lung parenchyma to the isolated organ, thereby mirroring normal physiology. The maximum perfusate flow rate achieved by this technique compared favourably with *in vivo* rates of blood flow and was superior to other perfusion experiments at the time (Hebb and Linzell 1951). However, this extensive set up has not been used since and lungs have subsequently been replaced by other means by which tissue oxygenation can be achieved (Hardwick and Linzell 1960). The simplest and most widely adopted gas

enrichment method is to channel gas directly into the perfusate reservoir prior to its circulation through the system. This approach was most likely adopted in those experiments in which the subsequent publications solely mention the use of "gassed" (Kietzmann, Löscher et al. 1993) or "oxygenated" (Bäumer and Kietzmann 1999) perfusates without further specification of the oxygenation system employed.

A suitable method to "gas" perfusate reservoirs is via the use of glassware with a sintered glass filter (Tindal 1957); however, a bubble oxygenator, which bubbles (pure) oxygen through the blood reservoir, represents an equally effective method (Smith, van Alphen et al. 1985). A slightly more sophisticated method adopts the use of a rotating disc oxygenator (Drapanas, Zemel et al. 1966, Cameron, Burger et al. 1972) whereby several parallel discs rotate within the reservoir containing unoxygenated blood and the gas exchange occurs at the disc-blood interface. More recently, the use of membrane or hollow fibre oxygenators (Butler, Rees et al. 2002, Mueller, Constantinescu et al. 2013), typically deployed during cardiopulmonary bypass (CPB) surgery or life support (extracorporeal membrane oxygenation), have been reportedly used in perfusion experiments. These systems generally follow the same concept as rotating disc oxygenators as oxygen exchange occurs at a porous membrane. A simple but effective adaptation of this principle is the use of gas permeable tubing exposed to room air in a custom made oxygenation chamber which has been shown to be effective for oxygenation of media containing erythrocytes (Hamilton, Berry et al. 1974, Patan, Budras et al. 2009).

By far, the most frequently used gas is carbogen with a composition of 95% oxygen (O_2) and 5% carbon dioxide (CO_2) as described in Kietzmann's model (Kietzmann, Löscher et al. 1993). This is due, at least in part, to the fact that the buffering capacity of commonly used cell free perfusion solutions is dependent on the presence of CO_2 (Mancina, Kalenski et al. 2015). Additionally, in solutions without oxygen carriers, an oxygen content significantly greater than room air is considered necessary to achieve the required O_2 supply to the tissues. Pure oxygen is rarely used in perfusion experiments (Drapanas, Zemel et al. 1966) and the use of carbogen of varying relative

CO_2-concentrations is commonplace (2.5% (Grosse-Siestrup, Pfeffer et al. 2002) to 7% (Hardwick and Linzell 1960)). Reasons for this include the possibility that high oxygen tensions which exceed physiological limits may lead to the production of free radicals (Fuller and Lee 2007) and the lack of any CO_2–associated buffering capacity may result in an excessive reduction in pH. Occasionally authors describe ambient air as sufficient for gassing the perfusion fluid; however, such set-ups are usually based on an erythrocyte containing perfusate, such as blood/ plasma (Patan, Budras et al. 2009) or blood/ dialysate mixtures (Wagner, Nogueira et al. 2003), to which a sub-physiological flow rate is applied (Wagner, Nogueira et al. 2003). For erythrocytes, the body's optimal oxygen carrier, room air is adequate to achieve satisfactory saturation of the perfusate while a low flow rate permits a sufficient time period for gas exchange in the oxygenation system.

Recently, specific perfusion solutions have been tested in the absence of a dedicated oxygenation system. Polyak et al. (2008) perfused an equine large colon with either an adapted cell free preservation solution or oxygenated whole blood. Organs perfused with the novel solution relied on ambient air as their sole source of oxygen. In this report, the authors concluded that the novel composition of specific (and partly well established) compounds within the perfusate prevented oedema formation (e.g. via modified hydroxyethyl starch, and mannitol) and provided a sufficient energy source (e.g. via ATP intermediates and dextrose). Furthermore, addition of prostaglandin E_1 and L-glutamine to the perfusate resulted in a reduction in inflammation and a positive effect on pathways involved in intestinal stress. L-glutamine may also be responsible for upregulation of heat shock proteins during ischemia, which in turn are associated with cell survival. Vascular (vascular resistance, pressure, flow) and biochemical (electrolytes, pO_2, pCO_2, pH, lactate, glucose) variables have also been shown to be superior when organs were perfused with the modified solution than with blood (Polyak, Morton et al. 2008). This suggests that a well-balanced artificial solution designed for a specific specimen is able to maintain the viability of a perfused organ, potentially without a dedicated oxygen source. Exclusion of an oxygenation system may lead to an easier perfusion set-up; however, developing and testing a highly

complex perfusate is both labour and cost intensive and may not be considered as a practical alternative in every instance.

1.3.4.2 Pressure and flow rate

Haemodynamic parameters, namely blood pressure (P, $\Delta P=P_{arterial}-P_{venous}$), blood flow (F), and vascular resistance (R) are interdependent as described by Ohm's Law:

$$F = \frac{\Delta P}{R}$$

While this equation applies to laminar flow conditions and thereby represents a simplified view of normal blood flow, it forms the basis for the artificial circuit set-up. Perfusion can either be controlled by flow rate or by pressure, as the flow rate is adjusted to reach a certain pressure, or *vice versa*. Flow controlled set-ups have been used most frequently (Chapman, Goldsworthy et al. 1961, Villeneuve, Dagenais et al. 1996, Grosse-Siestrup, Pfeffer et al. 2002, Zeitlin and Eshraghi 2002, Dragu, Birkholz et al. 2011); however, the latest evidence suggests that pressure controlled perfusions are preferred for organ preservation (Mancina, Kalenski et al. 2015).

In flow controlled perfusion experiments, two strategies may be applied: a low flow or a high flow approach. In low flow circuits, the average flow rate is below physiological limits, thus aiming for a perfusion pressure lower than that present in the live animal. In such a system, the flow, although low, is functional and fully reaches and supplies the capillary bed, as demonstrated by the use of dye solutions (Kietzmann, Löscher et al. 1993). Specimens seemed well preserved and remained viable for up to twelve hours (Cypel, Yeung et al. 2008, Mueller, Constantinescu et al. 2013). Low flow rate experiments compared favorably to high flow rate experiments based on histologically evident microvasculature impairment and subsequent hydrostatic oedema formation (Cypel, Yeung et al. 2008, Constantinescu, Knall et al. 2011, Mueller, Constantinescu et al. 2013). Systems which employ a high flow approach aim for physiological flow rates and perfusion pressures, thus mimicking the *in vivo*

situation more closely. As a higher flow rate leads to lower organ resistance, this also is indicative for the integrity of blood vessels (Barthel, Leonhardt et al. 1989, Bristol, Riviere et al. 1991, Wagner, Nogueira et al. 2003). Lactate levels in venous perfusate samples obtained during high flow experiments are lower than in low flow experiments and this could also imply better oxygenation of tissues (Wagner, Nogueira et al. 2003).

Although early experiments on hypothermic perfused kidneys failed to identify a difference between pulsatile versus constant flow (Pegg and Green 1976), other groups have shown pulsatile flow to be superior (Vang and Drapanas 1966, Finn, Naik et al. 1993, Sezai, Shiono et al. 1999). In cardio-pulmonary bypass experiments, pulsatile perfusion, using hydraulically driven by dual-chamber physiological pulsatile pumps, enabled better cerebral blood flow with lower resistance, compared with traditional roller pumps. This difference may be attributable to the generation of greater haemodynamic energy by the pulsatile perfusion system (Ündar, Masai et al. 2002). Overall, a true pulsatile perfusion is more reflective of the *in vivo* physiological situation, compared with non-pulsatile set-ups. Nevertheless the use of roller pumps remains a valuable option for research applications as they produce good results in ECP LA and allow more cost effective set-ups.

1.3.4.3 Temperature

Regarding temperature control, perfusates may be hypothermic or normothermic. Hypothermic perfusions are generally adopted for isolated organ and limb perfusions with the aim to promote organ preservation and facilitate replantation (Smith, van Alphen et al. 1985, Domingo-Pech, Garriga et al. 1991, Guarrera, Polyak et al. 2004, Guarrera, Polyak et al. 2004, Constantinescu, Knall et al. 2011, Mueller, Constantinescu et al. 2013). Hypothermia slows down cellular metabolism and therefore oxygen consumption, allowing metabolic demands to be met by perfusates without specific oxygen carriers delivered at low flow rates (Fuller and Lee 2007). Indeed, the use of lower flow rates may result in better preservation of the microcirculation (Cypel, Yeung et al. 2008) and might therefore be responsible for less

oedema formation reported with hypothermic perfusions (Constantinescu, Knall et al. 2011). Despite these advantages, others describe certain drawbacks of hypothermic pressure-driven flow rate perfusions, including weight gain and increased organ resistance due to the uncharacteristic sheer forces and viscosity associated with cold solutions (Fuller and Lee 2007). This weight gain may however be attributable to a variety of co-existing factors working together, rather than solely being due to the hypothermic perfusion itself. Low temperatures may also lead to reduced antioxidant defenses with the subsequent net accumulation of free radicals and toxic concentrations of superoxides within tissues (Fuller and Lee 2007). In contrast, studies of extracorporeal perfusion during cardiopulmonary bypass have demonstrated that hypothermia can reduce inflammation in the brain (Schmitt, Diestel et al. 2007). During hypothermia, neutrophil and monocyte migration is markedly reduced (Biggar, Bohn et al. 1984). Although such an effect which will undoubtedly reduce inflammatory responses, it may lead to a higher infection rate.

Reduced metabolism and altered inflammatory responses may render a hypothermic approach less suitable for most research applications. Consistent with this deduction, a normothermic approach is pursued in almost all scientific implementations of this type of methodology (Kietzmann, Löscher et al. 1993, Patan-Zugaj, Gauff et al. 2012). For studies with a physiological, pharmacokinetic or pharmacological focus (Roets, Verbeke et al. 1979, Bäumer, Mertens et al. 2002, Friebe, Schumacher et al. 2013) adoption of a hypothermic approach would appear contra-indicated.

1.3.4.4 Blood based solutions

Through its complex composition, blood provides perfectly balanced components as well as the most suitable oncotic pressure for perfusion. This is reflected in relatively low oedema-associated weight gain in experiments using whole blood as a perfusate (Patan, Budras et al. 2009, Constantinescu, Knall et al. 2011, Mancina, Kalenski et al. 2015). However one report demonstrated the opposite effect; namely, a greater weight gain in limbs perfused over five hours with diluted autologous blood (blood: Tyrode

solution 4:1) compared to limbs perfused over eight hours with adapted Tyrode solution containing sodium carboxymethyl cellulose (0.15g/L) (Friebe, Schumacher et al. 2013). Besides its ideal oncotic properties, whole blood contains erythrocytes which represent an optimal oxygen carrier and therefore enable sufficient oxygen transport to perfused tissues (Mancina, Kalenski et al. 2015).

As an alternative to autologous blood perfusions, several experiments have perfused using homologous blood or with specific blood components with no apparent negative effects (Hebb and Linzell 1951, Cameron, Burger et al. 1972, Butler, Rees et al. 2002). While this may simplify the experimental set-up and potentially reduce inter-animal variability, it is plausible that blood component incompatibility reactions could occur with a subsequent effect on the measured outcome variables. Consequently, the use of autologous blood remains the preferable option until further evidence supporting these alternative approaches can be obtained.

Besides the obvious advantages associated with autologous blood perfusions, due to inter-individual differences in the animals' blood composition, these approaches may result in slightly greater data variability, compared to perfusions with fully artificial solutions.

Unmodified blood is not suitable for perfusion purposes, as the addition of anticoagulants is a minimal necessity prior to its use. Dilution of whole blood may also be indicated to decrease viscosity and improve blood flow. This applies particularly to the capillary bed, where blood flow is comparatively slow and shear rates are low. As blood is a shear thinning non-Newtonian fluid, its viscosity is dependent on the extent of any shear rates present. Where shear rates are low (as in the capillary bed), blood viscosity is highest. Despite the reduction in the concentration of oxygen carriers which results from dilution, it does improve flow rates which lead to better tissue perfusion and oxygenation and consequently to superior organ function (Dittrich, Schuth et al. 2000). For dilution purposes, plasma (Patan, Budras et al. 2009) or artificial solutions such as Tyrode solution (Friebe, Schumacher et al. 2013), modified

Krebs Henseleit buffer (Mancina, Kalenski et al. 2015) or dialysate solution (acetate hemodialysis concentrate HD 22, Fresenius Medical Care, Bad Homburg, Germany, (Wagner, Nogueira et al. 2003)) have been used successfully.

Disadvantages associated with the use of whole blood mainly pertain to the logistical challenges associated with its harvesting and the processing required to render it a suitable perfusate. This is certainly more demanding and more time-consuming compared to the preparation of cell free solutions. Furthermore, any stresses experienced by the animals immediately prior to death may alter the composition of the blood; for example, adrenalin associated haemoconcentration in horses (Persson 1967). If autologous blood is to be used, it is typically harvested at the time of death, requiring both blood and tissue specimens to be processed at the same time. For homologous perfusions, blood and organs can be collected independently from separate donors, avoiding the potential problems associated with simultaneous collection following euthanasia or slaughter. Alternatively, in the case of autologous perfusions, blood could be collected just prior to euthanasia; although, the limited volume of blood available might necessitate the use of a recirculating system to ensure perfusion at adequate flow rates and over the desired length of time. Under such circumstances, the following considerations should be made in relation to closed or recirculating systems; they can result in damage to blood cells (Lee, Antaki et al. 2007, Watanabe, Sakota et al. 2007) and they result in the temporal accumulation of metabolic waste products such as lactate (Bristol, Riviere et al. 1991).

When using whole blood collected from animals under anaesthesia or following euthanasia, consideration should also be given to the potential for any drug residues to affect blood physiology (Barlow and Knott 1964, Gentry and Black 1976, Honkanen, McBath et al. 1995). Although collection of blood during post-slaughter exsanguination would seem the most appropriate option, this approach lacks sterility and carries the risk of bacterial contamination and subsequent bacterial growth, especially in experiments of a prolonged duration.

1.3.4.5 Cell free solutions

Cell free perfusion solutions are generally based on Ringer's isotonic solution containing sodium chloride (NaCl), potassium chloride (KCl), calcium chloride ($CaCl_2$), and sodium bicarbonate ($NaHCO_3$) as elementary ingredients. The solutions form the basis for the perfusate and are usually modified and enriched with various additives. The most commonly used variants for research purposes are Tyrode solution (Kietzmann, Löscher et al. 1993), Krebs Henseleit solution (Berhane, Elliott et al. 2006) and bicarbonated Krebs Ringer solution (Hansen, Hartmann et al. 2004). Perfusion of isolated digits with Tyrode solution was associated with good tissue viability (Friebe, Stahl et al. 2001). Tyrode solution was also used successfully in studies focusing on potential mucous membrane irritation of Lugol's iodine solution for the treatment of endometritis (Bäumer, Mertens et al. 2002) and in pharmacokinetic studies relating to joint disease (Friebe, Schumacher et al. 2013). Several specifically designed perfusion solutions have been reportedly used in relation to therapeutic organ transplantations, the most common being Eurocollins solution and the University of Wisconsin solution. The former is characterized by a relatively high glucose concentration (214mM/L) and is best suited for lung preservation (Hicks, Hing et al. 2006), while the latter is characterized by the inclusion of lactobionate, raffinose, and hydroxyethyl starch and is well-suited for kidney, liver and pancreas preservation (Hicks, Hing et al. 2006). Both of these solutions have been shown to be unsuitable for the preservation of muscle and extremities (Tsuchida, Kato et al. 2001, Tsuchida, Kato et al. 2003). As previously mentioned, Polyak et al. (2008) showed that the use of a novel unoxygenated artificial solution could maintain equine intestinal viability for twelve hours and was superior to the use of whole blood (Polyak, Morton et al. 2008).

Table 1-1: Basic compositions of commonly used solutions

Recipes vary between different research groups and suppliers. For perfusion experiments mixtures are often adapted to mimic the specie's plasma concentration of respective components.

Component in mM/L	Tyrode	Krebs Henseleit	Krebs Ringer (bicarbonated)
NaCl	137	118	115
KCl	2.7	4.7	5.9
$CaCl_2$	1.8	1.3	-
$MgCl_2$	1.05	-	1.2
$NaHCO_3$	12	25	25
$MgCl_2$	1.8	-	-
NaH_2PO_4	0.42	-	1.2
KH_2PO_4	-	1.2	-
$MgSO_4$	-	1.2	-
Na2SO4	-	-	1.2
Glucose	5.5	11	10

When compared with blood, one of the main advantages of cell free solutions is their relatively easy handling in a perfusion set-up. Such solutions are readily available, even in the large volumes that may be required when using an open system. The use of cell free solutions also permits standardization of the experimental environment, minimizes unwanted interactions and allows a refined focus on the behaviour of specific cell types. In contrast, a distinct disadvantage of their use is the associated risk of oedema formation due to inadequate oncotic pressure (Domingo-Pech, Garriga et al. 1991, Zeitlin and Eshraghi 2002). In the context of the presented work, specimen weight gain was indeed a concern but did not exceed values reported by other groups (see chapter 4.4.1). Nonetheless, weight gain of organs has also been reported in experiments using whole blood as a perfusate (dilution blood: Tyrode solution, 4:1) (Friebe, Stahl et al. 2001).

Table 1-2: Various applications for blood based and artificial perfusion fluids

The choice of a specific perfusion fluid depends on the perfused organ and the research question investigated. Care must be taken to select the perfusion fluid that best serves the intended use. This table gives a short overview of select applications of either blood based or artificial perfusion solutions. Specific recipes, compounds and additives to optimise the fluid's performance are subject to respective publications.

Perfusion fluid	Organ	Species	Research Area	Research Group/ Select Publications
Blood based	Heart	Porcine	Pathophysiology	Janse et al., 1980
	Kidney	Porcine	Organ preservation	Grosse-Siestrup et al., 2002a
	Limb	Equine	Pathophysiology	Patan-Zugaj et al., 2014; Patan-Zugaj et al., 2012; Patan et al., 2009; Gauff et al., 2014; Gauff et al., 2013
		Porcine	Pharmacology	Wagner et al., 2003
	Liver	Bovine	Organ preservation	Chapman et al., 1961
		Porcine	Perfusion	Adham et al., 1997
				Butler et al., 2002
				Grosse-Siestrup et al., 2002a; Grosse-Siestrup et al., 2002b
			Physiology	Cameron et al., 1972
				Drapanas et al., 1966
	Lung	Porcine	Organ preservation	Erasmus et al., 2006
	Udder	Bovine	Physiology	Cowie et al., 1951; Verbeke et al., 1959; Lauryssens et al., 1959; Lauryssens et al., 1960; Lauryssens et al., 1961; Wood et al., 1965
		Caprine	Physiology	Hebb and Linzell, 1951; Verbeke et al., 1957; Hardwick and Linzell, 1960; Hardwick et al., 1961; Hardwick et al., 1963; Hardwick, 1965, 1966; Linzell et al., 1967; Verbeke et al., 1968; Verbeke et al., 1972; Roets et al., 1974; Roets et al., 1979a; Roets et al., 1979b

Artificial	Heart	Porcine	Perfusion	Chinchoy et al., 2000
			Physiology	Araki et al., 2005
				Coronel et al., 1988
	Intestine	Equine	Organ preservation	Polyak et al., 2008
		Porcine	Physiology	Hansen et al., 2000; Hansen et al., 2004
				Rehfeld et al., 1982
	Kidney	Porcine	Pathophysiology	Köhrmann et al., 1994
			Organ Preservation	Mancina et al., 2015
	Limb	Equine	Pharmacology	Friebe et al., 2001; Friebe et al., 2013
		Porcine	Organ preservation	Constantinescu et al., 2011; Mueller et al., 2013
			Pharmacology	Wagner et al., 2003
	Lung	Porcine	Organ preservation	Cypel et al., 2008
			Physiology	Hellewell and Pearson, 1983
	Udder	Bovine	Pharmacology	Kietzmann et al., 1993; Kietzmann et al., 1995; Forster et al., 1999; Bäumer and Kietzmann, 1999, 2001; Ehinger and Kietzmann, 2000a, b; Ehinger et al., 2006; Kietzmann et al., 2008; Schumacher et al., 2011; Kietzmann et al., 2010

1.3.4.6 Additives

In an attempt to optimize the performance of the perfusion, various additives have been used. The most commonly used are presented here in relation to experimental design, specimen type and species from which the specimen was derived. Rarely used additives and those that are highly specific to organs or precise research questions are not covered.

The use of whole blood perfusates requires the addition of an appropriate anticoagulant for the prevention of thrombus formation and the consequent disturbance of blood flow. Furthermore, as clotting plays an important role in ischaemia/ reperfusion, the

incorporation of anticoagulants might ease the inflammatory response associated with this process (Blaisdell 2002). For this purpose heparin, an inhibitor of antithrombin III (Hirsh, Raschke et al. 1995), is the most widely used agent (Hardwick, Linzell et al. 1961, Patan, Budras et al. 2009, Constantinescu, Knall et al. 2011). In addition to volume expansion, dextran solutions also contribute thrombolytic and antithrombotic properties (Fischer, Mauzac et al. 1985, De Raucourt, Mauray et al. 1998) rendering them popular additives to perfusates (Tindal 1957, Drapanas, Zemel et al. 1966, Cameron, Burger et al. 1972, Rehfeld, Holst et al. 1982, Domingo-Pech, Garriga et al. 1991, Kietzmann, Löscher et al. 1993, Hansen, Hartmann et al. 2000).

Vasoconstriction, a core response in reperfusion injury, may be counteracted by the addition of vasodilators such as nitroglycerin (Domingo-Pech, Garriga et al. 1991) or prostacyclin (Erasmus, Fernhout et al. 2006) which consequently improve flow rates. Especially in udder perfusion studies, when relatively high flow rates are required, inhibition of 5-hydroxytryptamine induced vasoconstriction has been shown to be advantageous (Roets, Verbeke et al. 1974, Roets, Massart-LeëN et al. 1979, Roets, Verbeke et al. 1979).

Altering the perfusate's rheological properties is an additional means by which flow rates may be improved, especially when using whole blood perfusates. This prompted research groups to (haemo)dilute perfusates to modify blood viscosity and reduce vascular resistance, a technique widely applied in cardiopulmonary bypass procedures (Dittrich, Schuth et al. 2000). As previously mentioned, due to advanced circulatory function attributable to dilution, tissue oxygenation can be improved, despite a reduced concentration of erythrocytes (Dittrich, Schuth et al. 2000). Reported diluents include cell free solutions (Domingo-Pech, Garriga et al. 1991, Wagner, Nogueira et al. 2003, Erasmus, Fernhout et al. 2006, Friebe, Schumacher et al. 2013) or autologous plasma (Patan, Budras et al. 2009, Patan-Zugaj, Gauff et al. 2012, Patan-Zugaj, Gauff et al. 2014), the latter also having the added benefit of increasing oncotic pressure. The potential for cell free solutions to be associated with oedema formation, due to low oncotic pressures, can be addressed by adding components such as plasma proteins

(Verbeke, Peeters et al. 1968, Roets, Verbeke et al. 1974, Patan, Budras et al. 2009) and purified albumin (Rehfeld, Holst et al. 1982, Barthel, Leonhardt et al. 1989, Riviere, Bowman et al. 1989, Brunicardi, Kleinman et al. 2001). Plasma expanders/replacers used for clinical and research purposes may rely on alternative components to maintain oncotic pressure; these include dextran (Cameron, Burger et al. 1972, Kietzmann, Löscher et al. 1993), cellulose (Friebe, Stahl et al. 2001), hydroxyethyl starch (Mueller, Constantinescu et al. 2013) and mannitol (Domingo-Pech, Garriga et al. 1991, Labens, Lascelles et al. 2013). While mannitol is considered an inert substance, recent research has suggested possible effects on monocyte and neutrophil function (upregulation HLA-DR in monocytes, upregulation of CD11b in neutrophils and monocytes, and inhibition of neutrophil apoptosis (Turina, Mulhall et al. 2008)). Hydroxyethyl starch (Handrigan, Burns et al. 2005, Matharu, Butler et al. 2008) and cellulose (Hänsch, Karnaoukhova et al. 1996, Moore, Kaplan et al. 2001, Bae, Jin et al. 2004, Ewoldt, Anderson et al. 2004, Hernández, Galan et al. 2004, Hernandez, Fuste et al. 2009) have also both been shown to alter inflammatory responses due to their different effects on neutrophils. Although largely considered an energy source, responsible for the metabolism and survival of the specimen, glucose is also able to contribute to the maintenance of oncotic pressures within perfusates (Hicks, Hing et al. 2006).

Glycolysis represents the main energy source for living tissue and ensures ATP production under aerobic and anaerobic conditions (Silbernagl 2012). Glucose is metabolized by specimens in perfusion experiments and is therefore a commonly used additive in blood based solutions (Butler, Rees et al. 2002, Patan, Budras et al. 2009) and a standard component of the basic recipe of artificial fluids. When using closed systems, there is a requirement to regularly compensate for glucose loss.

To ensure aerobic metabolism, a sufficient oxygen supply is essential, and oxygen carriers are often added to artificial solutions. Isolated erythrocytes as the body's natural oxygen carrier are very well suited for this purpose, although their use in closed systems has the associated risk of mechanical cell damage over time (Lee, Antaki et

al. 2007, Watanabe, Sakota et al. 2007). In early experiments fluorocarbons were tested with equivocal results (Smith, van Alphen et al. 1985, Usui, Sakata et al. 1985).

Metabolic activity is also influenced by the pH of the perfusate and *vice versa*. Acidosis, potentially resulting from hypoxemia and/or hypoperfusion, leads to an increased level of lactic acid (Silbernagl 2012) which is initially buffered by alkalic substances such as $NaHCO_3$; consequently, such buffers are also standard components of perfusates (Cameron, Burger et al. 1972, Riviere, Bowman et al. 1989, Domingo-Pech, Garriga et al. 1991, Mancina, Kalenski et al. 2015). Although some authors report on gas flow rate adjustments to alter the partial pressure of carbon dioxide (pCO_2) levels and pH (Cypel, Yeung et al. 2008), this approach can be technically challenging within the constraints of most perfusion experimental set-ups.

Even though the harvesting process and the perfusion system are kept as clean as possible, bacterial contamination is still considered a concern as most perfusion experiments are conducted in an unsterile environment. To prevent bacterial overgrowth in perfusates and specimens, antibiotics have been used in selected applications. Most commonly, a standard combination of β-lactam antibiotics (usually penicillin (Hardwick, Linzell et al. 1961, Riviere, Bowman et al. 1989, Bristol, Riviere et al. 1991)) and aminoglycosides (usually streptomycin (Hardwick, Linzell et al. 1961) or gentamicin (Riviere, Bowman et al. 1989, Bristol, Riviere et al. 1991) were chosen. Drugs were generally administered via the perfusate either constantly (Riviere, Bowman et al. 1989, Domingo-Pech, Garriga et al. 1991) or intermittently at predetermined time intervals (Butler, Rees et al. 2002). However, many successful perfusion studies have been conducted without the use of antibiotics. In one particular study, no bacterial contamination was detected for up to 24 hours; neither in the specimen nor in the whole blood perfusate (Chapman, Goldsworthy et al. 1961). However, as the harvesting process and the system used in this particular report were sterile, bacterial contamination can still considered a concern in a lot of other set-ups, because most perfusion experiments are conducted in an unsterile environment.

Almost all perfused specimens undergo a period of warm and/ or cold ischemia. It is known that reperfusion of ischemic tissue leads to endothelial damage which is involved in vascular ischemia/ reperfusion injury (Blaisdell 2002). It is either mediated by IgM natural antibodies (Chan, Ding et al. 2004) or activation of the classical complement pathway by apoptotic endothelial cells (Mold and Morris 2001). This eventually leads to vascular leakage and subsequent oedema formation in perfusion experiments. Cardio pulmonary bypass surgery is also known to activate the complement system and trigger cytokine production (Butler, Rocker et al. 1993). To suppress this cascade, the use of glucocorticoids is widely accepted during CPB (Varan, Tokel et al. 2002). Methylprednisolone is generally used in perfusion experiments when organ preservation is required (Domingo-Pech, Garriga et al. 1991, Constantinescu, Knall et al. 2011); the common aim is to reduce inflammatory cytokine synthesis and the associated development of hydrostatic oedema.

Table 1-3: Most commonly used additives in perfusion experiments

Additive	Class	Function
Heparin	Anticoagulant	Prevention of thrombi
Dextran	Anticoagulant Impermeant	Prevention and lysis of thrombi Prevention of oedema
Mainly: **Penicillin** *and* **Streptomycin**	Antimicrobial agents	Prevention of bacterial overgrowth
Sodium bicarbonate	Buffer	Maintenance of pH levels
Methylprednisolone	Glucocorticoid	Prevention of general inflammation (reduction of vascular leakage)
Plasma proteins/ Serum albumin	Impermeant	Prevention of oedema
Glucose	Impermeant Metabolic substrate	Prevention of oedema Maintenance of metabolism
Aminoacids	Metabolic substrate	Maintenance of metabolism
Erythrocytes	Oxygen carrier	Enhancement of oxygen delivery and maintenance of aerobic metabolism
Cell free solutions	Rheological active agent	Haemodilution
Mainly: **Nitroglycerin** *or* **Prostacyclin**	Vasodilator	Improvement of vascular flow

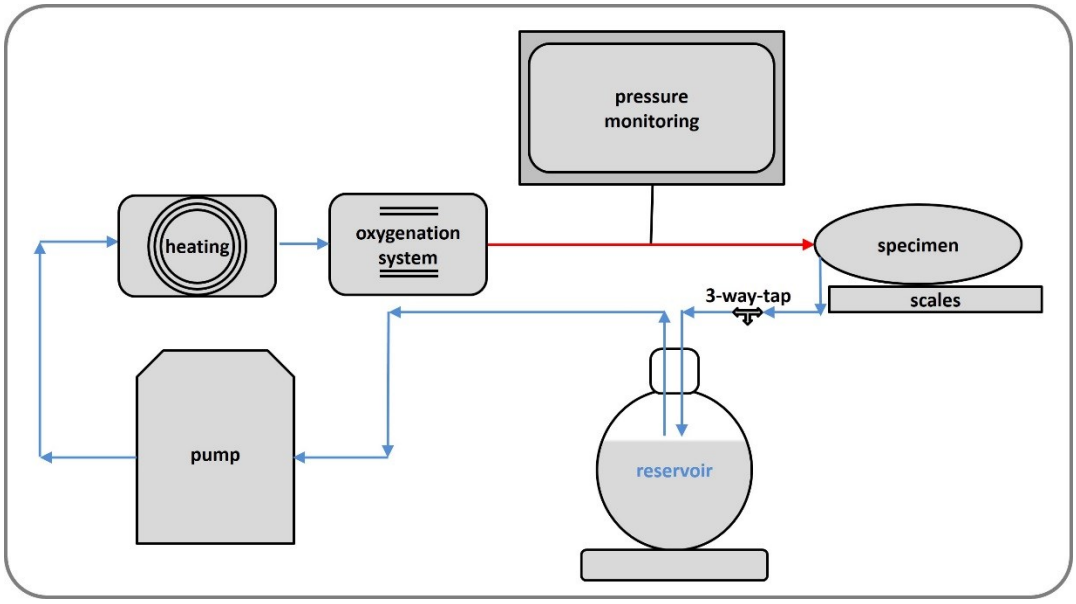

Figure 1-2: Potential set-up of a closed perfusion system

The perfusate is stored in a **venous reservoir** and propelled (blue arrows) by a **pump** to a **heat exchanger**, this could possibly be a water bath, which allows the perfusate to be warmed to body temperature. The perfusate flows through an **oxygenation system** e.g. a hollow fibre membrane oxygenator. The now oxygenated perfusate (red arrow) is eventually pumped through the **specimen's** main arteries, capillary network and venous system. A device for measuring the **perfusion pressure** is connected to the circuit. The venous return is fed back into the system via the cannulated main veins of the specimen. To asses oedema formation during perfusion the specimen rests on **scales**. Perfusate samples are taken via **3-way taps** which are incorporated into the tubing.

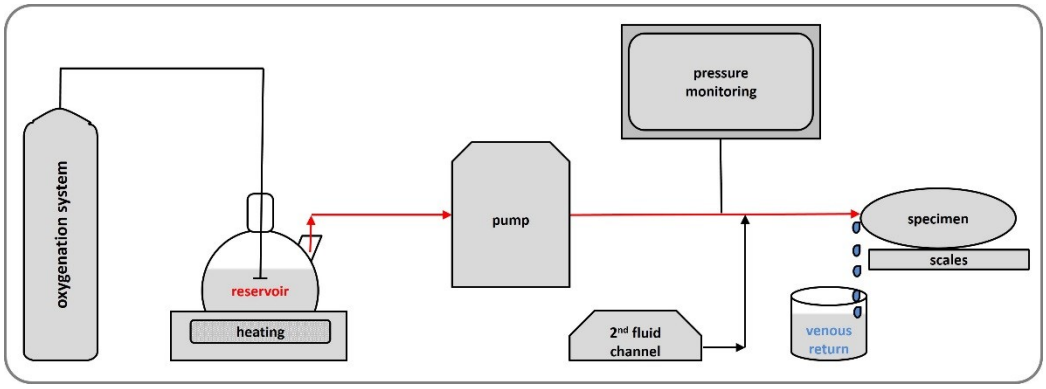

Figure 1-3: Potential set-up of an open perfusion system

An **oxygen source** is connected to the **arterial reservoir** and gasses the fluid e.g. via a sintered glass filter. The reservoir is warmed to body temperature by a **heating device**, this might be a water bath or hot plate. A **pump** propels (red arrows) the solution through the main arteries, capillary network and venous system of the **specimen**. The **venous return** (blue drops) drips freely into a beaker and could be collected at that point. Throughout the experiment the leg rests on **scales** to asses weight gain. A **pressure monitoring system** is connected to the system to inform on continuous perfusate pressures. A **second controlled fluid channel** is formed by another pump system and could introduce select additives into the system.

1.4 Perfusion: history and important findings

Since the early 20th century extracorporeal perfusion of large animal organs has been used to investigate a broad variety of research questions, thereby overcoming common draw backs of *in vitro* studies without suffering from ethical concerns associated with live animal research. The technique is in accordance with the 3R principles and represents an excellent opportunity to investigate in detail the physiology of organs under standardised conditions. It is also suitable for the translation of basic pre-clinical research into a more relevant arena prior to or avoiding altogether live animal research. Furthermore, organ perfusion has also been an important tool in developing methods of organ preservation for transplantation surgery. Yet due to the nature of the experiments, only short term observations can be made and while cells are still exposed

to their regional secretome, the whole organ itself is isolated from the body and correlations between organ-systems cannot be taken into consideration.

1.4.1 Transplantation, replantation and preservation

1.4.1.1 Organs

In the context of transplantation surgery, prolonged preservation using pulsatile perfusion has been shown to be superior to simple cold storage when assessing graft and patient survival, rate of delayed graft function and the need for post-transplant dialysis (kidney transplant, (Peter, Imber et al. 2002, Shah, Milgrom et al. 2008)). Standardization of perfusion set-ups was possible by the availability of commercially available perfusion systems (e.g. Waters RM 3, MOX-100, (Guarrera, Polyak et al. 2004)). This and the augmentation of perfusion solutions (Belzer MPS/ Vasosol MPS) with vasodilators (nitroglycerin, and prostaglandin E1), antioxidants (polyethylene glycol-superoxide dismutase, and N-acetylcysteine), Krebs cycle intermediates (α-ketoglutarate) and metabolic substrates (L-arginine) (Guarrera, Polyak et al. 2004, Guarrera, Polyak et al. 2004) improved results with organ preservations dramatically. To further optimise this methodology, recent studies have evaluated the differences between pressure- and flow-controlled perfusions and concluded that pressure controlled perfusions are superior with reference to renal haemodynamics and acid-base homeostasis (Mancina, Kalenski et al. 2015).

1.4.1.2 Limbs

The preservation of limbs represents a specific challenge due to the broad range of tissues involved and their variable tolerance to ischemia (Blaisdell 2002, Constantinescu, Knall et al. 2011).

In early ILP experiments, performing canine hind limb autotransplants, the best outcome was observed implementing continuous hypothermic perfusion with

solutions containing fluorocarbon as an oxygen carrier (Usui, Sakata et al. 1985). Despite these initial positive results, fluorocarbon containing solutions revealed only moderate success during clinical trials of human digital replantation following perfusions (Smith, van Alphen et al. 1985). Fluorocarbon is also known to reduce neutrophil infiltration, which might be an interesting characteristic in organ preservation but could affect outcomes in research applications of the perfusion model (Forman, Pitarys et al. 1992).

Another study was able to demonstrate that ILP over a period of 24 hours maintained viability of amputated canine hind limbs such that after six hours post replantation, limbs appeared healthy and peripheral vessels were well perfused. However, significantly and gradually over time increasing oedema formation (20 to 50% weight gain), due to increased vascular permeability (Blaisdell 2002), was observed in perfused legs. This phenomenon is indicative for the extent of ischemia/ reperfusion injury (Petrasek, Homer-Vanniasinkam et al. 1994). To improve results subsequent cooling of the perfusate and the use of peripheral vasodilators and steroids (Domingo-Pech, Garriga et al. 1991) was required, the latter to counteract inflammatory processes (Biggar, Bohn et al. 1984).

In order to optimize the experimental set-up, Tsuchida et al. (2001) assessed different perfusion pressures and solutions. Comparing replantation of amputated rat hind limbs after perfusion with the superior set-up (University of Wisconsin solution, high perfusate pressure) with replantation of non-perfused limbs, perfusion resulted in only slightly superior outcomes. This observation might be explained by the potential deterioration of vascular endothelial function and consequently blood flow with the use of University of Wisconsin solution (Tsuchida, Kato et al. 2003).

Recent preservation experiments in porcine limbs using autologous blood in a hypothermic set-up with sub-physiological perfusion pressures have demonstrated both the technical feasibility and great potential of this approach (Constantinescu, Knall et al. 2011). This is further supported by Mueller at al. (2013) who were able to

replant porcine front limbs after an extracorporeal perfusion time of twelve hours with only minimal impact of ischemia/ reperfusion injury as assessed by histopathology and measurement of markers of inflammation and endothelial cell activation. In order to reduce capillary leakage, methylprednisolone was added to the perfusate, a methodological refinement also adopted in several other studies (Mueller, Constantinescu et al. 2013).

1.4.2 Research models

1.4.2.1 Udder

The isolated perfused udder of various species, but predominantly ruminants, has been widely used in the study of milk synthesis and ejection. It has contributed to an improved understanding of lactation and has had a significant impact in the field of dairy research. It has also been used as a model for skin absorption in studies with a pharmacological focus.

The experimental methodology associated with the study of the isolated and perfused bovine udder is largely based on a technique described by Peeters and Massart (Peeters and Massart 1952). For this, abattoir derived specimens were perfused with normothermic oxygenated heparinized homologous blood for approximately two hours at a constant pressure. Different radioactively labelled substrates were added to the perfusate and subsequently measured in milk, venous return and tissue (James, Peeters et al. 1956, Verbeke, Lauryssens et al. 1959, Lauryssens, Verbeke et al. 1960). The O_2 uptake, as an indicator of tissue viability, compared well to the *in vivo* activity during the first two hours. Despite this physiological O_2 consumption, milk yield declined rapidly thereafter, resulting in sub-normal milk production (Lauryssens, Verbeke et al. 1961).

Upon consideration of the dependency of milk production on a relatively high flow rate which could not be achieved in these early experiments, Hebb and Linzell (1951) subsequently included isolated and perfused lungs in the circulatory system.

Justification for this modification was based on previous studies which demonstrated a reduction in the vasoconstrictive properties of blood following passage through the lungs (Eichholtz and Verney 1924, Newton 1933). Others have included vasodilators (dibenamine or dibenzyline) to improve flow rates (Tindal 1957). Hebb and Linzell's complicated technique was subsequently replaced by the availability of artificial oxygenation devices (Hardwick and Linzell 1960).

With the intent to enhance the viability of the used specimens, the udders were no longer obtained from dead slaughtered animals but carefully dissected from live animals under epidural anaesthesia, thus significantly reducing the time delay (two to 27min) between the interruption of blood supply and commencement of extracorporeal perfusion. Applying the definition of specimen oedema as a weight gain of 20% or more, oedema occurred in about half of the experiments reported and in most cases, once the weight gain exceeded 20%, milk secretion ceased within one hour. Nevertheless, following completion of the experiment, most secretory cells appeared normal during histological examination (Hardwick and Linzell 1960). Addition of an artificial kidney to the perfusion system permitted the maintenance of high flow rates for a longer period of perfusion. This additional apparatus consisted of ten metres of dialysis tubing in a reservoir containing 20L of adapted Krebs solution. This technique has since become more popular (Hardwick, Linzell et al. 1961, Hardwick, Linzell et al. 1963, Hardwick 1965, Hardwick 1966, Linzell, Annison et al. 1967, Verbeke, Peeters et al. 1968, Verbeke, Roets et al. 1972, Roets, Verbeke et al. 1974, Roets, Massart-LeëN et al. 1979, Roets, Verbeke et al. 1979). In the 1990s, the isolated perfused bovine udder was used for pharmacokinetic research, with the seminal work of Kietzmann et al. supporting the application of this model to therapeutic studies on mastitis (Kietzmann, Löscher et al. 1993). In these studies, warmed and oxygenated Tyrode solution was the perfusate of choice (Ehinger, Schmidt et al. 2006, Kietzmann, Niedorf et al. 2010).

The potential for the application of the model to studies on skin inflammation became evident with the collection of data which supported good skin viability during a six

hour period of perfusion; these data included the following; glucose consumption, lactate production, lactate dehydrogenase activity, and pH in the perfusate, histological examination. Additional measurement of the udder skin-fold thickness demonstrated the absence of oedema formation (Kietzmann, Löscher et al. 1993). Subsequently, different anti-inflammatory drugs were tested for their effect on eicosanoid synthesis. These were either administered "systemically" (i.e. via the perfusate) or applied topically on the skin (Bäumer and Kietzmann 2001). The perfusion model also served as the basis for studies on the transdermal absorption potential of vitamin E acetate from cosmetic formulations (Lampen, Pittermann et al. 2003). More recently, the isolated bovine udder, perfused with Tyrode solution for five hours, was shown to be applicable to preclinical trials into biodegradable magnesium implants (Schumacher, Stahl et al. 2011).

1.4.2.2 Internal organs

Heart

The isolated perfused heart is an extensively used *ex vivo* whole organ research model which has helped to gain a better understanding of cardiac physiology (contractile function, blood flow and, metabolism) and pathophysiology (ischemia/ reperfusion injury). Furthermore, the model forms the basis for the collection of viable cardiac myocytes or for the measurement of electrical activity (Bell, Mocanu et al. 2011). The technique dates back to Langendorff who, in 1897, introduced a model of retrograde perfusion of the isolated mammalian heart via the aorta, later known as the Langendorff heart. For this, the aortic root is slipped over a fixed cannula in the perfusion system which is in turn connected to a reservoir containing a gassed and warmed perfusion solution, most commonly a modified Krebs Henseleit solution. The model can either be used under constant flow or constant pressure conditions. It facilitates the investigation of a broad spectrum of physiological, morphological, biochemical and pharmacological parameters and is generally accepted as an appropriate model to study drug-induced cardiotoxicity and electrical conductivity (Skrzypiec-Spring, Grotthus et al. 2007, Bell, Mocanu et al. 2011). In comparison, the

isolated heart can also be perfused in the working heart mode, whereby the perfusate enters the left atrium via the pulmonary vein, flows into the left ventricle and onwards into the aorta (Chinchoy, Soule et al. 2000, Araki, Usui et al. 2005). The right side of the heart is not included in this system as this would necessitate a biventricular working heart set-up, in which the right heart performs a physiological low pressure ejection (Demmy, Magovern et al. 1992, Chinchoy, Soule et al. 2000).

Uterus

Another application of isolated organ perfusion is represented by the use of the bovine uterus for the study of mucosal inflammation. For such inflammation studies, a mixed Tyrode/ homologous blood perfusate was used (ratio 1:4), whereas irritancy studies were carried out on only Tyrode perfused uteri. The average weight gain of the specimen throughout the five hour perfusion period was reported at 20% for Tyrode-perfused organs with no diminished oedema formation in haemoperfused uteri (Bäumer, Mertens et al. 2002, Braun and Kietzmann 2004).

Liver

In 1961, Chapman et al described for the first time the successful perfusion of isolated calf livers for up to 24 hours by cannulating the hepatic artery and portal vein simultaneously. This report demonstrated tissue viability based partly on the measurement of oxygen consumption, the constancy of blood flows and pressures and only minimal changes in histologic parameters. The authors also postulated that the perfusate (autologous blood diluted with Krebs-Henseleit solution to a final haematocrit value of 25 to 35%) could be maintained free of bacteria throughout a twelve hour perfusion without the addition of antimicrobials (Chapman, Goldsworthy et al. 1961). A similar approach, but using homologous porcine blood with several additives (Tisusol, Rheomacrodex© 5% in dextrose, calcium glucoheptonate, heparin, xanthocholate), was successfully used to model hepatic metabolic clearance (Cameron, Burger et al. 1972). Following further improvements to the set-up and the addition of a dialysate circuit, autologous haemoperfusion of the isolated pig liver also yielded good results and was shown to be a promising tool for the study of whole organ

liver function and hepatotoxicity (Grosse-Siestrup, Pfeffer et al. 2002). Drapanas et al (1966) also reported on haemoperfusion of the isolated pig liver, using heterologous blood (human) modified with low molecular weight dextran and heparin. In contrast to the results of Grosse-Siestrup et al (2002), four hours of perfusion resulted in mild to moderate interstitial oedema, reduced oxygen consumption and a sample weight gain of about 20%. Half of this reported total weight gain occurred during the initial wash out period (20 to 30 minutes) with cold Ringer's solution, thus illustrating the inadequacy of this perfusate solution for maintenance of oncotic pressures (Drapanas, Zemel et al. 1966). In comparison, a five hour human liver perfusion with Krebs bicarbonate buffer containing 20% prewashed human or bovine red blood cells, bovine serum albumin, α1-acid-glycoprotein, calcium and glucose resulted in normal histological liver architecture. Nevertheless, the reservoir contained increased levels of alanine aminotransferase, likely reflective of endothelial cell damage resulting from ischemic injury (Villeneuve, Dagenais et al. 1996).

Intestine

Few attempts to perfuse isolated large animal intestine have been made. For absorption studies, isolated porcine duodenum or ileum was perfused under normothermic conditions with Krebs Ringer bicarbonate solution containing various additives, including washed bovine or human erythrocytes, dextran T70, glucose, amino acids or cyclooxygenase inhibitors (Rehfeld, Holst et al. 1982, Messell, Harling et al. 1992, Hansen, Hartmann et al. 2000, Hansen, Hartmann et al. 2004). The perfusion set-up described by Messell et al. (1992) is based on an open system first developed for pancreas perfusion (Jensen, Kühl et al. 1975). In that study, only perfusion pressure was continuously recorded which, upon analysis showed an association with nerve function. No viability related data was provided; however, stimulation by various means seemed to have influenced the activity of intrinsic nerves during the six hour perfusion period (Messell, Harling et al. 1992). Similarly, despite the failure to report on specific measures of tissue viability, Hansen et al. (2000), utilising the same model, demonstrated normal motor activity of the gut, with contractions leading to a short increase in perfusion pressure. To inform on intestinal function and pathophysiology

in the context of ischemia/reperfusion injury, Polyak et al. (2008) developed a model of an isolated and perfused equine large colon. Using this model, twelve hours perfusion with a novel organ preservation solution and without any means of oxygenation proved superior to the use of oxygenated whole blood, based on the measurement of arterial blood pressure and flow, intra-vascular resistance, electrolyte concentrations and an assessment of mucosal integrity (Polyak, Morton et al. 2008).

Kidney

Efforts to establish and improve techniques for isolated kidney perfusion have been ongoing since 1903 (Pavy, Brodie et al. 1903) with the main focus on the organ's functional preservation for subsequent transplantation surgery. The first successful attempts were made using dog kidneys and normothermic perfusion conditions under physiological perfusion pressure in a closed system with a customised oxygenator supplying an O_2-CO_2-mixture. Two different blood preparations were used and weight gain was reported to be 15±2% (Waugh and Kubo 1969). Use of Tyrode or barium sulphate ($BaSO_4$) solutions for perfusion were associated with well-preserved histological morphology in experiments investigating shockwave induced lesions (Köhrmann, Back et al. 1994). Perfusion with cell free Tyrode solution was comparable with autologous blood preparations in terms of reperfusion injury, but inferior with respect to the preservation of renal function (Hoechel, Lehmann et al. 2003).

Lung

The use of an isolated and perfused large animal and canine lung has been described for physiological modelling. For this purpose, either autologous whole blood (Bhattacharya and Staub 1980) or Krebs' solution augmented with 4,5% Ficoll 70 as a colloid oncotic agent (Hellewell and Pearson 1983) was used as the perfusate. Attempts to establish a set-up for prolonged lung preservation have yielded promising results after six hours of perfusion, although impairment of lung function occurred towards the end of the experiment. The perfusate of choice was blood diluted with Steen® solution (final haematocrit 15%), from which leucocytes and platelets were

eliminated using a Cell Saver (Cat II®; Fresenius Hemocare, Emmercompascum, the Netherlands, (Erasmus, Fernhout et al. 2006)). Maintenance of a stable lung function for up to twelve hours of perfusion has since been reported using cell free Steen® solution as the perfusate (Cypel, Yeung et al. 2008).

1.4.2.3 Limbs

The technique of isolated limb perfusion (ILP) has the potential to serve a variety of research interests and objectives. In the context of equine laminitis, an open ILP system using gassed Krebs-Henseleit solution was used to demonstrate that endothelium-derived nitric oxide could modulate the response to vasoconstrictors, thus supporting its potential role as an important regulator of blood flow in the equine digit (Berhane, Elliott et al. 2006). In the same field of research, Patan et al. (2009) demonstrated excellent viability of the laminar tissue following up to ten hours of perfusion with autologous whole blood, applying constant (non-pulsatile), physiological blood pressures throughout (Patan, Budras et al. 2009). Employing the described set-up, the authors were also able to show the model's ability to respond to an inflammatory stimulus, created by addition of lipopolysaccharide to the perfusate (Patan-Zugaj, Gauff et al. 2012, Patan-Zugaj, Gauff et al. 2014).

Another application of ILP is represented by its use in pharmacokinetic studies, whereby an *ex vivo* perfusion model is used to assess drug distribution in the synovial fluid and synovial clearance after both, intra-articular injection and systemic administration via the perfusate (Friebe, Stahl et al. 2001, Friebe, Schumacher et al. 2013). In this context, the authors were able to show that, following a perfusion period of eight hours with gassed Tyrode solution and sodium carboxymethyl cellulose, the intimal layer of the equine fetlock joint capsule appeared unchanged; in comparison, the subintimal connective tissue developed mild signs of oedema. In this study, four minimal criteria for an effective ILP of the equine distal digit were postulated; namely, glucose utilization ≥200mg/h, lactate production ≤400mg/h, LDH activity ≤10U/h, skin surface temperature ≥26°C (Friebe, Stahl et al. 2001). However, these reference

criteria can only be applied to similar experimental models, as metabolic parameters are tissue and perfusion dependent. For example, a closed system may lead to the accumulation of lactate or the use of blood-based perfusates may increase overall LDH levels due to the mechanical cell damage the pump inflicts on cellular blood components. Similarly, measured metabolic data will also be influenced by the weight of the specimen and the volume of perfusate.

Due to the similarities between porcine and human skin, perfused isolated porcine limbs have been used for transdermal absorption studies. Such work has included a comparison between low (100ml/min) and high (physiological) flow (230-250ml/min) perfusions, in which higher flow rates were shown to improve oxygen supply and reduce the risk of oedema formation, features attributed to the comparatively lower organ resistance (perfusion flow/perfusion pressure) and improved blood vessel integrity. An additional comparison of two different perfusate solutions in the high flow group revealed improved haemodynamic parameters when a dialysate solution augmented with bovine serum and autologous erythrocytes was compared with a whole blood dialysate mixture (Wagner, Nogueira et al. 2003).

Table 1-4: Selected perfusion models and their use in research

Organ	ECP LA suitable for	Findings	Model developed by
Limb (equine)	Modelling inflammatory responses in the context of laminitis	Endotoxin plays a role as causative agent for equine laminitis (Patan-Zugaj, Gauff et al. 2012, Patan-Zugaj, Gauff et al. 2014)	Patan et al., 2009; Gauff et al., 2013
	Investigating the role of hyperinsulinaemia in the context of laminitis	Hyperinsulinaemia alters endothelin-1 expression in the equine laminar tissue which suggests endothelin receptor antagonists as a potentially new class of agents in the treatment of laminitis (Gauff, Patan-Zugaj et al. 2013, Gauff, Patan-Zugaj et al. 2014)	

Limb (equine)	Pharmacokinetic studies in the context of joint disease	Acetylsalicylic acid and salicylic acid accumulate in the synovial fluid after systemic administration, despite subsiding systemic levels (Friebe, Schumacher et al. 2013)	Friebe et al., 2001
Limb (porcine)	Prolonged limb preservation for transplantation	Prolonged limb preservation barely influences ischemia/ reperfusion injury, ECP LA is a promising technique for use in transplantation surgery (Mueller, Constantinescu et al. 2013)	Constantinescu et al., 2011
Udder (caprine)	Exploring physiological concepts (milk synthesis)	Metabolism of various substrates and their contribution to milk synthesis, e.g. (Hardwick 1965, Roets, Verbeke et al. 1979)	Hebb and Linzell, 1951; Hardwick and Linzell, 1960
Udder (bovine)	Pharmacokinetic skin absorption studies Pharmacokinetic studies in the context of mastitis (intra-mammary and systemic administration)	No cytotoxicity was recorded for various delivery systems, some formulations were superior regarding their maximum vitamin E delivery to deeper skin layers (Lampen, Pittermann et al. 2003) Cefquinome exceeds the MIC_{90} values of common mastitis pathogens after a combined systemic and intra-mammary application (Ehinger, Schmidt et al. 2006)	Kietzmann et al., 1993
Udder (bovine)	Exploring physiological concepts (milk synthesis)	Metabolism of various substrates and their contribution to milk synthesis, e.g. (James, Peeters et al. 1956, Verbeke, Lauryssens et al. 1959)	Peeters and Massart, 1952; Lauryssens et al., 1959

Uterus (bovine)	Modelling inflammatory responses	The mucosal irritation potential of Lugol's iodine solution has been shown on the Tyrode-perfused uterus. In addition a haemoperfused uterus has demonstrated its potential as a model for inflammatory responses (Bäumer, Mertens et al. 2002)	Kietzmann et al., 1993; Bäumer et al., 2002

End article

1.5 Summary and aims

Against the background of these various approaches, it becomes evident that no gold standard model exists for research in the field of OA (Lampropoulou-Adamidou, Lelovas et al. 2014). In comparison, for RA, transgenic and chemically induced models may accurately reflect the naturally occurring disease. Despite this, *in vitro* models barely reflect the complexity of the diseases and the gap between laboratory-based single cell models and live animal experiments remains wide. It would therefore be beneficial to develop an *ex vivo*, whole organ joint model with a view to bringing *in vitro* research into a more relevant arena prior to the initiation of live animal research. Isolated limb perfusion (ILP), a technique in which appendices are separated from the body's blood circulation but maintained under physiologic conditions using an extracorporeal circuit, has the potential to fill this gap. Following development of the model, the longer term plan would be to adopt its use for testing new anti-inflammatory agents and drug delivery systems in the context of arthritis. The technique would not only reduce live animal experiments in accordance with the 3R's principle but also facilitate the development of cost-efficient pre-clinical trials with great translational potential. It is however imperative to emphasise that the ILP model should not be seen as a disease model, but a tool for pharmacological research with focus on arthropathies and the joint in general.

Chapter 2 Materials and methods

2.1 Ethical approval and origin of specimens

Specimens were either waste material from food production (local licensed abattoir) or licensed experiments of other research groups or obtained from twelve pigs that were specifically sacrificed for this project. Blood was collected at the time of exsanguination either at the abattoir or from the twelve project specific pigs. All of these procedures were approved by the university's Veterinary Ethical Review Committee.

Tissues obtained from live animals were harvested during terminal procedures, in which students practised their surgical skills. All of these procedures were approved by the Institutional Animal Care and Use Committee (Reference number 09-148-T).

For the work presented in chapter three 22 specimens were used (abattoir derived and waste material from other research groups).
Data collection for chapters four and five was based on the use of 18 abattoir derived specimens, twelve specimens derived from terminal experiments of other research groups and twelve animals sacrificed for the presented study.

2.2 Neutrophil isolation and staining

Neutrophils were isolated from autologous heparinized (20.000IU/L) porcine blood collected at the time of exsanguination and immediately aliquoted in 30mL tubes (Sarsted, AG&Co, Nümbrecht, Germany). After transportation to the laboratory under non-cooled conditions (median transport time: 100min; Q1: 96.25; Q3: 105.00; IQR: 8.75) samples were allowed to settle for 45min to generate leukocyte rich plasma. Neutrophils were isolated by density gradient separation (Ficoll®-Paque, Sigma-Aldrich). The sedimented leucocyte rich plasma fraction (10mL) was layered over five

milliliter Ficoll®-Paque aliquots, followed by centrifugation at 1800rpm for 20min. The density of granulocytes was sufficiently high at the given oncotic pressure to travel through the Ficoll®-Paque medium and accumulate at the bottom of the tube. Any residual erythrocytes within the plasma are aggregated by Ficoll PM400 (an ingredient of Ficoll®-Paque); consequently, these also settle at the bottom of the tube. Everything but the granulocyte pellet was aspirated and discarded and the cell pellet was gently re-suspended in six milliliter sterile water (hypotonic) for one minute to lyse the erythrocytes. The isotonicity was restored by adding six milliliter of hypertonic 1.8% saline solution to the tube. The cells were then further suspended in 40ml Hanks' Balanced Salt Solution (HBSS, Life technologies) without additives. Manual cell counts and cell viability assessments were conducted on a 20uL aliquot of the cell suspension mixed with an equal volume of trypan blue (Sigma Aldrich), using a haemocytometer. Cells were subsequently re-suspended to a defined cell count per milliliter ($1x10^7$cells/mL) in HBSS. The dye CMFDA (2µg/mL) was added to the solution to stain cells for later multiphoton microscopy and the mix incubated for 30min. Next, stained cells were washed twice (2x centrifugation at 1000rpm, 8min, re-suspension in HBSS). As a final step, cells were suspended in the appropriate volume of 5% porcine serum in HBSS without magnesium and calcium (HBSS --) to achieve the desired final cell concentration (experiment dependent; ranging from $5x10^6$ to $20x10^6$ cells/mL) and transferred to 20mL syringes (BD DiscarditTM II).

2.3 Multiphoton

The principle of multiphoton microscopy is based on the use of long-wavelength light (infrared lasers) that excites fluorescent dyes. Two photons of comparably low energy (E), and therefore long wavelength (λ) ($E = \frac{hc}{\lambda}$, h: Planck constant, c: speed of light), are simultaneously absorbed in a single event. In order to achieve the necessary number of two-photon absorption events, a high power (pulsed) laser is required and photons are spatially and timely concentrated. When these physical principles are combined, the advantage of multiphoton laser scanning microscopy against one-

photon techniques becomes evident: light with longer wavelengths is scattered less in mediums having a variable refraction index, such as biological tissues. Therefore, two-photon excitation allows more light to propagate through the tissue to the focus plane, and subsequently attain a greater penetration depth. Additionally, no absorption occurs out-with the focus plane, thus also contributing to a greater depth of penetration. These properties supersede the requirement for a pinhole, resulting in images which contain less background fog and better contrast. In light of these facts, an approach which adopted this multiphoton technology was considered ideal for microscopic visualisation of the relatively thick specimens and intact, unprocessed tissue samples.

2.3.1 Live and dead cell staining

Assigned samples were stained with 5-chloromethylfluorescein diacetate (CMFDA, live cells, green) and propidium iodide (PI, dead cells, red). The staining was carried out in a dark environment and all tubes were light protected with aluminum foil. One vial CMFDA powder (Life technologies) was dissolved in 50µL dimethyl sulfoxide (DMSO; Sigma-Aldrich®) and an aliquot of the above solution transferred to 150mL Dulbecco's Modified Eagle Medium (DMEM; ThermoFisher Scientific) containing 1% penicillin/ streptomycin. The remainder of the dye was stored for further use. The mix obtained was enriched with 75µL PI (ThermoFisher Scientific). The solution was aliquoted into suitable containers and samples were submerged in the liquid for 75min at room temperature. Subsequently, specimens were fixed in 4% formaldehyde in 0.9% NaCl v/v for 24 hours at 4°C. As appropriate, samples were then transferred to phosphate-buffered saline (PBS) and stored at 4°C. Finally, samples were mounted into Petri dishes, submerged in PBS and the viability of cartilage and joint capsule samples was assessed using multiphoton laser scanning microscopy (MP7, Zeiss) and 3D image processing (Imaris, Bitplane) by computing a live to dead cell ratio.

2.3.2 Second harmonic generation

The second harmonic generation effect (SHG) was utilized to provide further information regarding collagen fibers in samples. In order to be suitable for SHG imaging, tissues have to be of non-centrosymmetric structure in order to interact with incoming photons in a way that converts them into photons with twice the energy, and hence half the wavelength and twice the frequency. The multiphoton microscope is capable of detecting variations in this frequency doubling and subsequently transforming the obtained data into an image. For the purpose of this study, a differentiation between forward and backward direction of the signal was not considered.

2.4 Lactate dehydrogenase activity assay

The enzyme lactate dehydrogenase (LDH) reduces nicotinamide adenine dinucleotide (NAD) to NADH and is involved in the conversion of lactate to pyruvate in glucose biosynthesis and anaerobic glucose metabolism (Berg, Tymoczko et al. 2013). Elevations in LDH levels are indicative of cell injury/death (Legrand, Bour et al. 1992) and can be assessed using a colorimetric assay (Lactate Dehydrogenase Activity Kit, Sigma-Aldrich). The NADH produced via LDH enzymatic activity interacts with a particular probe which in turn produces a dyed substance. The absorbance of this colour was measured at 450nm using a spectrophotometric plate reader (1420 Multilabel Counter, VICTOR³ TM, PerkinElmer precisely). LDH concentration within the sample was calculated by reference to a standard curve derived from serial dilutions of an NADH standard solution provided with the kit. Five to 35µL of respective venous return samples (= fluid which drops freely from the veins after flowing through the limb) from perfusion experiments were mixed with the assay's reagents to a final volume of 100µL per reaction. The first measurement ($A_{450initial}$) was obtained two minutes following completion of the pipetting (96 well flat bottom plate ($T_{initial}$)). Measurements were subsequently obtained every five minutes until the most active sample displayed a higher value than the highest standard. Between

measurements the plate was incubated at 37ºC. To ensure that all readings fell within the limits of the standard curve, the absorbance values used for further calculations ($A_{450final}$) represented the penultimate readings obtained (T_{final}). For each plate, readings obtained for construction of the standard curve were all corrected for background noise.

The difference in absorbance between $T_{initial}$ and T_{final} was calculated for each sample:

$$\Delta A_{450} = A_{450final} - A_{450initial}$$

Comparison of sample results with the standard curve permitted the calculation of the amount of NADH produced by the reaction between the time points $T_{initial}$ and T_{final} using the following equation:

$$LDH\ activity = \frac{B\ x\ sample\ dilution\ factor}{reaction\ time\ x\ V}$$

B was defined as amount of NADH generated between the initial and the final measurement in nmol. The sample dilution factor for the assay was set to one. The reaction time (min) was the elapsed time between the initial and final measurement. The volume (ml) of sample used per reaction is referred to as V.

The unit of LDH activity is nmol/min/mL or mU/mL, with one unit of LDH activity described as the quantity of LDH required to produce 1µmol of NADH per minute at a temperature of 37ºC.

2.5 RNA extraction, analysis and processing

2.5.1 RNA extraction

Samples (approx. 100mg) were submerged in 1.5mL RNAlater® (ThermoFisher Scientific) and incubated for 24h at room temperature. Subsequently the fluid was removed and samples stored at -80°C. The frozen and minced tissue sample was placed in a liquid nitrogen cooled dis-membranator flask together with 500µL guanidinium thiocyanate-phenol (TRIzol, ThermoFisher Scientific). The flask, containing tissue, TRIzol and a grinding ball, was subsequently mounted into the dis-membranator (Oscillating mill MM200, Retsch) and subjected to a constant oscillation at a frequency of 30.0Hz for 90s in order to disrupt and homogenise the tissue. The remaining powder was scraped into and Eppendorf tube containing 500µL of TRIzol and mixed by shaking the tube. Samples were then stored at -80°C until further processing. Between samples, all equipment was thoroughly cleaned (e.g. flask, ball, spatula, forceps etc.) by sequentially submerging in sterile water, 10% NaOH and sterile water again for four minutes, respectively.

After thawing, the mixture was incubated for 45min at room temperature prior to centrifugation (11773.44rcf/12000rpm, 4°C; Centrifuge 5415 R, Eppendorf, rotor radius 73mm) for ten minutes in order to remove remaining tissue and cell fragments. The supernatant was transferred to a clean tube and mixed with 200µL chloroform using a Vortex mixer (PV-1 Vortex Mixer, Grant). The solution was incubated at room temperature for three minutes and centrifuged (4°C, 12000rpm) for 15min. The supernatant was decanted to another tube and washed with 400µL of 70% ethanol (ThermoFisher Scientific). For the following steps, the RNeasy® Mini Kit (Qiagen) was used. The protocol is based on the supplier's handbook. The reagents were mixed by pipetting gently up and down and a fraction of 700µL was immediately transferred into an RNeasy® Mini spin column mounted into a 2mL collection tube from the same kit and centrifuged for 30s at 8000rcf. The flow-through was discarded and the procedure repeated with the remainder of the above ethanol solution. For on-column DNA digestion, 350µL Buffer RW1 was applied to the column and the tube subjected

to centrifugation (30s, 8000rcf). Subsequently the flow-through was discarded, 80µL DNase in Buffer RDD added directly to the RNeasy® spin column membrane (15min, room temperature) and the Buffer RW1 washing step repeated. This was followed by two washing steps using 500µL Buffer RPE each (1st: 30s, 8000rcf, 2nd: 2min, 8000rcf). To dry the membrane and remove any carryover of Buffer RPE, the spin column was placed in a new 1.5mL collection tube and centrifuged for one minute at 8000rcf. To complete the RNA extraction, 30µL RNase-free water was applied directly to the spin column membrane and centrifuged for one minute at 8000rcf. Following spectrophotometric quality assessment (see below), the extracted RNA was stored at -80°C.

2.5.2 RNA purity

Purity of the extracted RNA was evaluated for all samples using the NandoDrop™ 1000 Spectrophotometer (Thermo Scientific). The assessment is based on the measurement of the absorbance (A) of light at λ=260nm to determine the optical density of the RNA molecules present in the tested solution. In contrast to RNA which absorbs at λ = 260nm, possible contaminants usually absorb either near λ = 280nm or λ = 230nm. Accordingly, ideal ratios reflecting acceptable RNA purity were defined as approximately 1.8 for A260/A280 and between 2.0 and 2.2 for A260/A230. Using the results obtained, RNA concentration was calculated based on a modified Beer-Lambert equation with *c* being the nucleic acid concentration in ng/µL, *A* being the absorbance in AU, *e* being the wavelength-dependent molar absorptivity coefficient in ng-cm/µL and *b* being the path length in centimeters:

$$c = \frac{Ae}{b}$$

The absorbance of interest was at λ = 260nm. A value of 40ng-cm/µL is commonly accepted as the molar absorptivity coefficient for RNA. Consequently, the final equation applied was as follows:

$$c = \frac{A260 * 40}{b}$$

2.5.3 RNA to cDNA

Via reverse transcription (RT), the extracted RNA was subsequently converted to complementary DNA (cDNA). The reaction required a total volume (including all reagents) of 20µL and the desired final concentration of cDNA per reaction was 1000ng. Based on these values and the known RNA concentration derived from the spectrophotometric analysis, the volume (µL) of RNA required was calculated as follows:

$$volRNA = \frac{1000}{cRNA}$$

For the conversion to cDNA, the Omniscript® RT Kit (Qiagen) was used. Firstly, the calculated volume of RNA was mixed with nuclease-free water (Qiagen): the volume of water was dependent on the volume of RNA used to ensure that the total volume of 20µL was not exceeded. This mix was incubated for five minutes at 65°C in a heat block (Dri-Block® DB-2D, Techne). During the period of incubation, a master mix was prepared containing 2µL 10x RT buffer (Omniscript® RT Kit, Qiagen), 2µL deoxynucleotide triphosphates mix (dNTP mix, 5mM, Omniscript® RT Kit, Qiagen), 0.2µL Oligo (dT) 15primer (0,5mg/mL, Promega), RNasin® Plus inhibitor (40U/µL, Promega), 2µL dithiothreitol (DTT, 100mM, Promega). Immediately prior to use, 1µL Omniscript® RT (Omniscript® RT Kit, Qiagen) was added. RNA and master mix were carefully vortexed, briefly centrifuged and incubated for 60min at 37°C in a thermal cycler (G-Storm GS4822, labtech.com). In the same batch, negative controls of randomly assigned samples for the following qPCR were also prepared. The above protocol was used with the following exceptions: one reaction lacked reverse

transcriptase (no RT control, NRTC) and one reaction was conducted without an RNA template (no template control, NTC). The final products were stored at -20°C.

2.6 Quantitative polymerase chain reaction

Quantitative polymerase chain reaction (qPCR) was used to quantitatively assess the level of expression of both the genes of interest (GOI) and the housekeeping genes (HKG). This method allows quantification of the amplified product by linking it to a fluorescent probe. For the main experiment, the dye of choice was PrecisionPLUS MasterMix (premixed with low level ROX and inert blue (Primerdesign Ltd)), which is widely used for non-specific detection and intercalates into amplified DNA. Once bound to DNA, the fluorescence can be detected at 520nm and the generated target can be calculated as it is proportional to the amount of incorporated dye.

2.6.1 Selection of housekeeping genes

To identify appropriate housekeeping genes (HKG), which are stably expressed independent of different sample treatments, a porcine specific geNorm™ Reference Gene Selection Kit (Primerdesign) was used. The following six genes were tested according to the manufacturer's protocol: β-actin (ACTB), ATP synthase, H+ transporting, mitochondrial Fo complex subunit C1 (subunit 9) (ATP5G1), β2 microglobulin (B2M), glyceraldehyde-3-phosphate dehydrogenase (GAPDH), glucose-6-phosphate isomerase (GPI), ubiquitine C (UBC). Samples used were sourced from auxiliary joints of non-perfused limbs, perfused limbs and perfused limbs with injected (intra-articular) superparamagnetic iron oxide nanoparticles (SPIONs, n=4 for each group). Respective cDNA was diluted with RNase/DNase free water to obtain a final concentration of 5ng/µL. A separate master mix was made for each potential HKG containing 1µL of respective primers (designed by Primerdesign, sequence not provided), 10µL SYBR green (Primerdesgin 2x PrecisionPLUS™) and 4µL RNase/DNase free water. Master mix (15µL) and cDNA (5µL) were transferred

into designated wells of a 96 well plate. Water controls were also used to provide information regarding potential contamination. The manufacturer provided an amplification protocol for the experiment as shown in Table 2-1.

Table 2-1: Amplification protocol geNorm™ Reference Gene Selection Kit

Number of cycles	Stage	Temperature in °C	Time in seconds
1	**Activation**	95	120
	Amplification		
40	Denaturation	95	10
	Data collection	60	60
	Dissociation	95	60
1	(optional)	55	30
		95	30

Generated data was analysed with qbase+ (www.biogazelle.com) using the default M and V analysis tool. The variable M represents the average stability of the tested gene, whereby a low M value is desirable as it indicates a more stable HKG which is less susceptible to potential differences in expression between cDNA samples from various experiments (e.g. treated vs. control group; ideal: $M \leq 0{,}5$). The variable V assesses the ideal number of HKGs in the intended experiment to allow for an optimal normalisation of data. The V value is calculated by a pairwise variation V (n/n+1) and is considered optimal when below 0.15.

2.6.2 Design and validation of primers for genes of interest

2.6.2.1 Isolation and stimulation of porcine peripheral blood mononuclear cells (PBMCs)

After several unsuccessful attempts to validate primers on samples obtained from perfusion experiments, it was decided to test primers for all the genes of interest (GOIs) on concanavalin A (ConA) stimulated porcine peripheral blood mononuclear cells (PBMCs), as they have been shown in the literature to sufficiently express most

GOIs and thus permit appropriate validation of sequences (Dozois, Oswald et al. 1997).

The isolation and stimulation process is adapted from Dozois et al. (1997). Porcine whole blood was obtained as a byproduct of food production at a local licensed abattoir. Five hundred millilitres mixed arterial and venous blood was collected into a heparinised glass bottle (10.000IU/ 500mL) during the exsanguination process, followed immediately by careful aliquoting into 50mL Falcon tubes (Sarstedt). Tubes were transported to the laboratory within 1h, where they were immediately centrifuged for 20min (3000rcf, 21°C). The brakes were disabled on the centrifuge to minimize the likelihood of cellular resuspension due to vibrations associated with rapid deceleration. The buffy coat was carefully removed and diluted with PBS (1:1). This solution was carefully layered on an equal volume of Ficoll (GE Healthcare) and tubes centrifuges for 20min (1800rpm). Cells were separated during this process by density gradient and the layer between phases, containing the PBMCs, was transferred to another tube and washed with PBS (10mL, 10min, 300rcf). Following centrifugation, the supernatant was decanted and discarded and the cell pellet re-suspended in PBS (10mL). Manual cell counts and cell viability assessments were performed using a haematocytometer and trypan blue (ThermoFisher Scientific). Tubes were further centrifuged (8min, 1000rpm) and following the removal of the supernatant, re-suspended to a final concentration of two million cells per milliliter in Complete Medium (Oswald, Gazzinelli et al. 1992). Finally, six-well-plates were loaded with 2mL of the above solution per well (= $4x10^6$ cells/ well) and 2µg ConA (Sigma-Aldrich®). Cells were incubated for 36h at 37°C and 5% CO_2.

Table 2-2: Complete Medium according to Oswald et al., 1992

Ingredient	Concentration
DMEM **RPMI**	Ratio 1:1
FBS	10%
Penicillin	100U/mL
Streptomycin	100µL/mL
Glutamine	2mM
HEPES	300mM
2-ME	0,5µM

2.6.2.2 RNA extraction from PBMCs

Following the 36h incubation period, cells were further processed using the RNeasy® Mini Kit (Qiagen) according to the manufacturer's protocol. The Complete Medium was removed and 600µL of RLT buffer re-suspended in β-mercaptoethanol (β-ME) was added to each well to disrupt cells and release the RNA. Adherent cells were scraped off using a cell scraper and the lysate was transferred into an RNase/DNase free Eppendorf and vortexed. Subsequently, the lysate was pipetted into a QIAshredder spin column for homogenisation and spun for two minutes at top speed. An equal volume of 70% ethanol was then added directly to the collection tube. The subsequent steps relating to RNA extraction, RNA quality control and generation of cDNA were the same as described in sections 2.5.1, 2.5.2 and 2.5.3, respectively.

2.6.2.3 Primer design

Appropriate sequences were identified using the publicly available Ensemble genome browser (www.ensembl.org). On the basis of these sequences, suitable primers were designed with Primer3web, version 4.1.0 (http://primer3.ut.ee/). Care was taken to ensure that selected primers had a melting temperature close to 60°C, a low guanine and cytosine content, were located near the 3' end and were intron spanning. Specificity of primers was confirmed with Primer Blast of NCBI (https://blast.ncbi.nlm.nih.gov/Blast.cgi) (Ye, Coulouris et al. 2012). Several sequences for potential HKGs and GOIs were designed and tested. If self-designed

primers failed validation after multiple attempts of optimization, respective primers were commercially designed and tested (Primerdesign Ltd).

2.6.2.4 Primer validation

An optimal PCR would accomplish a doubling of the DNA target with every cycle which would result in an efficiency of 100%. In reality however the efficiency might deviate from this value for several reasons (e.g. template quality, thermal profile, primer). It is therefore advisable to establish a standard curve of several dilutions (1:5 to 1:160, triplicates). For this purpose the cycle threshold values (Ct) were plotted against the initial template quantity. The slope (m) of the line relates to the amplification efficiency as follows:

$$y = mx + b$$
$$m = \frac{y - b}{x}$$

Y was defined as the vertical change ($\Delta y = y_2 - y_1$), *x* as the horizontal change ($\Delta x = x_2 - x_1$) and *b* as the y-intercept.

PCR efficiency in percent was defined as:

$$E = \left(10^{-\frac{1}{m}} - 1\right) * 100$$

To confirm whether the size of obtained products was consistent with the expected product size, gel electrophoresis was performed. With this technique, negatively charged DNA molecules are separated by size during migration through an agarose gel exposed to an electric field. Smaller molecules are able to move quicker through the pores of the gel and, compared with larger molecules, will travel a greater distance within a given time.

The gel cassette was loaded with 1% agarose gel containing the intercalating stain GelRed™ (Biotium). Samples were mixed with a dye (Promega) and gel pockets were loaded in duplicates. A DNA ladder (100bp; Promega) was run with the samples as a standard against which the samples could be compared. An electric potential of 70V was applied for 60min. Gels were assessed using Kodak's Gel Logic 200 Imaging System.

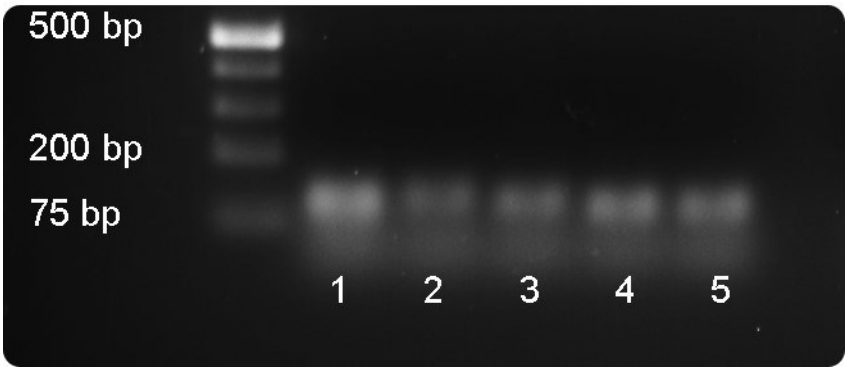

Figure 2-1: Example of gel electrophoresis

1 IFN-γ (150bp) **2** IL-6 (149bp) **3** COX-1 (142bp) **4** IL-1β (126bp) **5** TNF-α (124bp)

Product sizes of the final oligonucleotides were consistent with expected product sizes (shown in brackets).

2.6.3 Data processing

Data were processed with an adapted 2-ΔΔ method described by Livak et al. (Livak and Schmittgen 2001). As a first step the arithmetic mean of measured Ct values was calculated for each GOI and both HKGs. Ultimately, the geometrical mean for the HKGs was determined. The averaged Ct values were used to calculate ΔCt for a pre-defined experimental group ($\Delta Ct_{experimental}$) and its control ($\Delta Ct_{control}$).

$$\Delta Ct = \sqrt[2]{(\overline{Ct_{HKG1}}) * (\overline{Ct_{HKG2}})} - \overline{Ct_{GOI}}$$

From these values, ΔΔCt could be worked out.

$$\Delta\Delta Ct = \Delta Ct_{experimental} - \Delta Ct_{control}$$

A positive ΔΔCt value indicates a greater GOI expression, relative to the control samples; whereas, a negative ΔΔCt value indicates a lower GOI expression, relative to the control samples.

Ultimately ΔΔCt could be used to determine the fold change, which indicates the magnitude of GOI expression (greater or lesser) relative to the HKG.

$$Upregulation: fold\ change = log2(\Delta\Delta Ct)$$

$$Downregulation: fold\ change = \frac{1}{log2(\Delta\Delta Ct)}$$

Chapter 3 Design of a porcine ILP model to study short term events and interventions in the context of arthritis

3.1 Abstract

Arthritis is a disease associated with great morbidity, affecting the quality of life of human and veterinary patients alike. Therapeutic advances are aided by the use of *in vivo* rodent models; however, their translational value for human disease has been questioned. Therefore, alternative models using large animals have come to the forefront of translational research; yet, despite the potentially greater translational validity of experimental observations derived from such models, they understandably invoke a greater degree of ethical concern and debate. Isolated limb perfusion (ILP), a technique in which appendices are separated from the body's blood circulation but maintained under physiologic conditions using an extracorporeal circuit, is well established in transplantation surgery and selected research applications. Extending this principle to the use of porcine cadaver limbs to maintain joint viability offers a potentially unique means by which short-term events and interventions, as they relate to acute inflammation and arthritis, can be studied in a relatively physiological environment. This novel approach promises to facilitate translation of pre-clinical research into a more relevant arena prior to the initiation of live animal research, thereby addressing some of the common concerns associated with *in vitro* studies. Preliminary results on the use of ILP as a basis for a large animal whole organ joint model are presented in this chapter.

3.2 Introduction

Arthritis is a disease affecting veterinary patients and humans alike. It has a marked effect on the quality of life of approximately ten million people in the UK alone (www.nhs.uk). In the equine patient it is the principal acquired disorder leading to loss of performance (Goodrich and Nixon 2006).

To treat the disease, or at least alleviate the associated symptoms, the use of anti-inflammatory drugs is indicated. These can be delivered either locally via intra-articular injection or systemically via the blood stream. In light of the compartmentalised structure of the joint, it is of both interest and therapeutic relevance to advance our understanding of the mechanisms of cellular migration and drug pharmacokinetics within this unique environment. A whole organ joint model with functional blood supply mimics both the compartmentalised nature of this structure and its interface with the circulatory system. Such a model offers a significant opportunity to study new drugs and delivery systems without the requirement for live animal experiments. Isolated limb perfusion (ILP) is a technique that features both properties; namely, an intact 3D structure and a functional blood supply. Extracorporeal perfusion of organs has been successfully used for decades to address various research questions in the fields of (patho)physiology, pharmacology, organ preservation and transplantation surgery. In the presented work the principle was expanded to the use of isolated perfused porcine distal limbs to model short term events and interventions in the context of arthritis. Due to their physiological and anatomical similarities to humans, pigs are considered a suitable model for translational research which has applicability to humans (Kobayashi, Hishikawa et al. 2012). Pigs are also of a sufficient size to serve as a large animal model for research directed to the equine field; thus a porcine model would maximise the potential for cross-species translational application of data. Availability of abattoir derived specimens permitted access to healthy, fresh tissue samples without the necessity to sacrifice animal life specifically and exclusively for research purposes.

The following section summarises the preliminary work that has been conducted in order to allow a pilot study on the perfused limb.

3.3 Materials and methods

3.3.1 Perfusion set-up

The perfusion set-up (e.g. hardware, temperature, perfusate) was designed based on a thorough literature review as presented in chapter one. Most suitable approaches for the intended work were identified and combined to a novel model.
English and German articles were taken into consideration. The search engines PubMed and Google Scholar were used. Keywords were "perfusion/ perfused", "isolated" "extracorporeal", "preservation", "*ex vivo*" and "animal model". Additional materials referenced in the articles initially identified were also included where suitable. The focus was on research conducted in large animal organs (bovine, porcine, equine, ovine, and caprine).

3.3.2 Specimen

Limbs for dissection were either obtained from a licensed local abattoir or from the university's associated farm. Used specimens were waste material either from food production or licensed experiments of other research groups. For this part of the project no animals were sacrificed solely for the sake of the presented study. Pigs were female with a body weight ranging between approximately 150 to 250kg. Animals were either Landrace, Large White or hybrids of both breeds. Both hind- and front limbs were collected. Limbs were transected at the level of the tarsus (n=20) or carpus (n=1) using either large shears, a saw or a knife. Practical considerations, e.g. specimen availability and time frame, dictated the final sample size for respective groups (see Figure 3-1).

In order to be able to source specimens for perfusion experiments from the abattoir, the cut level of limbs was set to the carpal and tarsal area respectively. This avoided

any conflict between the relative availability of material for the perfusion experiments and for food production. Pigs at the local abattoir were skinned, whereby the skin was mechanically removed via tension force. To stabilise the carcass during this process, chains were wrapped around both metacarpal areas. It was not possible to harvest front limbs prior to completion of this process. One front limb and two hind limbs were transected/ amputated at the level of the mid humerus/ femur. Specimens were either stored at -20°C and thawed prior to use (for native dissections only) or used immediately following collection. Immediate use was always undertaken if intra-arterial infusions were planned.

Skin was removed from all specimens (for perfused specimens this happened after ILP) and anatomical dissection was focussed on the vasculature and joints. Arteries and veins were identified according to renowned veterinary anatomical textbooks (Nickel 2005). Where appropriate, the vascular network of specimens was stained via the perfusion of designated arteries using haematoxylin, eosin or India ink, thus permitting better visualisation of small vessels. For arterial cannulation, winged and pencil style catheters (Venocan™) of different sizes were tested. To secure the catheter in the artery during perfusion, the use of a Chinese Finger Trap suture was compared to the use of tissue adhesive (3M Vetbond™). To determine the most suitable joint for subsequent intra-articular injections, the main metcarpophalangeal joints (MTPIII or MTPIV joint) and the auxiliary joints (MTPII or MTPV) were injected with dye to assess whether joint injection had been successful.

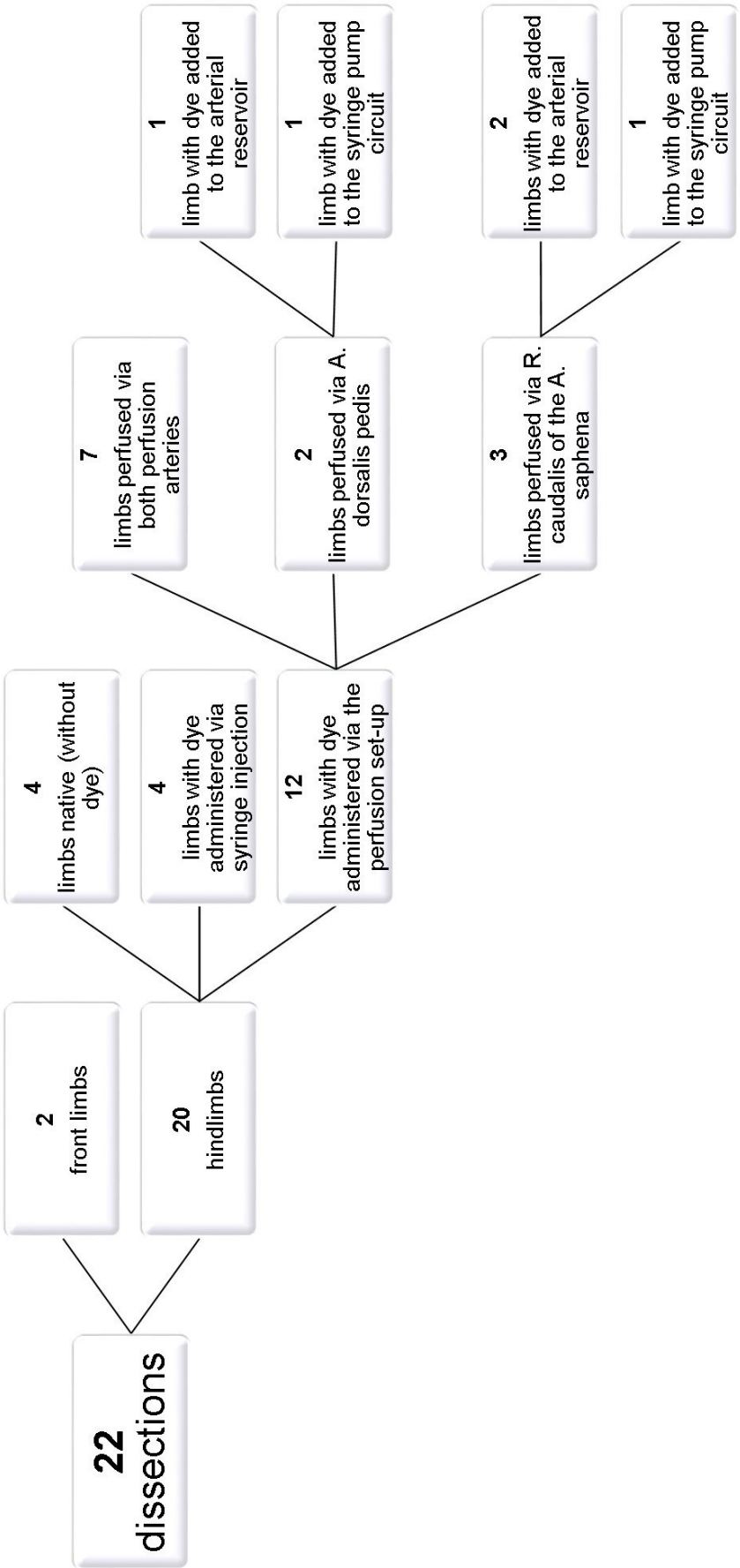
22
dissections
2
front limbs
20
hindlimbs
4
limbs native (without dye)
4
limbs with dye administered via syringe injection
12
limbs with dye administered via the perfusion set-up
7
limbs perfused via both perfusion arteries
2
limbs perfused via A. dorsalis pedis
3
limbs perfused via R. caudalis of the A. saphena
1
limb with dye added to the arterial reservoir
1
limb with dye added to the syringe pump circuit
2
limbs with dye added to the arterial reservoir
1
limb with dye added to the syringe pump circuit

Figure 3-1: Flowchart of dissected limbs

A total of 22 limbs was dissected. Amongst other reasons the front limb was ruled out due to its complex arterial branching. Four native (unstained) dissections of hind limbs revealed the caudal ramus of the *A. saphena* and the *A. dorsalis pedis* as best suited for perfusion experiments. This was confirmed by an even distribution of dye, injected into both arteries, within the vessels (n=4). Findings were further substantiated by dissection of twelve limbs perfused with dye solution, which also showed the functionality of the perfusion set-up. The connection between the dorsal and plantar arterial systems became evident after perfusion via just one of the designated perfusion arteries, which still resulted in an evenly stained vasculature (n=2 and 3 respectively). This was the case for dye added to the arterial reservoir as well as added to the syringe pump circuit. Confirmation that additives added to the syringe pump system reached all vessels in the limb was of particular importance in the context of the planned neutrophil experiments (see Chapter 5).

3.4 Results

3.4.1 Perfusion set-up

Based on the above targeted literature review, the following model was developed.
With regard to donor selection it was decided to predominantly utilise abattoir derived porcine limbs. In addition, through close working relationships with other research groups of the university, specimens were also obtained from their experimental animals. These limbs were harvested as by-products following euthanasia in terminal research experiments. Finally, due to unforeseen circumstances in relation to the final experiments, it was deemed necessary to sacrifice twelve animals specifically for the presented work. This was approved by the university's Veterinary Ethical Review Committee.

After collection of the limbs, respective perfusion arteries were cannulated immediately and flushed with heparinised (20.000U/L), ice cold preservation solution (adapted Tyrode solution) to arrest warm ischemia (Patan, Budras et al. 2009). Specimens were subsequently placed on ice and transported to the laboratory (median time 100min, n=43, (VanGiesen, Seaber et al. 1983), where they were connected to

the perfusion system without delay. The flow rate and temperature of the perfusate were then gradually increased over a period of 30min to allow for a slow equilibration period.

Perfusate was administered at physiologic body temperature of pigs (39°C) (Biggar, Bohn et al. 1984). With regard to warming the perfusate to body temperature, preliminary experiments yielded better results when the arterial reservoir was placed within a thermostatically controlled water bath (Thermostatic water bath, WBS 4, 4,5L, LabScientific Inc). It also became evident during preliminary experiments that a combination of the temperature differential between the perfusate reservoir and room temperature and the variability in room temperature necessitated insulation of the tubing. Therefore the tubing was sheathed with a double foil faced bubble membrane tape (Spiral Pipe Wrap, ThermaWrap). The temperature of the perfusate was measured at the level immediately prior to connection to the limb. To achieve a physiologically appropriate perfusate temperature at this point of the circuit, it was necessary to maintain the arterial reservoir at 59ºC to compensate for cooling of the fluid during its flow throughout the circuit.

The system was designed as an open circuit with the perfusate supplied by the arterial reservoir passing through the circuit once. The majority of venous return was discarded; however, an aliquot was sampled hourly while dripping freely from the cut surface of the limb. This permitted a regular and temporal viability assessment of the perfused limb. Potassium concentration, and glucose and oxygen consumption were also measured. The arterial perfusate reservoir was contained within a glass double neck flask (Rotilabo®-double neck round bottom flask, 1L, ACE6.1, Carl Roth) in combination with a Drechsel head with sintered glass filter (Drechsel-head (NS29), KX53.1, Carl Roth) serving as an oxygenation system. A gas bottle containing a mix of 95% O_2 and 5% CO_2 (BOC, Linde Group, BJ industries) was connected to the Drechsel head. The chosen perfusate was adapted Tyrode solution (aTS) (Friebe, Stahl et al. 2001) (10mmol/L D(+)-$C_6H_{12}O_6$ x 1H_2O, 136.8mmol/L NaCl, 5.4mmol/L KCl, 1.8mmol/L $CaCl_2$ x 2H20, 1.05mmol/L $MgCl_2$ x 6H_2O, 0.416mmol/L NaH_2PO_4 x

$2H_2O$, 11.9mmol/L $NaHCO_3$) with double glucose (10mmol/L) and mannitol (20mmol/L). Potassium levels were adjusted to approximate the concentration in porcine blood. Glucose levels were increased to match levels used in previous experiments by the group.

A peristaltic pump (Masterflex L/S digital drive, 100 RPM, 115/230 VAC, Cole Parmer) (Patan, Budras et al. 2009) was used to propel the perfusate through the system (final flow rate: 5mL/min per tube) via Masterflex BioPharm platinum-cured silicone pump tubing (L/S 14, Cole Parmer), the inner diameter of which was chosen to reflect the diameter of the blood vessel used for perfusion (*A. dorsalis pedis*, *R. caudalis* of the *A. saphena*). This represents a flow controlled circuit. The flow rate was adjusted to achieve approximately half of the physiological blood pressure (Constantinescu, Knall et al. 2011). An intra-arterial pressure monitoring system (Datascope 2000®), connected to the system via a 3-way-tap, was incorporated to provide perfusion pressure data (Patan, Budras et al. 2009) in later experiments. A syringe pump (IVAC® P6000 Mk II, Alaris® Medical Systems) was used to introduce isolated autologous neutrophils into the system. The pump was connected via a 3-way-tap (flow rate: 10mL/h).

To assess the level of oedema formation, scales (UltraShip 55 lb. Digital Postal Shipping & Kitchen Scale, Amazon) were incorporated into the perfusion system (Patan, Budras et al. 2009). Venous return was collected hourly for subsequent measurements of LDH. Tissue samples for analysis of viability and inflammation were collected immediately following termination of the perfusion.

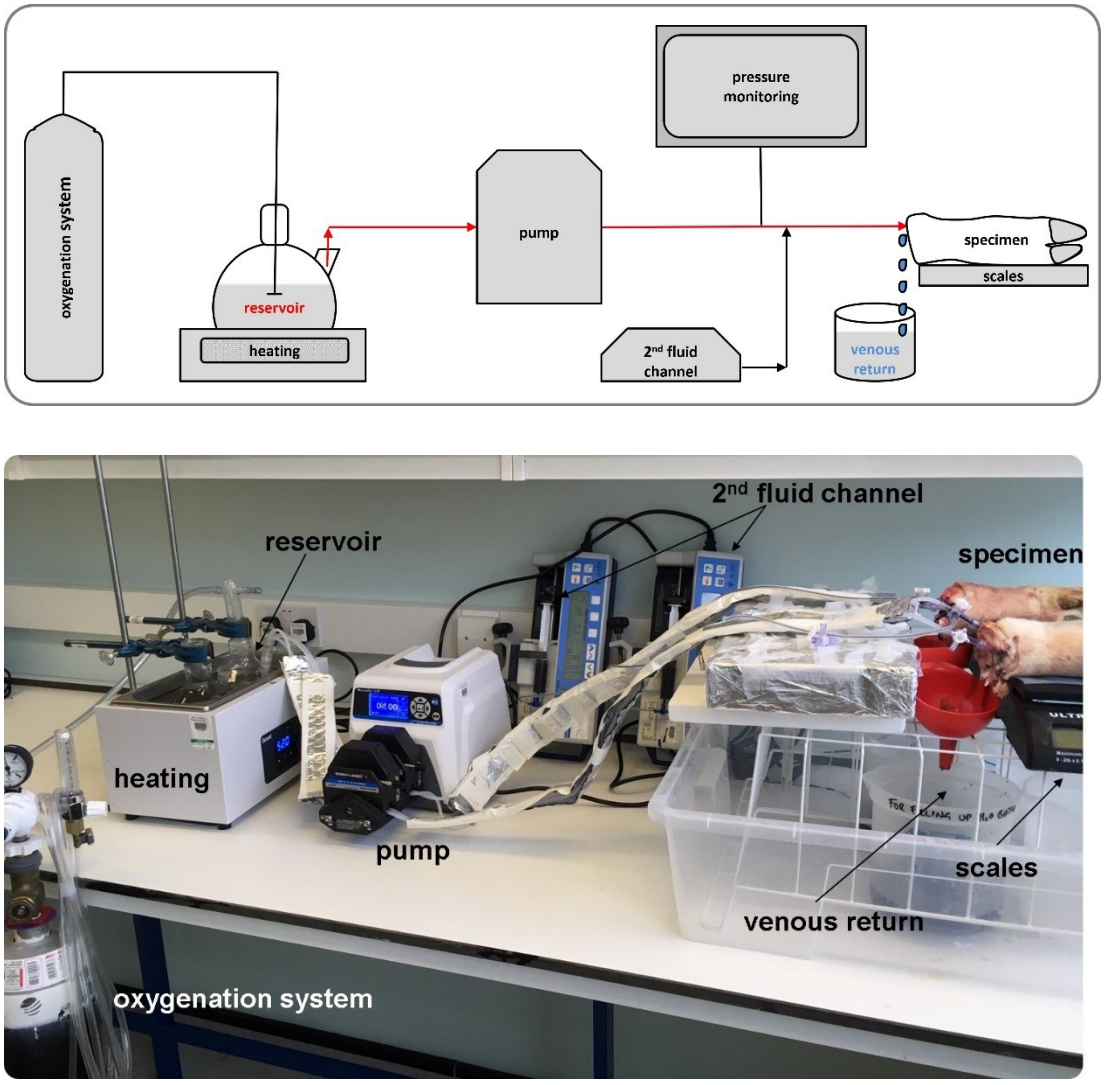

Figure 3-2: Set-up ILP system

An oxygen cylinder was connected to a gas wash bottle according to Drechsel and oxygenates the arterial reservoir via a sintered glass filter. The perfusate was heated by a water bath. A peristaltic pump propelled (red arrows) the oxygenated perfusate through the main arteries and capillary network of the porcine limb. The venous return (blue drops) dripped freely into a beaker and was sampled at this point. Throughout the experiment the specimen rested on scales to permit the assessment of weight gain. An intra-arterial pressure monitoring system was connected to the circuit to inform on continuous perfusion pressures. A second controlled fluid channel was formed by a syringe pump to facilitate the subsequent introduction of isolated autologous neutrophils in later cell migration experiments. Schematic illustration adapted from: "Extracorporeal perfusion of isolated organs of large animals – review of the research method bridging the gap between in vitro and in vivo studies" CR Daniel, R Labens, D Argyle, TF Licka, ALTEX-Alternatives to animal experimentation 35(1): 77-98

3.4.2 Specimen

Inspection of the forelimbs revealed callus formation in the carpal area, considered to reflect repeated external pressure on this anatomical site. Dissection of front limbs revealed a relatively complex vascular pattern at the level of the carpus that would have necessitated cannulation and/or ligation of numerous vessels (see Figure 3-1). Overall, upon consideration of the notable tension force on the forelimb, the abnormal condition of the skin close to the area of interest and the extensive branching of the vasculature, it was concluded that the forelimb was unsuitable for the planned perfusion experiments.

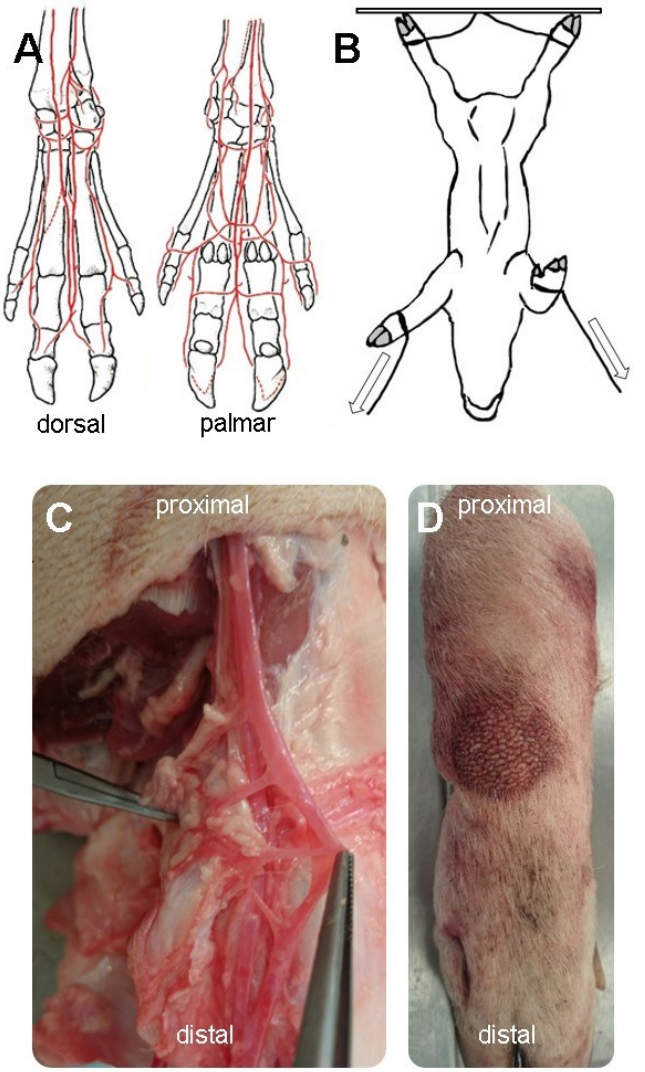

Figure 3-3: Drawbacks front limb

Vasculature in the front limb is more complex compared to the hind limb (**A**). In particular, at the level of the carpus (the intended site of limb transection), there are numerous arteries that would necessitate extensive cannulation and/or ligation, thus rendering the use of front limbs for perfusion impractical. Dissection confirmed the complex branching at this level (**C**). Additionally, callus formation was present at carpi in dissected specimens (**D**). Due to technical requirements at the abattoir, front limbs could only be collected after the carcass had been skinned (**B**), which necessitated the application of marked tension forces (arrows) to the front limb via chains secured around the pastern area. This was considered to have a potential, yet unpredictable effect on joint integrity.

Picture A adapted from “Lehrbuch der Anatomie der Haussäugetiere, Band 3, Kreislaufsystem, Haut und Hautorgane”, Nickel, Schummer, Seiferle, 4th edition, Parey Verlag, 2005, Stuttgart, p. 100/101 (Nickel 2005)

At the cut surface of the hind limb, two major arteries could be identified. Dorsally, the *A. dorsalis pedis* and on the plantar aspect of the limb, the caudal branch of the saphenous artery (*R. caudalis* of the *A. saphena*). Minor branches of the *Arcus plantaris profundus* could not be identified in the native specimen and were therefore considered unsuitable for cannulation. After injection of dye (H&E) into the main arteries, connecting branches between the dorsal and plantar system were identified and matched to relevant textbooks. A decision was made to use the *A. dorsalis pedis* and the *R. caudalis* of the *A. saphena* as designated perfusion arteries without ligating additional vessels; this was based on both a robust connection between the dorsal and plantar vascular systems and an even and complete staining of the vasculature of the whole distal limb without injecting or cannulating minor branches of the *Arcus profundus* (Figure 3-4; Figure 3-5; Figure 3-6). Indwelling pencil-style catheters (20G, Venocan™ Pencilstyle IV Catheter) proved best suited for cannulation of designated perfusion arteries. The use of tissue adhesive proved most effective in securing the catheter within the vessel during both transportation and experimentation.

Intra-articular injection of the MTPIII and IV joints was technically challenging; however, both auxiliary joints could be successfully injected with dye in all cases.

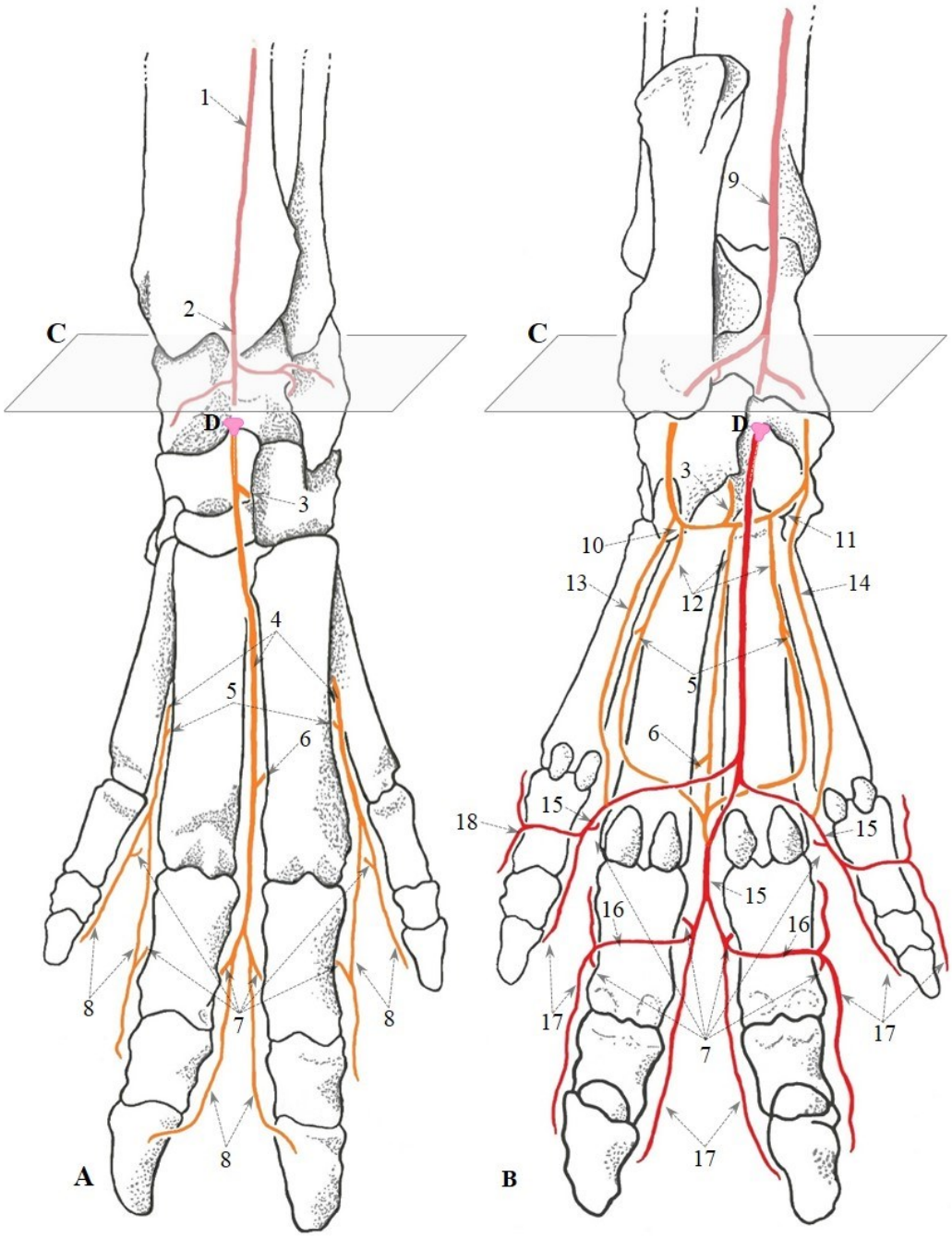
1
2
C
D
3
4
5
6
8
7
8
8
A
9
C
D
3
10
11
13
12
14
5
6
18
15
15
15
16
16
17
17
7
17
B

Figure 3-4: Arteries of the left distal porcine hindlimb

A dorsal view **B** plantar view **C** level of cut surface **D** site of catheter placement

Orange: arteries mainly supplied by the dorsal system during perfusion

Red: arteries mainly supplied by the plantar system during perfusion

1 *A. tibialis cranialis* ***2*** *A. dorsalis pedis* ***3*** *A. tarsea perforans distalis* ***4*** *Aa. metatarseae dorsales II-IV* ***5*** *Rr. perforantes proximales II* and *IV* ***6*** *R. perforans distalis III* ***7*** *Rr. dorsales phalangium proximalium* ***8*** *Aa. digitales dorsales propriae* ***9*** *R. caudalis* of the *A. saphena* ***10*** *R. profundus* of the *A. plantaris lateralis* ***11*** *R. profundus* of the *A. plantaris medialis* ***10+11*** *Arcus plantaris profundus* ***12*** *Aa. metatarseae plantares II-IV* ***13*** *R. superficialis* of the *A. plantaris lateralis* ***14*** *R. superficialis* of the *A. plantaris medialis* ***15*** *Aa. digitales plantares communes II-IV* ***16*** *Rr. plantares phalangium proximalium* ***17*** *Aa. digitales plantares propriae* ***18*** *A. digitalis plantaris V abaxialis*

Adapted from “Lehrbuch der Anatomie der Haussäugetiere, Band 3, Kreislaufsystem, Haut und Hautorgane”, Nickel, Schummer, Seiferle, 4th edition, Parey Verlag, 2005, Stuttgart, p. 158/159(Nickel 2005)

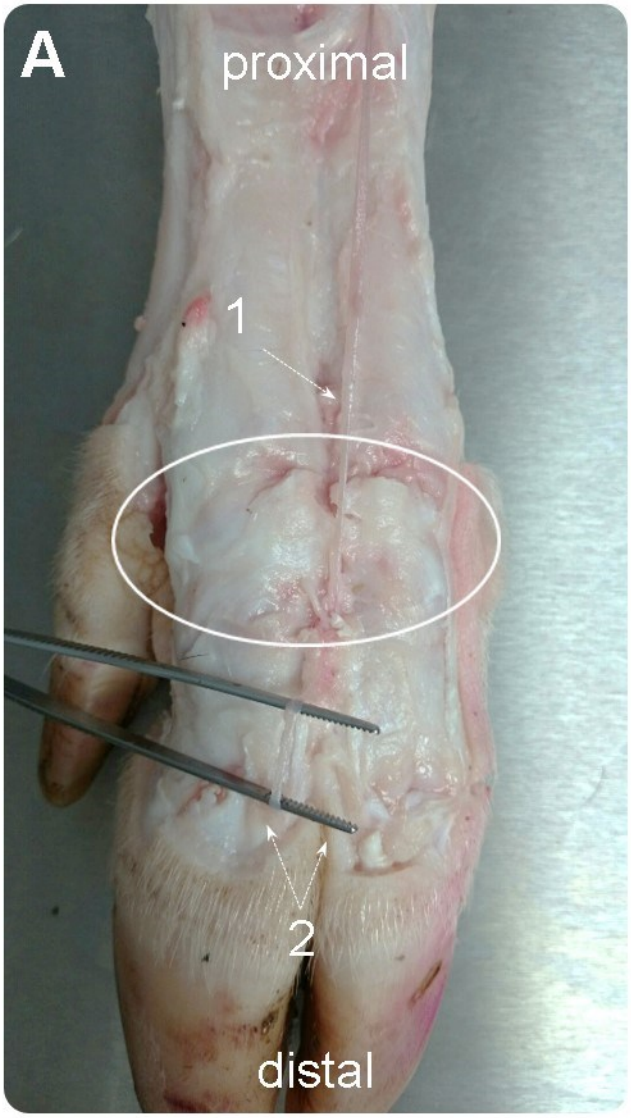
A
proximal
1
2
distal

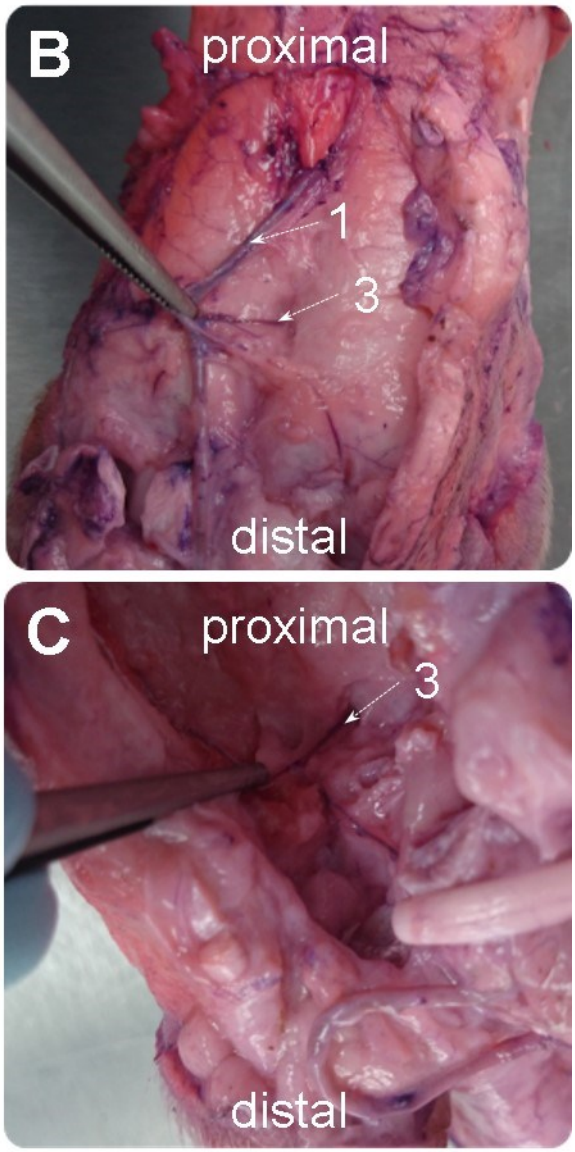

Figure 3-5: Dissection arteries with focus on *R. perforans distalis III*

A Dorsal view **B** Dorsal view **C** Plantar view

B and **C** are close-ups of the circled area in view **A**.

1 *A. dorsalis pedis* **2** *Aa. digitales dorsales propriae* **3** *R. perforans distalis III*

Dissection of the dorsal arteries in an undyed limb (**A**). The close-ups are showing a connecting branch (**3**) between the dorsal (**B**) and plantar (**C**) system. For better visibility of the arteries during dissection the dedicated perfusion arteries have been injected with eosin/ haematoxylin diluted in water.

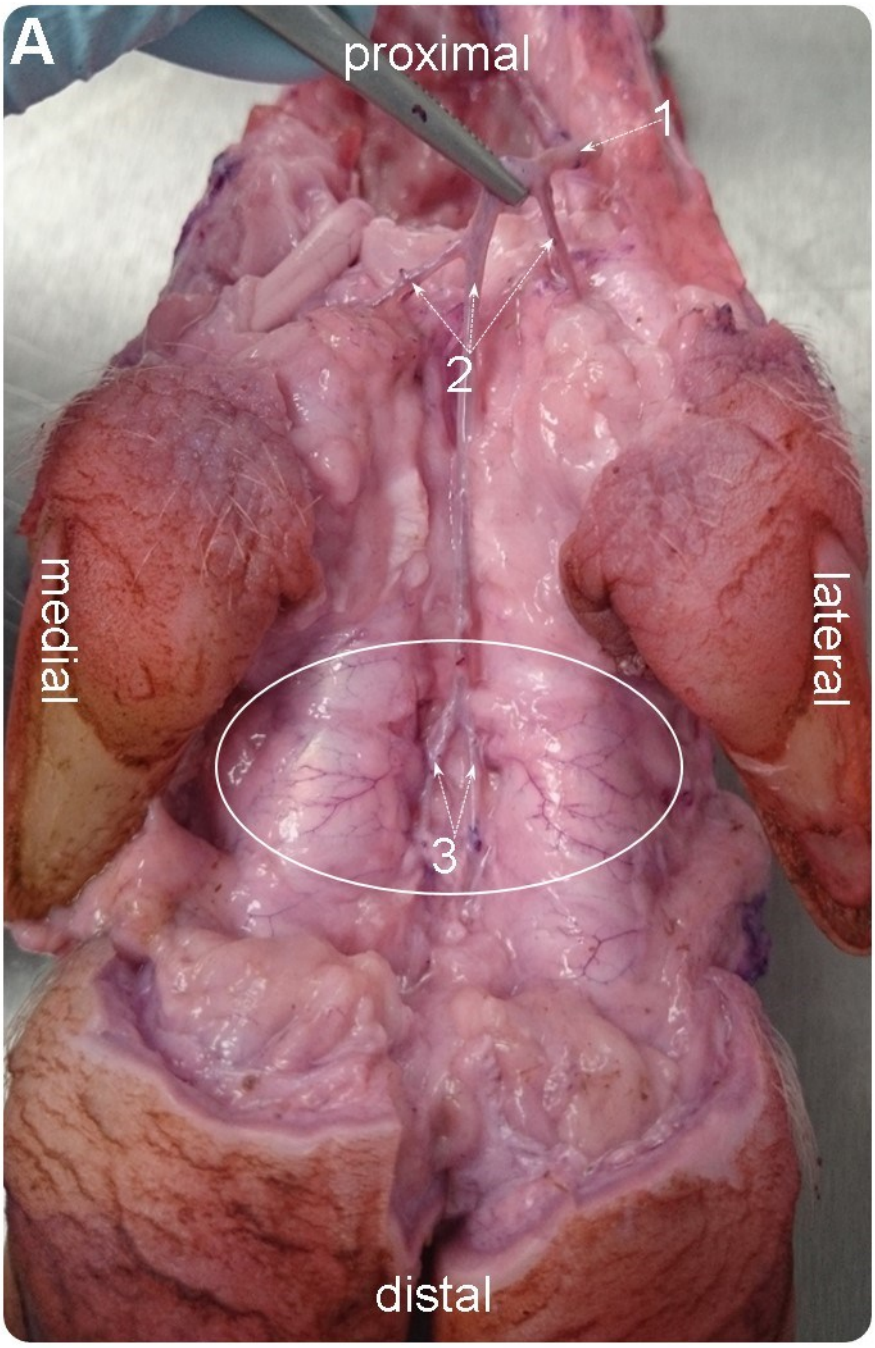
A
proximal
1
2
medial
lateral
3
distal

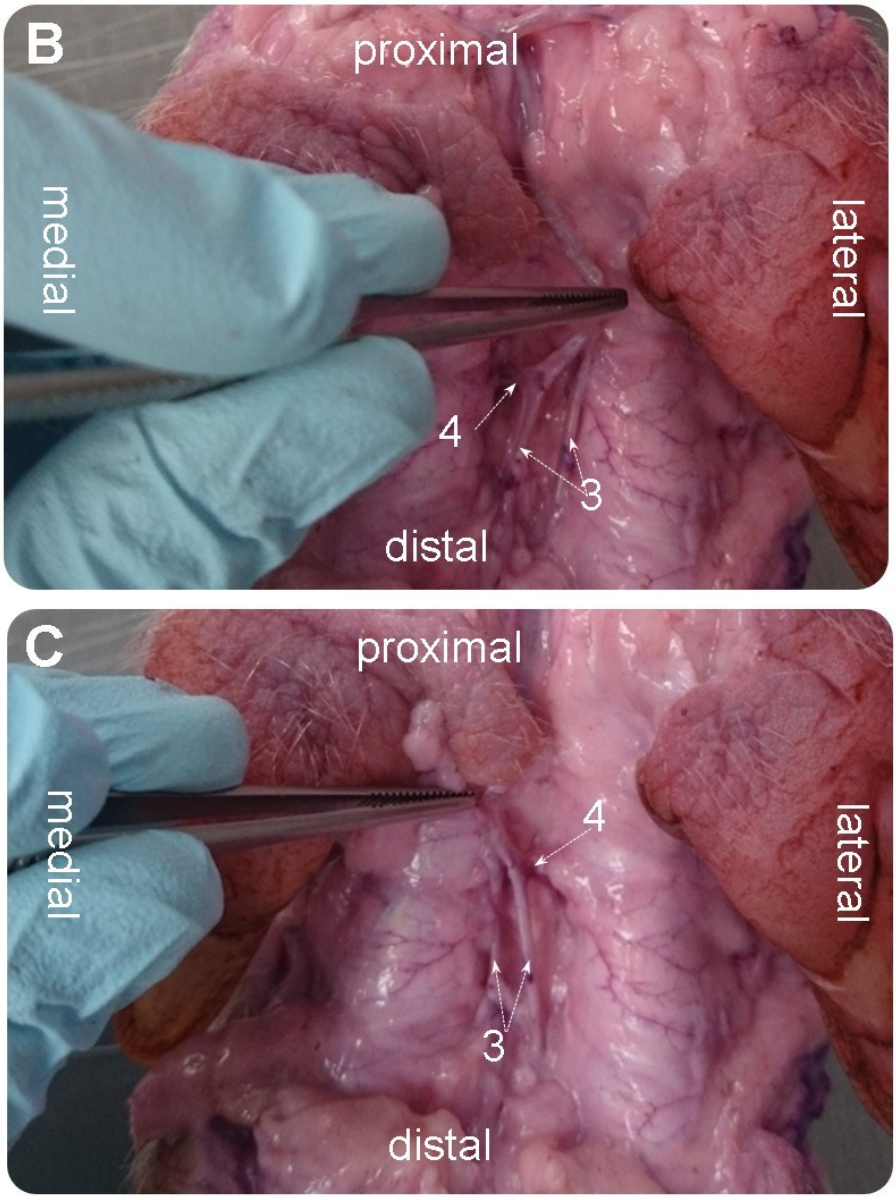

Figure 3-6: Dissection arteries with focus on *Rr. dorsales phalangium proximalium*

A, B, C Plantar views

B and **C** are close-ups of the circled area in view **A**.

1 *R. caudalis* of the *A. saphena* **2** *Aa. digitales plantares* communes II-IV **3** *Aa. digitales plantares* **4** *Rr. dorsales phalangium proximalium*

Dissection of the plantar arteries (**A**). The close-ups are showing connective branches (**4**) between the dorsal (**B**) and plantar (**C**) system. For better visibility of the arteries during dissection, the dedicated perfusion arteries have been injected with eosin/ haematoxylin diluted in water.

To further support data obtained from dissection of the dye injected limbs, dye was added to the perfusate of twelve perfused limbs and dissections were subsequently performed. The colourant was evenly distributed in the vasculature, including the capillary bed and could also be seen in joint related tissues (see Figure 3-7).

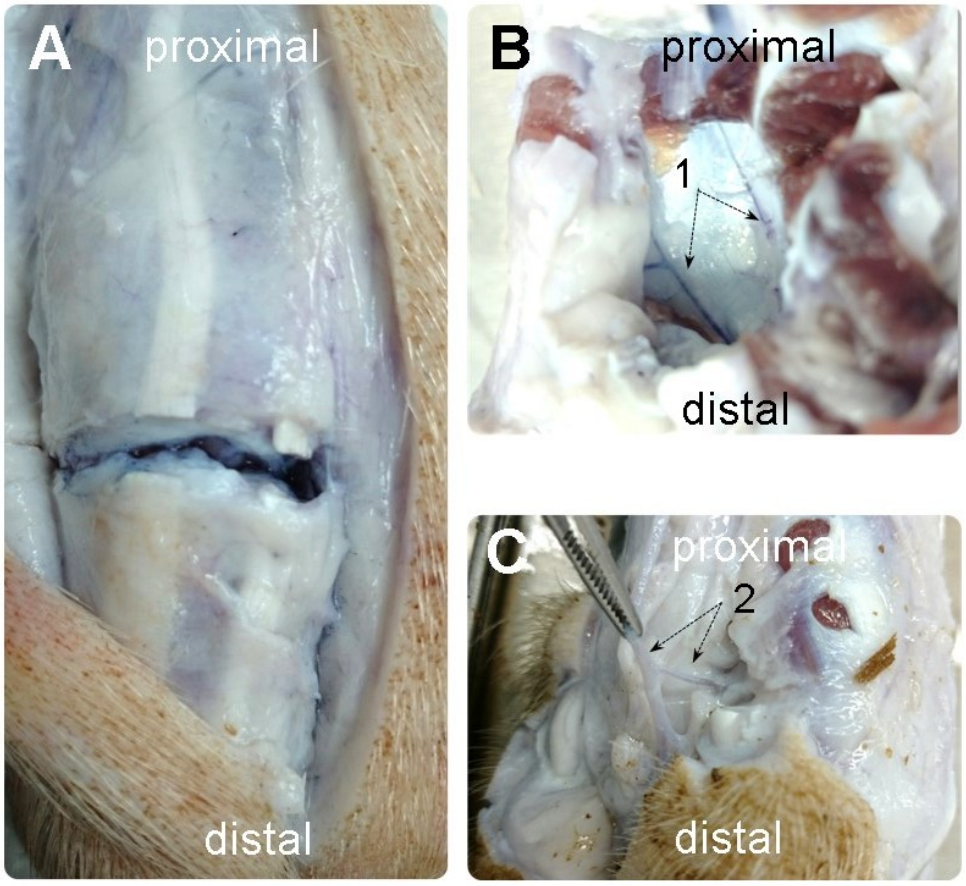

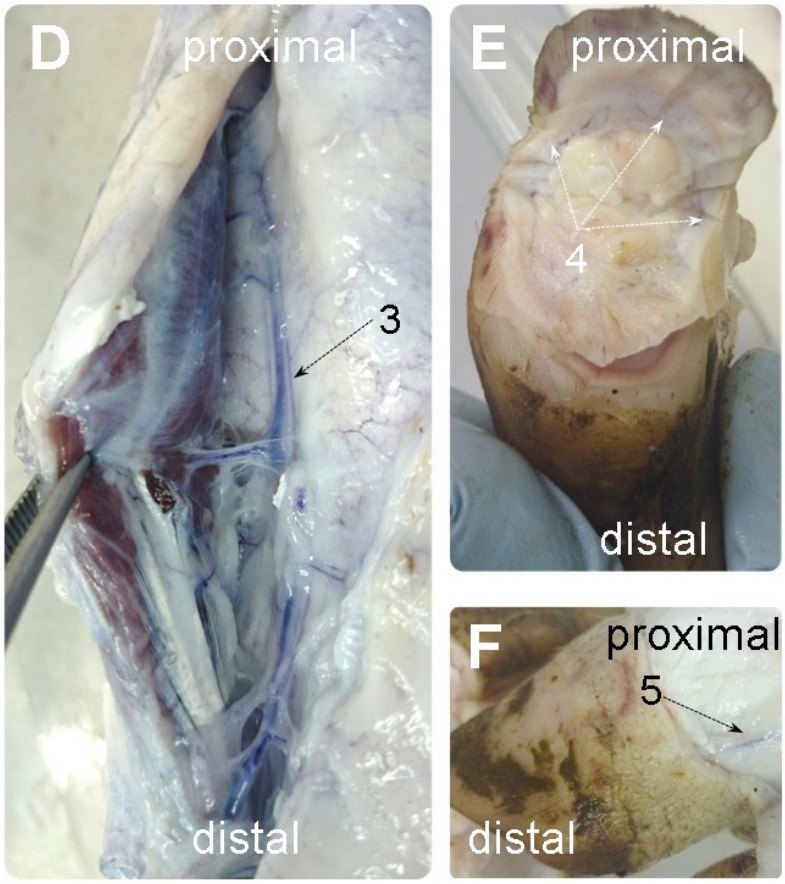

Figure 3-7: Perfusion with dyed solution

A Dorsal view **B** Plantar view **C** Plantar view **D** Dorsal view **E** Proximodistal view **F** Lateral view

1 *Arcus plantaris profundus* **2** *A. digitalis plantaris* and its *R. dorsalis phalangium proximalium* **3** *A. dorsalis pedis* **4 + 5** Small collateral vessels

After perfusion with a dyed solution the colourant could be detected in joint tissues (**A**). Important connections between the dorsal and the plantar system (**1 + 2**) were dyed as well as the dedicated dorsal perfusion artery (**3**). In addition to that, the solution reached the most distal parts of the limb (**4** and **5**), indicating a functional perfusate supply during perfusion. Limbs were perfused with Tyrode solution enriched with Haematoxylin for various time periods.

An adequate supply of perfusion fluid to the joint could also be observed during dissection of an additional limb perfused without dye. Residual blood visibly evident

throughout the tissues (including below the articular surface) prior to perfusion was completely washed out thereafter, suggesting a functional circulation (see Figure 3-8).

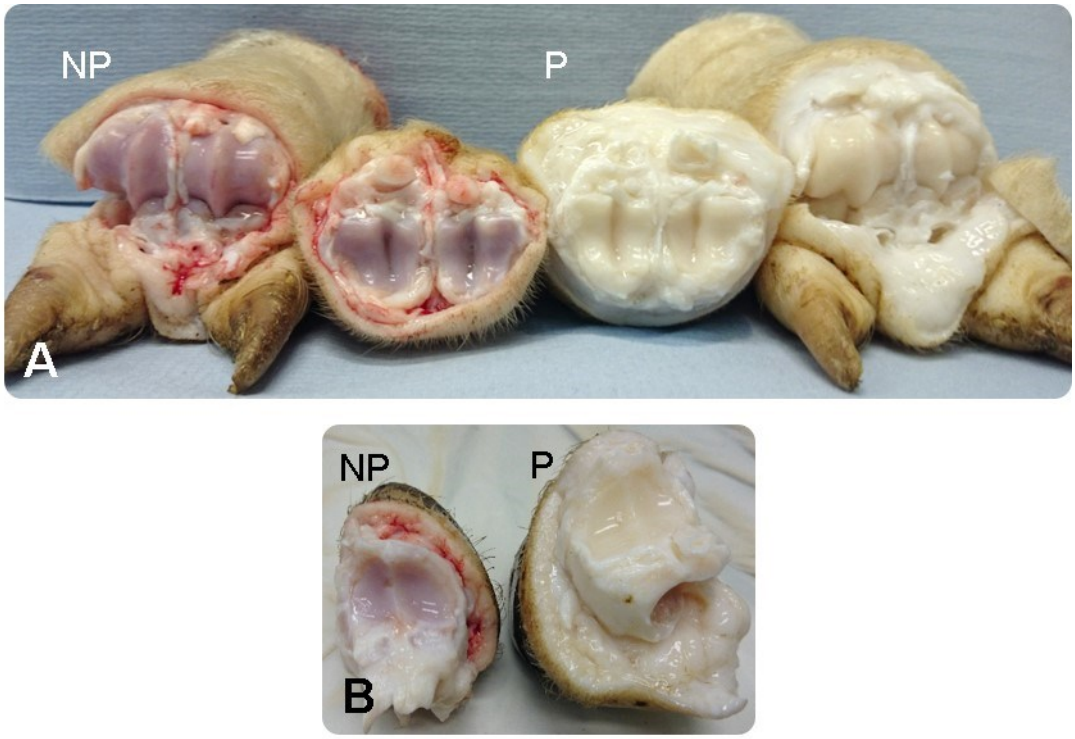

Figure 3-8: Washed out cartilage after perfusion

A MTP joint **B** DIP joint **NP** non-perfused **P** perfused
Remaining blood from the subchondral bone shimmers through the cartilage in the non-perfused leg (**NP**). After perfusion with Tyrode solution the blood was completely washed out in the perfused leg (**P**), indicating a functional perfusate supply during perfusion. This phenomenon was not only seen in the MTP joint (**A**), but also in the more distally located DIP joint (**B**). Cartilage defects were inadvertently induced by dissection.

To further confirm the presence of a connection between dorsal and plantar vessels in the porcine limb and to show that fluids administered via only one of the systems will still be evenly distributed in the specimen, perfusions were performed via only one of the designated perfusion arteries. The dye was either added to the arterial reservoir Figure 3-9, Figure 3-10) or administered via the syringe pump circuit (see Figure 3-11), thus confirming the likely distribution of cells throughout the entire limb in

subsequent cell migration experiments. These experiments also confirmed the absence of any backflow from the syringe pump circuit into the arterial reservoir.

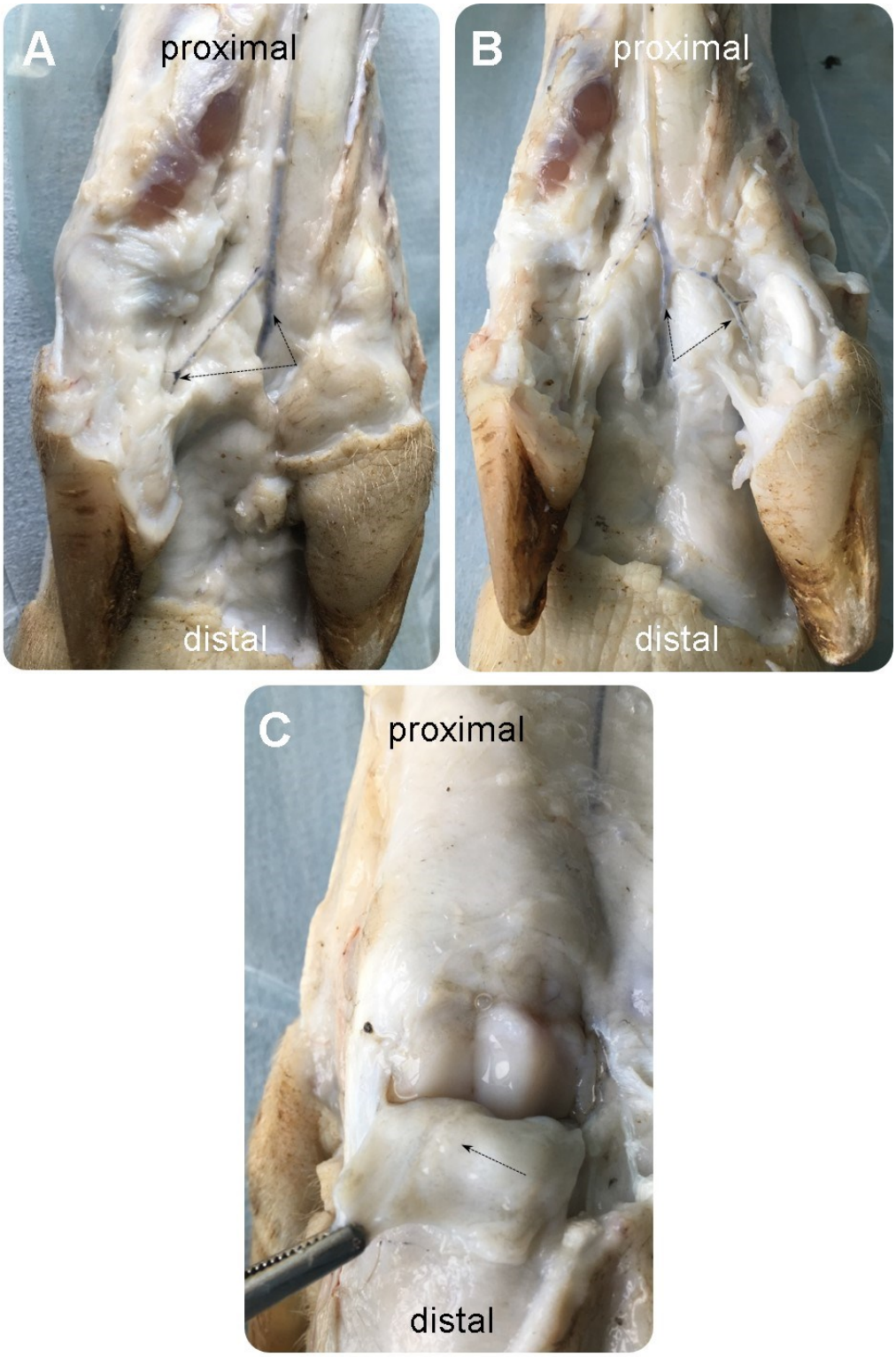

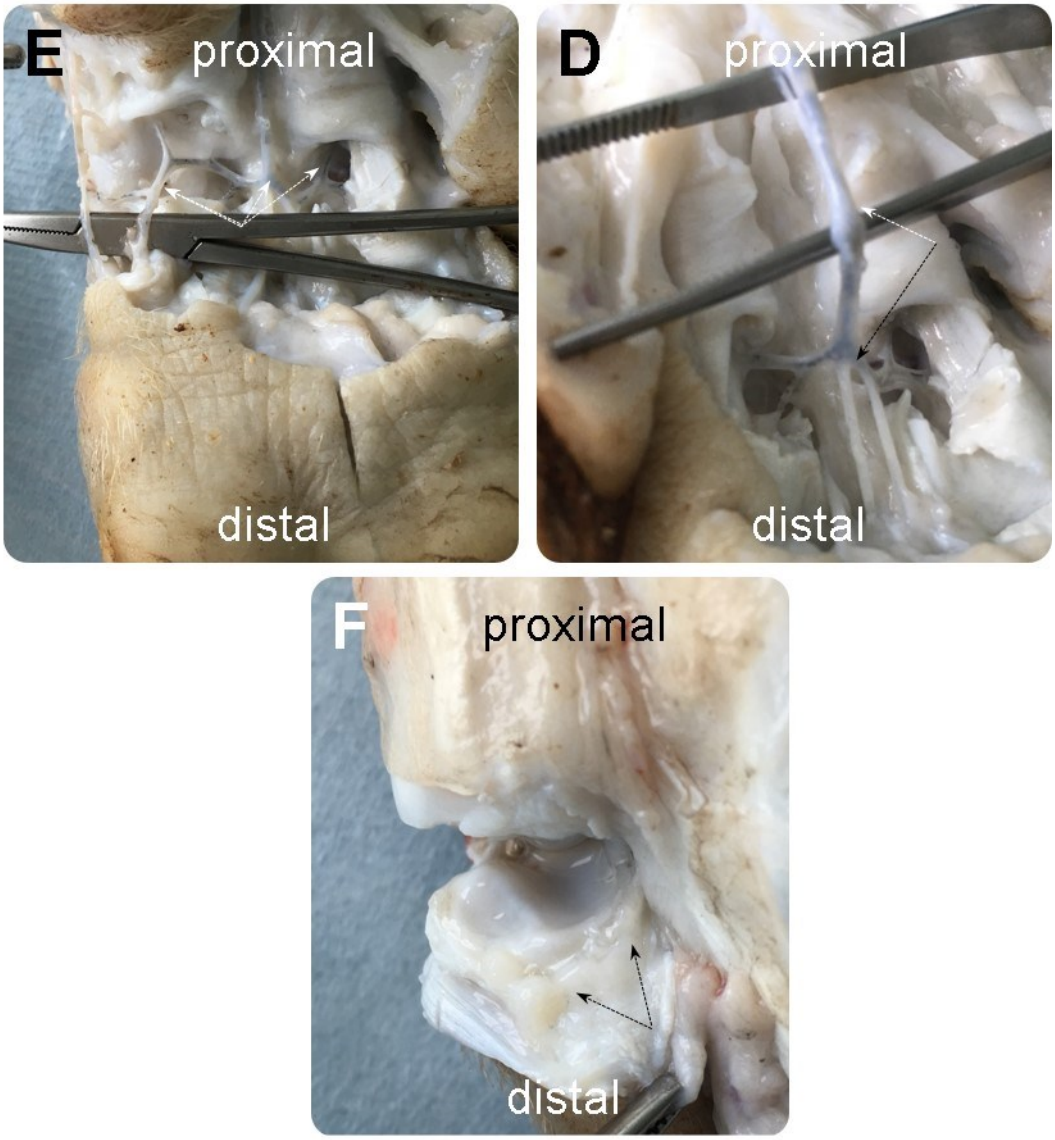

Figure 3-9: Perfusion solely via *A. dorsalis pedis*

A, **B**, **D**, and **E** Plantar views, **C** and **F** dorsal views

After perfusion with dyed Tyrode solution solely via the dorsal system (*A. dorsalis pedis*), respective arteries in the plantar system were stained as well (**A**, **B**, **D**, and **E, arrows**) indicating a functional connection between dorsal and plantar vessels. The synovium in the MTP joint (**C**) showed traces of dye (**arrow**). Slight traces could also be detected in the synovial membrane of the auxiliary joint (**F, arrows**), even though they appeared less pronounced compared to the MTP joint or following perfusion solely via the plantar system (see Figure 3-10). The limb was perfused with adapted Tyrode solution enriched with India ink for two hours.


A
proximal
distal
B
proximal
distal

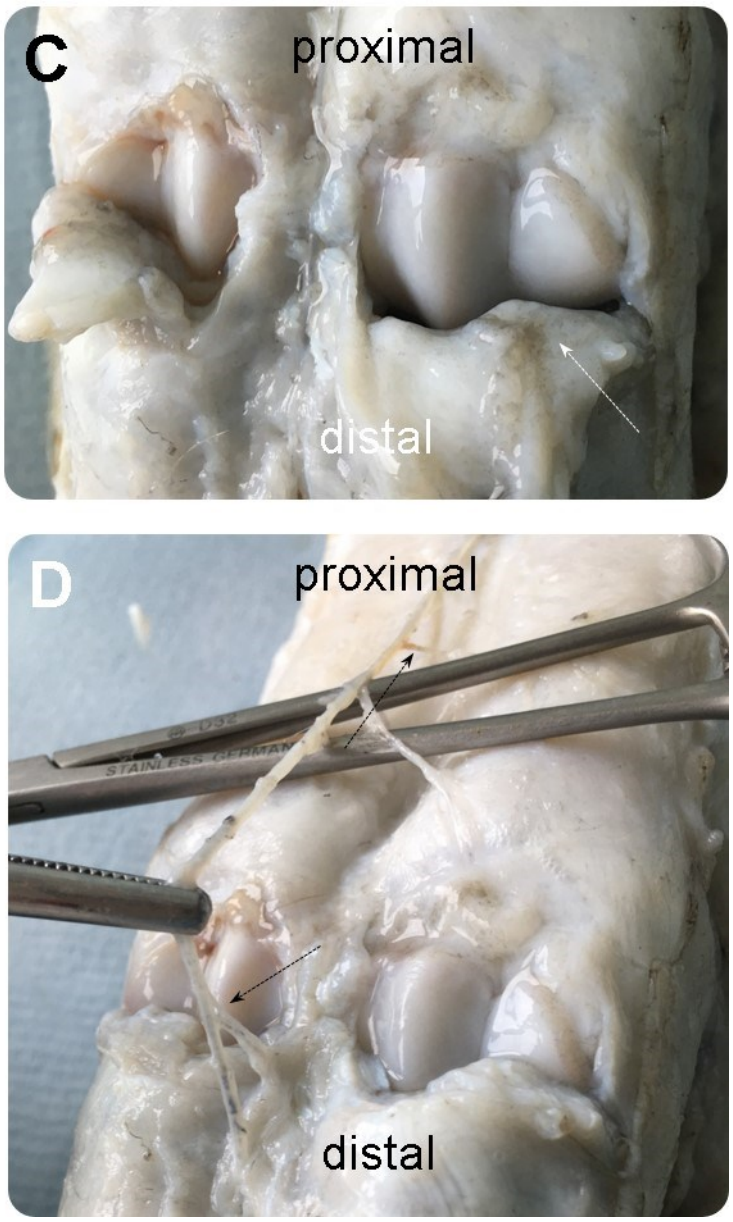

Figure 3-10: Perfusion solely via *R. caudalis* of *A. saphena*

A, B, **C**, and **D** Dorsal views

After perfusion with dyed Tyrode solution solely via the plantar system (*R. caudalis* of *A. saphena*), respective arteries in the dorsal system were stained as well (**A** and **D**, **arrows**) indicating a functional connection between dorsal and plantar vessels. The synovium in the MTP joint (**C**) showed traces of dye (**arrow**). Dye could also be detected in the synovial membrane of the auxiliary joint (**B**, **arrow**). Synovial structures appeared slightly more stained compared to perfusion solely via the dorsal system (see Figure 3-9). The limb was perfused with adapted Tyrode solution enriched with India ink for two hours.

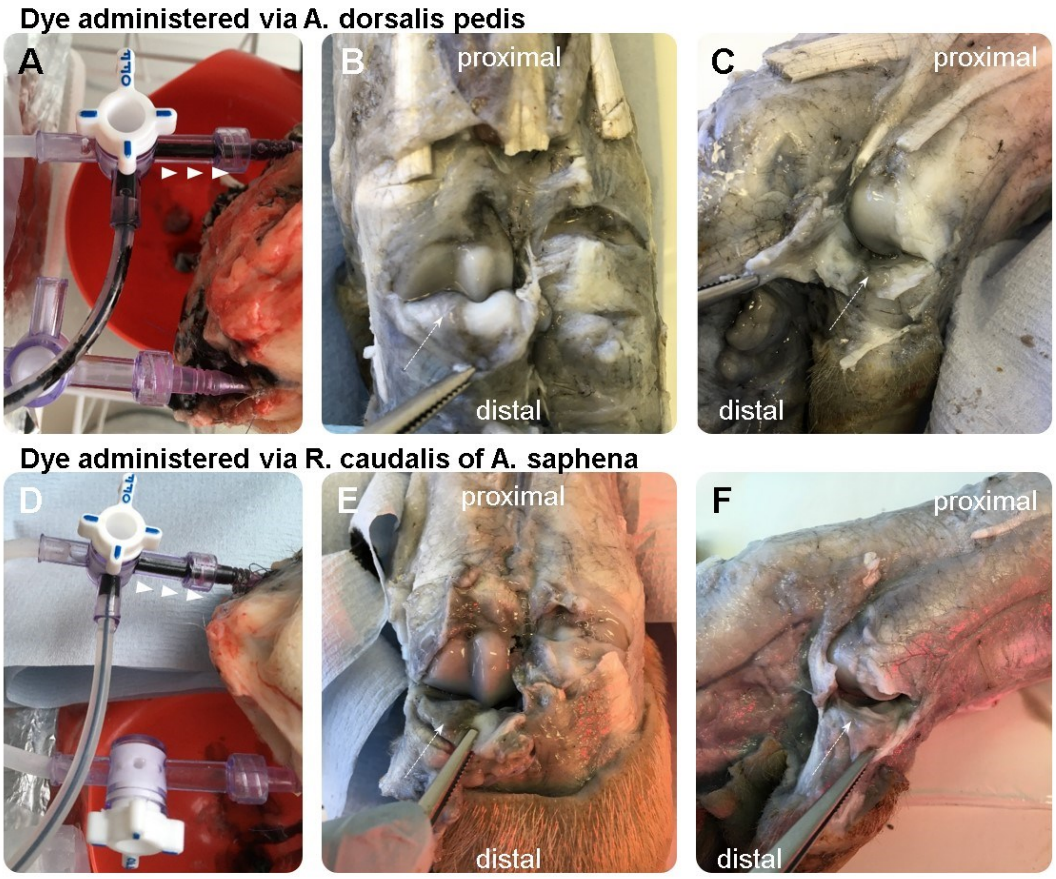

Figure 3-11: Perfusion with dye administered via syringe pump circuit

When dye was administered via the syringe pump circuit at a flow rate of ten millilitres per hour no back flow towards the reservoir could be seen, the dye mixes well with the Tyrode solution and streams into the connected artery (**arrow heads**). Dyed venous return could be detected at the cut surface of the limb (**A**) and in the red collection funnel (**A** and **D**). This was true for the use of *A. dorsalis pedis* (**A**) as well as *R. caudalis* of *A. saphena* (**D**) as dedicated arteries. Dye delivered via the dorsal system stained the synovium of the MTP joint (**B, arrow**) and the auxiliary joint (**C, arrow**) equally. When administered via the plantar system, synovial structures were also stained consistently with no obvious intra-leg difference between the MTP joint (**E, arrow**) and auxiliary joint (**F, arrow**) or inter-leg difference in comparison to pictures **B** and **C**. These results were consistent with a successful substance supply to the joint which was independent of the artery chosen for delivery. The overall staining of specimens further supported previous experimental results showing that dorsal and plantar systems are very well connected. Limbs were perfused with adapted Tyrode solution for three hours. Syringe pump circuit with India ink was connected to the system after an equilibration period of 40min with a flow rate of 10mL/h.

3.5 Discussion

Advantages and disadvantages of the perfusion set-up were discussed in chapter one.

Due to their size, the use of porcine specimens seemed ideal in the current project as they represented a model with potential direct applications to large animal research, the main area of interest to the group. Indeed, as pigs are also widely used in projects modelling human disease, the translational value of the model was potentially even further reaching. The availability of specimens, both as by-products of food production and derived from already existing research projects, added to the advantages of a porcine model and also complied with the 3R guidelines. The use of specimens derived from pigs specifically slaughtered for this project clearly does not support these ideas; however, this was only necessary due to the unforeseen cessation of pig processing by the local abattoir. Without this approach, the project could not have been completed within the available time frame.

The front limbs were considered unsuitable for perfusion for the following reasons: (a) in comparison to hind limbs, they had a more complex vascular pattern; (b) the necessary application of tension forces directly to the anatomical area of interest during carcass processing of abattoir derived material; (c) the presence of callus formation on several dissected carpi, reflecting repeated trauma to this region which could have an unpredictable effect on joint health. The level at which the limb was amputated was largely dictated by the carcass processing procedure adopted by the abattoir, as the porcine limb distal to the level of the tarsus is considered a by-product of meat production. Therefore, limiting the specimen collection to a level distal to the tarsus avoided any detrimental effect on the availability of material for food production. The use of the distal porcine limb also minimized the amount of muscle tissue in the perfused specimen, a beneficial factor considering the high susceptibility of muscle to ischemia and reperfusion injury (Blaisdell 2002, Steinau 2013). Compared to certain other large animal species (e.g. equine) the pig has well developed fleshy muscles on the distal part of the limb (*M. extensor digitalis brevis, Mm. interossei, M. flexor digit* II/ V, *M. abductor digiti* II/ V and *M. adductor digiti* II/ V); yet, the blood supply of

respective muscles was conserved during the harvesting process which enables a complete perfusion of respective tissues during ILP (Nickel 2005).

The use of *A. dorsalis pedis* and *R. caudalis* of the *A. saphena* as designated perfusion arteries allowed easy and quick access to respective arterial stumps, necessary for the timely cannulation and flushing of the harvested specimen. The clear connection between dorsal and plantar arterial vasculature (see Figure 3-5 and Figure 3-6) permitted allowances to be made for the potential under perfusion which may have resulted from a failure to cannulate branches of the *Arcus plantaris profundus*. It was therefore decided that *A. dorsalis pedis* and *R. caudalis* of the *A. saphena* were suitable for connecting the limb to the extracorporeal blood circuit, while maintaining a fully functional perfusate supply.

Joint injections were technically easier to perform on auxiliary joints; namely, those which connect the metatarsus and proximal phalanx of the second and fifth toe. It was therefore agreed to use these joints as target joints in this study. Unlike the third and fourth toes, the second and fifth toes are non-weight bearing and therefore rudimentary in the pig, a factor which may influence the relative composition of cartilage and synovium (Eggli, Hunzinker et al. 1988, Huber, Trattnig et al. 2000). Consequently, it may be necessary to adopt a degree of caution when translating ILP study data derived from these joints to fully weight bearing joints. Nevertheless, auxiliary joints are also diarthroses; consequently ILP remains a valuable tool for pharmacokinetic studies utilising these joints.

Immediately following harvesting, the specimen was flushed with an ice cold heparin-containing preservation solution (Patan, Budras et al. 2009). As with the perfusion fluid, the preservation solution should be formulated to avoid any oedema formation resulting from unbalanced oncotic pressure (Drapanas, Zemel et al. 1966). For the experiments presented here, perfusion fluid supplemented with heparin was used as a preservation solution. The cold flushing procedure does not only prevent thrombus formation but also slows down anoxic cell injury in oxygen dependent cells (De Groot

and Rauen 2007). To maintain a low metabolic rate in the limb during transport, the specimens would ideally either be submerged in the electrolyte solution or wrapped in swabs saturated with electrolyte solution and stored on ice (VanGiesen, Seaber et al. 1983). Inevitably there is a degree of bacterial colonisation of the skin of harvested limbs; this is likely to contaminate the transport fluid and subsequently the specimen. Furthermore the use of soaked swabs and fluid filled bags in preliminary experiments was shown to compromise the integrity of the tissue glue used for securing the catheter within perfusion arteries. For these reasons, despite being considered as the second best option for transport (VanGiesen, Seaber et al. 1983), storage of the specimen on ice seemed to be most appropriate in the present studies.

The presented perfusion circuit has been designed as an open, non-recirculating system. One drawback of the use of an open system is a greater requirement for perfusion fluid as it is discarded after one pass through the system. Considering the high volumes required to perfuse large animal organs for several hours (e.g. up to 6L/h for the equine distal limb (Patan, Budras et al. 2009) or up to 9L/h in the porcine limb (Mueller, Constantinescu et al. 2013)) the use of expensive perfusates or blood based solutions with limited availability are not ideally suited to such open systems. However, a re-circulating system has been shown to cause greater mechanical damage to cells in the perfusate and is associated with a greater risk of infection and waste product accumulation due to the repeated use of the perfusate (Bristol, Riviere et al. 1991, Lee, Antaki et al. 2007, Watanabe, Sakota et al. 2007). If used in a closed system, the addition of cells (e.g. neutrophils) would require a very concisely formulated perfusate to provide a suitable culture medium for added cells, as they are exposed to the perfusate over a long period of time. Commonly used basic cell free solutions (e.g. Tyrode solution) are most likely not able to fulfil the cells requirements and would therefore suddenly become unsuitable for perfusion experiments. This represents an additional challenge which is not easy to overcome. Considering the intended application of the model in these studies, the use of Tyrode solution was deemed appropriate (Friebe, Stahl et al. 2001, Bäumer, Mertens et al. 2002, Friebe,

Schumacher et al. 2013), especially as it can be prepared in the large volumes required when adopting an open system.

The recipe for Tyrode's solution was adapted to reflect the pig's plasma concentration of specific components. Oedema formation is a significant concern in perfusion experiments, despite best efforts to adapt artificial solutions to minimise this occurrence. Plasma expanders, such as purified albumin (e.g. (Riviere, Bowman et al. 1989, Brunicardi, Kleinman et al. 2001)) or plasma proteins (e.g. (Roets, Verbeke et al. 1974, Patan, Budras et al. 2009)), help to minimise oedema formation; however, their availability and cost renders them less suitable for an open perfusion system. Artificial plasma replacers like cellulose (Friebe, Stahl et al. 2001), dextran (e.g. (Cameron, Burger et al. 1972, Kietzmann, Löscher et al. 1993)) or hydroxyethyl starch (Mueller, Constantinescu et al. 2013) are also considered beneficial for oedema prevention; these polymers have been shown to impair neutrophil migration and inflammatory processes, a key consideration when using the perfusion model to study inflammation and cell (e.g. neutrophils) migration (e.g. in the context of arthritis) . (Hänsch, Karnaoukhova et al. 1996, Moore, Kaplan et al. 2001, Bae, Jin et al. 2004, Ewoldt, Anderson et al. 2004, Hernández, Galan et al. 2004, Handrigan, Burns et al. 2005, Matharu, Butler et al. 2008, Hernandez, Fuste et al. 2009). Indeed, a cell free solution was specifically adopted in the current set up to focus on the migration behaviour of one specific cell type (neutrophils) in subsequently planned experiments (see Chapter 5).

Although mannitol is a potent oncotic agent with few side effects, relatively little is known about its influence on the immune system. Recently, mannitol exposure has been shown to upregulate CD 11b expression in neutrophils after 24h; TNF-α and IL-6 were not affected (Turina, Mulhall et al. 2008). In light of the predicted time course of the planned experiments and the absence of an effect on TNF-α and IL-6, both genes of interest in subsequent studies (see Chapter 5), mannitol was incorporated as an appropriate component of the adapted Tyrode recipe for these studies. Increasing the glucose concentration of the perfusate to 10mM was also considered an additional

means of maintaining an appropriate oncotic pressure (Hicks, Hing et al. 2006). An additional benefit of a relatively high glucose level within the perfusate included the provision of an adequate neutrophilic nutrient source, as demonstrated by Ussing chamber experimental protocols (Labens, Lascelles et al. 2013).

To ensure a sufficient oxygen supply, it was decided to gas the perfusate with mixture of 95% O_2 and 5% CO_2, an approach commonly adopted in perfusion experiments. In light of the absence of oxygen carriers (e.g. haemoglobin) within the perfusate, the higher oxygen content, compared to room air, was considered appropriate; however, pure oxygen is rarely used, as its high oxygen tension may result in excessive production of free radicals (Fuller and Lee 2007). Furthermore, the buffering capacity of Tyrode solution is dependent on the presence of CO_2 and the use of O_2 alone has the potential to result in a significant reduction in pH (Mancina, Kalenski et al. 2015). The use of a gas wash bottle, according to Drechsel, with a sintered glass filter was considered a simple and cost-effective approach to achieving oxygenation of the perfusate. This or similar approaches, in which gas was bubbled into the arterial reservoir, have been successfully adopted in various research applications (Tindal 1957, Smith, van Alphen et al. 1985, Kietzmann, Löscher et al. 1993, Bäumer and Kietzmann 1999). More sophisticated methods have been described, including the use of rotating disc oxygenators (Drapanas, Zemel et al. 1966, Cameron, Burger et al. 1972) or hollow fibre oxygenators (Butler, Rees et al. 2002, Mueller, Constantinescu et al. 2013), whereby gas exchange occurs at a porous membrane. However, for the purpose of these studies the additional benefit of adopting such techniques was not considered to be justifiable, largely due to the additional costs which would have been incurred. Although experimental set ups based on blood based solutions have utilised room air as an oxygen source (Patan, Budras et al. 2009), in the absence of oxygen carriers, such a source was considered inadequate to achieve sufficient oxygen transport via the perfusate. Despite the apparent success of perfusion experiments on equine large colon in the absence of any specific oxygenation system (Polyak, Morton et al. 2008), this approach was not considered suitable for the presented model. It was concluded that the highly specialised perfusion fluid used by Polyak et al (2008) could

not be simply translated to a different tissue (i.e. porcine limb). Furthermore, the volume of fluid necessary to perfuse the porcine limb in a non-recirculating system would have exceeded the available financial budget.

In perfusion experiments, the perfusate can be administered under hypothermic or normothermic conditions. A hypothermic approach is mainly adopted in perfusion set-ups focusing on organ preservation potentially prior to re-/ transplantation (Smith, van Alphen et al. 1985, Domingo-Pech, Garriga et al. 1991, Guarrera, Polyak et al. 2004, Guarrera, Polyak et al. 2004, Constantinescu, Knall et al. 2011, Mueller, Constantinescu et al. 2013). Hypothermia decreases the metabolic demands of tissue, thus permitting lower perfusion flow rates and potentially less oedema formation due to better preserved microvasculature (Cypel, Yeung et al. 2008, Constantinescu, Knall et al. 2011) (see Chapter 1.3.4.2). During cardio pulmonary bypass surgery, low temperatures have been shown to supress inflammatory responses in the brain (Schmitt, Diestel et al. 2007), potentially due to reduced neutrophil and monocyte migration (Biggar, Bohn et al. 1984). Despite such advantages, hypothermic conditions may also increase the risk of infection, also via a hypothermia-induced reduction in neutrophil migration as well as a hypothermia-induced impairment of antioxidant defences, the latter potentially leading to an accumulation of toxic superoxides and free radicals (Fuller and Lee 2007). In light of the intended use of the model in this series of studies, it was considered highly inappropriate to adopt experimental conditions (e.g. hypothermia) which could potentially alter the inflammatory response.

Normothermic conditions were achievable via the use of a heated arterial reservoir, as previously demonstrated by our research group. Although the insulation of tubing resulted in a reduction in heat loss within the system, a significant drop in perfusate temperature was noted between the reservoir and the specimen. Although heating the arterial reservoir above physiological temperatures (59°C) accounted for the heat loss within the system, this compensatory approach is clearly only applicable to a cell free perfusate solution. In this model, the perfusate had cooled to physiological

temperatures (39°C) by the time it reached the level at which neutrophils were introduced (see Chapter 5).

Either pulsatile or constant flow can be used in ECP LA and despite early experiments failing to demonstrate any difference between constant and pulsatile flow (Pegg and Green 1976), subsequent studies have clearly evidenced the superiority of a pulsatile flow (Vang and Drapanas 1966, Finn, Naik et al. 1993, Sezai, Shiono et al. 1999). This was further supported by CPB experiments showing a better cerebral blood flow with the use of pulsatile pumps (Ündar, Masai et al. 2002). Undoubtedly true pulsatile perfusion more accurately reflects the *in vivo* situation; however, the use of roller pumps is more economical and this approach has been widely adopted in various research settings with remarkable results (e.g. (Friebe, Stahl et al. 2001, Patan, Budras et al. 2009). The use of roller pumps usually results in a flow controlled set-up in which the flow rate is adjusted to achieve a certain perfusion pressure; although recent findings suggest that pressure controlled set-ups might be better suited for organ preservation (Mancina, Kalenski et al. 2015). In relation to the current project, the well-established roller pump set-up seemed both applicable and practical.

It was considered important to weigh the limbs before and after perfusion as an indirect measure of oedema formation (Patan, Budras et al. 2009). This will be discussed in detail in Chapter 4. As part of the viability assessment, it was considered appropriate to measure perfusate pressures in all perfusion experiments (e.g. (Wagner, Nogueira et al. 2003, Patan, Budras et al. 2009, Constantinescu, Knall et al. 2011)). For this purpose, an intra-arterial monitoring system, similar to those commonly used in clinical anaesthesia, was connected to the circuit. Syringe pumps, similar to those used in a clinical setting to facilitate the controlled and constant rate administration of specific additives, were selected for use in the perfusion set-up.

3.6 Conclusion

The presented data forms the foundation for developing a cost-effective whole organ *ex vivo* joint model on the basis of ILP, a technique with a potentially high applicability to various research studies. Porcine hind limbs were obtained from the local abattoir. They were flushed with ice cold preservation solution (aTS with heparin) and stored on ice during transport to the laboratory. The model was set up as an open system utilizing oxygenated aTS as perfusate. The specimen was connected to the tubing via an indwelling catheter within the *A. dorsalis pedis* and *Ramus caudalis* of the *A. saphena*.

A peristaltic pump was used to maintain perfusate flow through the system. The heated arterial reservoir and insulated tubing allowed the perfusate to be delivered to the model at body temperature. Perfusion pressure and weight gain were assessed during the experiment.

To validate the model's functionality as a tool for pharmacokinetic studies, a pilot study focused on the assessment of the viability of the specimen was conducted as a next step.

Chapter 4 Validation of a porcine ILP model with a focus on the assessment of specimen viability

4.1 Abstract

The following chapter aims to show that isolated limb perfusion (ILP) is capable of maintaining joint viability, thus facilitating the study of the effect of new therapeutic agents on acute joint inflammation. In this context, viability data were derived from experiments conducted to evaluate the use of the isolated perfused porcine cadaver limb as a large animal whole organ joint model.

As an indicator of vascular integrity, oedema formation was assessed by the temporal increase in specimen weight. A perfusion period of six hours resulted in a median weight gain of 13.31% (n=38; Q1: 9.27; Q3: 16.2; IQR: 6.94). Over the same time course, the median perfusate pressure was at 28.0mmHg (n=141; Q1: 24.0; Q3: 32.5; IQR: 8.5). Perfusate gas analysis results were consistent with good overall tissue viability. Median oxygen uptake from a fully saturated reservoir was 7.75% during six hours of perfusion (n=178; Q1: 2.90; Q3: 11.9; IQR: 8.95) and the mean metabolic consumption of glucose was 1.44 ± 0.61mmol/L (n=178). Relatively constant median lactate (1.84mmol/L (n=180); Q1: 1.56; Q3: 2.40; IQR: 0.838) and potassium (5.20mmol/L (n=176); Q1: 5.10; Q3: 5.40; IQR: 0.3) levels further substantiate functionality of the model. To inform on joint specific viability, cartilage and synovium samples were stained for live and dead cells and analysed using multiphoton laser scanning microscopy. Synovium samples showed a median viability of 92.36% (n=29; Q1: 69.21; Q3: 97.66; IQR: 28.45) after six hours of perfusion and corresponding cartilage samples consisted of 99.34% (n=31; Q1: 96.45; Q3: 99.76; IQR: 3.31) viable cells.

4.2 Introduction

Perfusion of isolated organs and limbs can bridge the gap between *in vitro* and *in vivo* research. When attempting to use such models to their full potential, either as a precursor or substitute for live animal experiments, it is important to mimic the physiological situation as closely as possible. Such efforts are aimed at maintaining a viable specimen throughout the duration of the experiment. In the literature, different measured outputs have been used to monitor viability. In this context, viability measurements can be regarded as either those which apply to all specimens or those which are organ specific; for example, bile production (Drapanas, Zemel et al. 1966), milk synthesis (Hardwick and Linzell 1960), endocrine response (Jensen, Fahrenkrug et al. 1978) or responsiveness to an electric stimulus (Constantinescu, Knall et al. 2011). Metabolic data (e.g. oxygen uptake, glucose consumption and lactate levels) is routinely used to provide information on the general tissue viability of the specimen. Furthermore, to assess cell viability during perfusion, indicators of cell injury/ death, such as LDH activity and potassium concentration (reflecting cellular potassium efflux), have been used (Kietzmann, Löscher et al. 1993, Friebe, Stahl et al. 2001, Polyak, Morton et al. 2008, Patan, Budras et al. 2009, Constantinescu, Knall et al. 2011). The integrity of blood vessels is essential in perfusion experiments as it ensures a functional blood/perfusate supply. Generally, blood vessel integrity is assessed indirectly by the measuring the magnitude of oedema formation (Verbeke, Roets et al. 1972, Mueller, Constantinescu et al. 2013). Histologic analysis of tissues, generally following conclusion of the experiment, can also provide valuable information on tissue viability. Although retrospective, such information can help to inform the design of future experimental set-ups. Despite such temporal and retrospective measurements being applicable to a variety of tissues, the absolute values obtained are however highly tissue specific and dependent on the mass of the perfused specimen. Therefore, it is generally not considered appropriate to apply cut off values from one study to another; caution should be exercised when making any such extrapolations. The following chapter presents viability data derived from the current series of studies and makes comparisons with previously reported experiments.

4.3 Materials and methods

The data presented in the following chapters is derived from the perfusion of 59 limbs obtained from 42 individual pigs. Specimens were either obtained from a local licensed abattoir (by-products of food production; n=18), collected from animals which were sacrificed at the conclusion of other licensed terminal research projects within the university (n=12) or harvested from pigs specifically purchased and sacrificed for the current study (n=12). All animals were female and either Landrace, Large White or a hybrid of both breeds; body weights ranged from approximately 60kg to 250kg. It was not possible to obtain body weight measurements for all live animals due to technical requirements at the abattoir. Median specimen weight however was 476g (Q1: 446; Q3: 700; IQR: 254). No data regarding the animal's age could be collected. As the data was derived from experimental set-ups which developed over time, it was not possible to acquire a full data set from each individual perfused limb. Sample sizes for presented data are specified accordingly.

4.3.1 Oedema and perfusate pressure

Specimens were harvested and prepared for perfusion as previously described (see Chapter 3). To assess weight gain as an indicator of oedema formation, legs were positioned on electronic scales (UltraShip 55lb. Digital Postal Shipping and Kitchen Scale, Amazon) and their weight recorded at the beginning and conclusion of the experiment. For constant perfusion pressure monitoring, an intra-arterial pressure monitoring system (Datascope 2000®) was connected to the catheter placed into designated perfusion arteries. Limbs were perfused with a flow rate of 5mL/min/artery. Therefore, with two designated perfusion arteries (*A. dorsalis pedis*, caudal branch of the saphenous artery), a total perfusate volume of 10mL/min was administered.

4.3.2 Metabolic data

To assess the tissue's viability, several analytes were measured in the perfusate (arterial reservoir AR and venous return VR) at the beginning of the experiment and hourly thereafter, using a portable blood gas analyzer system (epoc®, Woodley Equipment). Samples were obtained directly at the cut surface of the limb by collecting 1,5mL into an Eppendorf tube. A preliminary study validated the use of the analyser to measure gas in the Tyrode solution; measurements of the arterial reservoir were taken (n=22) and compared to the known composition of the perfusate. In addition, non-specific oxygen loss attributed to the perfusion system alone was investigated and ruled out by comparison of metabolic data obtained from the AR and values measured in the perfusate after it was propelled through the system, but before it entered the limb (n=5).

Oxygen consumption was calculated by the difference in oxygen saturation of the AR and the VR. Further metabolic information was gained by collecting data on glucose consumption ($glucose\ concentration_{\ AR} - glucose\ concentration_{VR}$) and lactate concentration. Potassium levels were also measured to inform on cell function and integrity.

4.3.3 LDH assays

As a predictor of cell injury/death, LDH levels were measured in VR samples with a colorimetric assay (Lactate Dehydrogenase Activity Kit, Sigma-Aldrich, (Legrand, Bour et al. 1992, Patan, Budras et al. 2009). LDH's enzymatic activity produced NADH which interacts with a specific probe in the kit, producing a dyed substance. Using a spectrophotometric plate reader (1420 Multilabel Counter, VICTOR³ TM, Perkin Elmer precisely), the colour produced was measured at a wavelength of 450nm. The assay was performed according to the supplier's manual and subsequently the LDH concentration within the sample was calculated by reference to a standard curve based on the manufacturers NADH standard solution (see chapter 2.4). Results are presented in nmol/min/mL or mU/mL, with one unit of LDH activity described as the

quantity of LDH needed to produce 1µmol of NADH per minute at a temperature of 37ºC.

4.3.4 Assessment of cell viability using multiphoton microscopy

At the conclusion of the experiment, samples of the joint capsule and the abaxial sesamoid bones were harvested from either the third or fourth metatarsophalangeal joint. This was performed after either six (synovium: n=29, cartilage: n=31) or ten (both n=4) hours of perfusion. For comparison, samples were also taken from non-perfused legs after the same time periods (n=4 per time period and tissue). Samples were stained with 5-chloromethylfluorescein diacetate (CMFDA, live cells, green) and propidium iodide (PI, dead cells, red) for 75 minutes at room temperature. Subsequently, specimens were fixed in 4% formaldehyde in 0,9% NaCl v/v for 24 hours at 4°C. Immediately prior to imaging, the tissues were mounted onto petri dishes using skin glue (3M Vetbond™, USA) and submerged in PBS. Viability of the cartilage and joint capsule sample was assessed using multiphoton laser scanning microscopy and 3D image processing (Imaris, Bitplane, Switzerland) by computing a live to dead cell ratio (see Chapter 2.3).

4.3.5 Statistical analysis

All data were statistically analysed using commercially available software (Minitab 17, Statistical Software). Data was non-parametric and analysed using Mann-Whitney tests.

4.4 Results

4.4.1 Oedema formation and perfusate pressure

Over a perfusion period of six hours, the specimen's median weight gain was 13.31% (n=38; Q1: 9.27; Q3: 16.2; IQR: 6.94). This, however, increased after ten hours perfusion (median increase in weight 27.31%; n=4; Q1: 19.19; Q3: 31.28; IQR: 12.09). The difference in specimen weight gain between the 6h and 10h time points was statistically significant (p=0.004).

Over six hours of perfusion, a median arterial perfusate pressure of 28.0mmHg (n=141; Q1: 24.0; Q3: 32.5; IQR: 8.5) was calculated. However, there was extensive variability between measurements with outliers of a minimum value of 13mmHg and a maximum value of 102mmHg (see Figure 4-1).

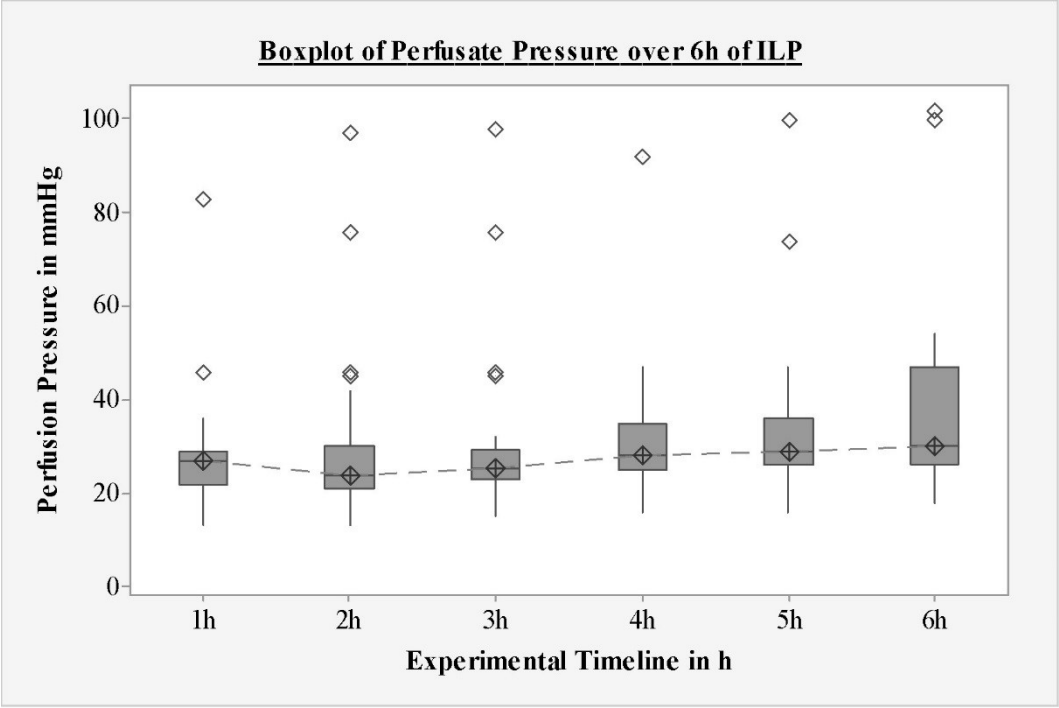

Figure 4-1: Boxplot of perfusate pressure

The arterial perfusate pressure remains fairly constant over time with a median value of 28.0mmHg (n=141; Q1: 24.0; Q3: 32.5; IQR: 8.5). However quite large outliers can be observed. This could be due to biological reasons (e.g. oedema formation) or due to

technical complications with the perfusion set-up or the intra-arterial blood pressure measurement. No measurements were taken within the first hour of ILP as the equilibration period falls into this time frame and flow rate and hence perfusate pressure had to slowly be adjusted. Limits of the box represent interquartile range, and whiskers, the minimum and maximum values. Crossed squares indicate the median values of respective data sets, dotted squares represent outliers.

4.4.2 Metabolic data

A one-sample Wilcoxon signed rank test showed no statistically significant difference between data measurements taken from the AR and the known composition of the perfusate (potassium, calcium, glucose), therefore showing that the analyser is suitable for use with Tyrode solution.

Oxygen

Non-specific oxygen loss attributed to the perfusion system could be ruled out as oxygen saturation in the AR and the perfusate were identical (saturation 100%) for all measurements.

Over the six hour perfusion, a median oxygen uptake from the AR of 7.75% (n=178; Q1: 2.90; Q3: 11.9; IQR: 8.95) was calculated by the difference between the 100% saturated AR and respective VR samples. Oxygen saturation was significantly different between AR and VR samples (p=0.000), as was partial oxygen pressure (p=0.000). A statistically significant increase in oxygen consumption could be observed after one hour of perfusion (p=0.0013). Thereafter values remained relatively constant (see Figure 4-2).

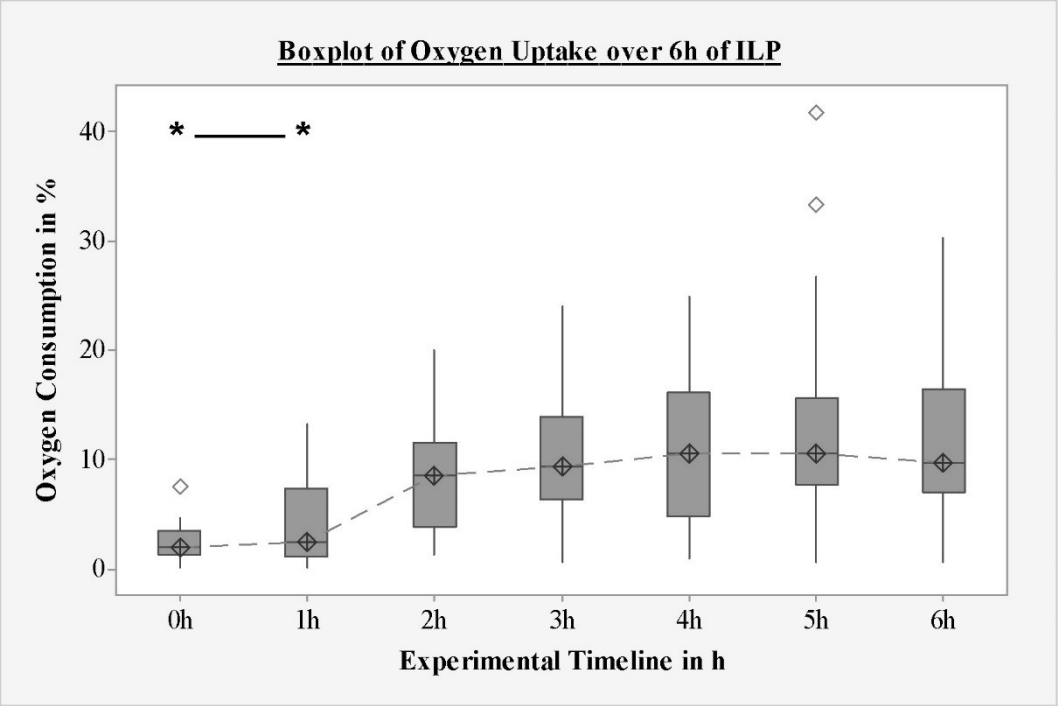

Figure 4-2: Boxplot of oxygen uptake

Oxygen consumption was calculated by the difference in oxygen saturation of the AR and the VR. Median uptake of oxygen was 7.75% (n=178; Q1: 2.90; Q3: 11.9; IQR: 8.95). An initial increase in values over the first two hours of perfusion are attributed to a slowly starting metabolism after the cooled and hypoxic transport. A statistically significant increase in oxygen consumption could be observed after one hour of perfusion (p=0.0013). Eventually oxygen uptake stabilised for the remainder of the experiment. Limits of the box represent interquartile range, and whiskers, the minimum and maximum values. Crossed squares indicate the median values of respective data sets, dotted squares represent outliers. Asterisks indicate statistically significant results.

Glucose

Porcine limbs consumed a mean of 1.44±0.61mmol/L (n=178) glucose. This value was greatest immediately following commencement of perfusion (mean at time point 0h: 1.748±0.60mmol/L; n=25) and decreased after five hours of perfusion (mean at time point 6h: 1.187±0.69mmol/L; n=15). However, despite these peaks and troughs, there

was no statistically significant difference in glucose concentration between time points 0h/ 1h or 5h/ 6h (p=0.475 and p=1.00 respectively; see Figure 4-3).

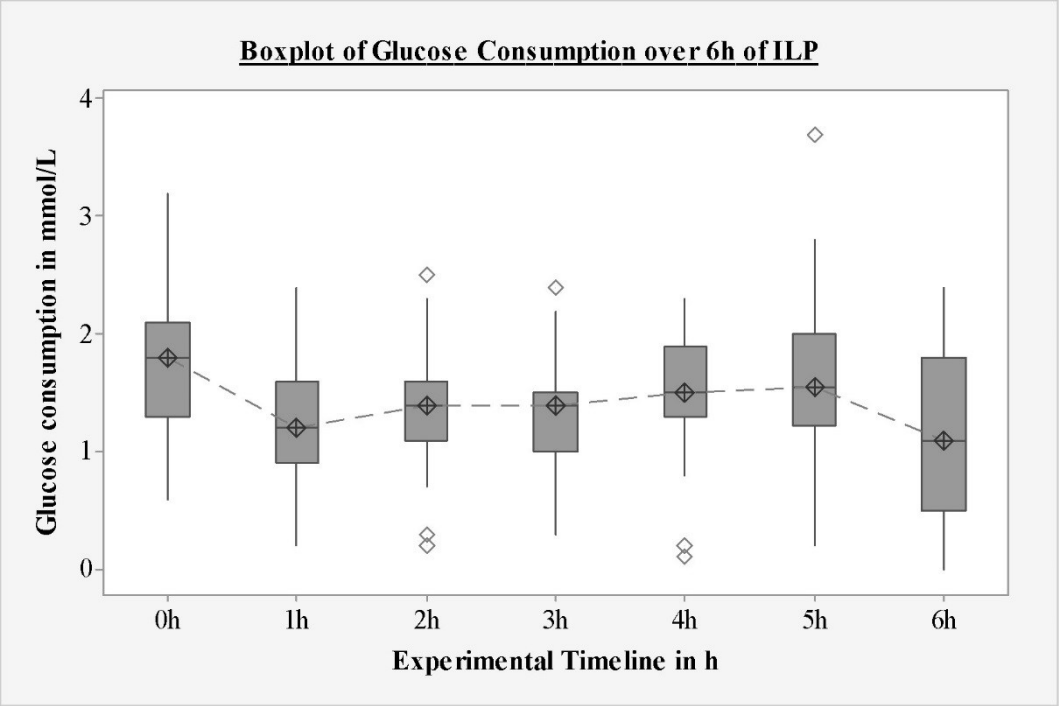

Figure 4-3: Boxplot of glucose consumption

A mean overall glucose consumption of 1.44±0.61mmol/L was calculated from 178 single measurements. Upon initiation of perfusion a higher consumption was observed, potentially due to higher metabolic demands during the equilibration process. A slight fall in glucose uptake after five hours could be attributable to reduced tissue viability. However the initial higher value (difference time points 0h/ 1h; p=0.475) as well as the lower consumption (difference between points 5h/ 6h; p=1.00), were not significantly different. Limits of the box represent interquartile range, and whiskers, the minimum and maximum values. Crossed squares indicate the median values of respective data sets, dotted squares represent outliers.

Lactate

Initially, relatively high lactate values were detected (median at time point 0h: 2.410mmol/L; Q1: 1.720; Q3: 2.870; IQR: 1.150; n=25); this was statistically different

to the measurements taken at time points 1h (p=0.0062), 2h (p=0.0394), and 3h (p=0.0460). Throughout the subsequent duration of the perfusion, the lactate concentration of the perfusate remained relatively constant (median 1.840mmol/L; n=180; Q1: 1.56; Q3: 2.40; IQR: 0.838; see Figure 4-4).

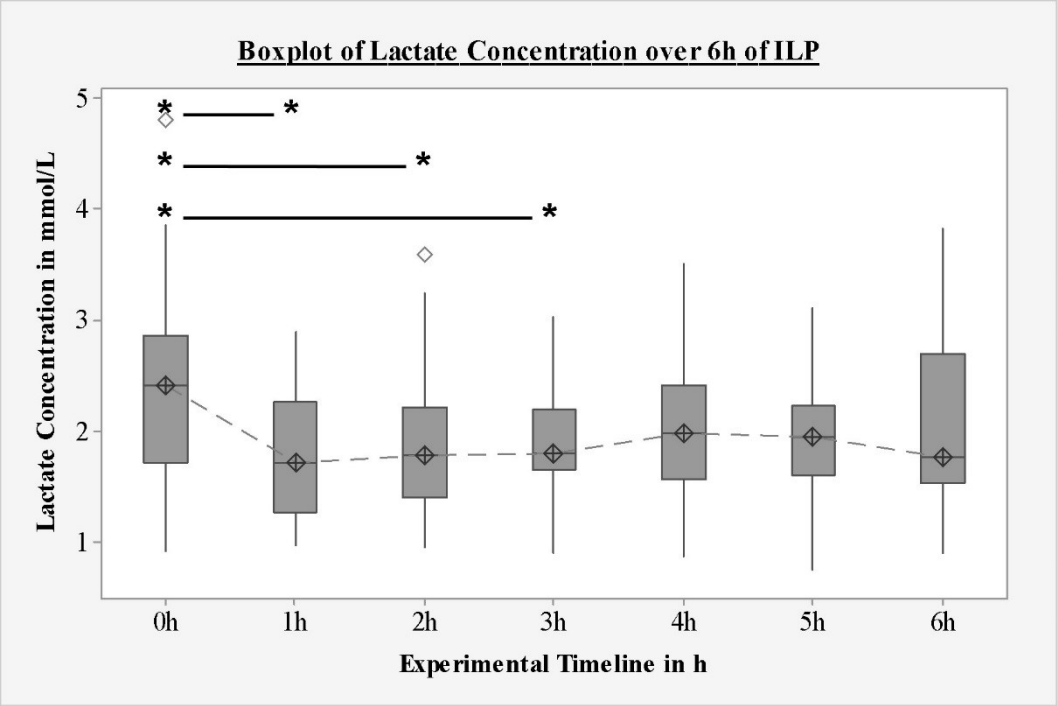

Figure 4-4: Boxplot of lactate concentration

The overall median of lactate concentration was 1.840mmol/L (n=180; Q1: 1.56; Q3: 2.40; IQR: 0.838). Data collected at time point zero were statistically significant different to 1h (p=0.0062), 2h (p=0.0394), and 3h (p=0.0460). This is considered to represent lactate accumulation during anaerobic transport of the specimen. Limits of the box represent interquartile range, and whiskers, the minimum and maximum values. Crossed squares indicate the median values of respective data sets, dotted squares represent outliers. Asterisks indicate statistically significant different results.

Potassium

The median potassium concentration measured in VR samples was 5.200mmol/L (n=176; Q1: 5.10; Q3: 5.40; IQR: 0.3). Whereas the AR showed a median

concentration of 5.3mmol/L (n=29; Q1: 5.00; Q3: 5.50; IQR: 0.5). This difference was not statistically significant (p=0.9340). However, the initial high potassium concentrations were statistically different from the measurements obtained at time points 1h (p=0.0064), 2h (p=0.0226) and 3h (p=0.0385).

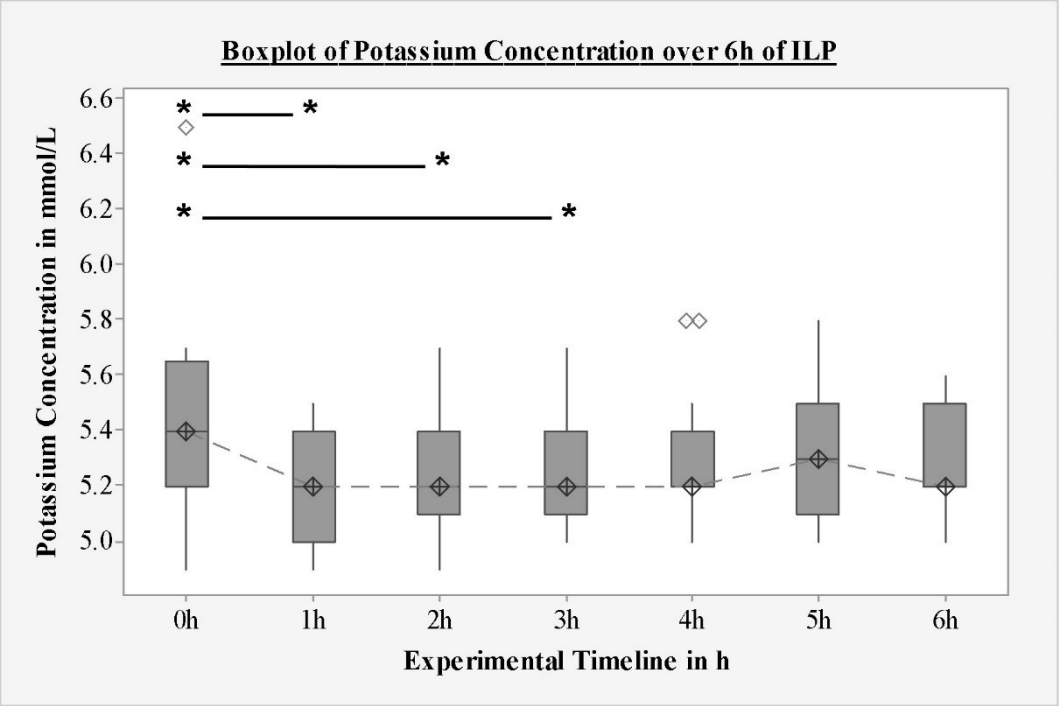

Figure 4-5: Boxplot of potassium concentration

The median value of potassium concentration was 5.200mmol/L (n=176; Q1: 5.10; Q3: 5.40; IQR: 0.3). This is slightly above the physiological range due to the adapted Tyrode recipe. The initial high potassium concentration was significantly different from the measurements obtained at time points 1h (p=0.0064), 2h (p=0.0226) and 3h (p=0.0385), most likely due to an accumulation of potassium during transport. Limits of the box represent interquartile range, whiskers the minimum and maximum values. Crossed squares indicate the median values of respective data sets, dotted squares represent outliers. Asterisks indicate statistically significant different results.

4.4.3 LDH assays

LDH

Median LDH activity over a perfusion time of six hours was 8.581mU/mL (n=135; Q1: 5.50; Q3: 13.81; IQR: 8.30). The baseline (time point 0h) LDH activity was significantly greater (p=0.0003) than time point one. However, there was no significant difference (p=0.1462) in LDH activity between the time points during the first half of the perfusion, after the equilibration period (time points 1h, 2h, 3h) and those during the second half of the perfusion, after connection of the syringe pump circuit containing neutrophils (time points 4h, 5h, 6h).

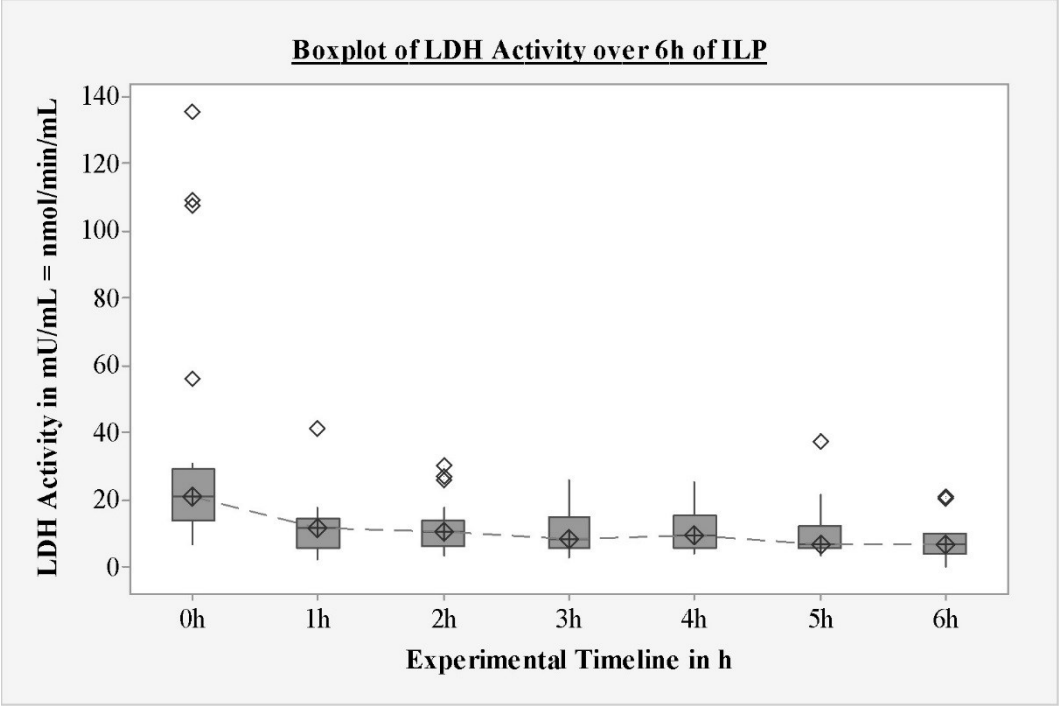

Figure 4-6: Boxplot of LDH activity

Activity of LDH stayed constant from 1h following commencement of perfusion until the end of the experiment. The initial higher values, measured immediately following connection of the limb to the system, were attributed to an accumulation of dead cells during ischemia while transporting the specimen. It could be hypothesised that a significant efflux of neutrophils within the VR from the 4h time point onwards would have resulted in an increase in LDH activity; however, this was not observed. Reasons for this remain unclear; however, this may reflect retention of the infused neutrophils within the specimen. Limits of the box

represent interquartile range, and whiskers, the minimum and maximum values. Crossed squares indicate the median values of respective data sets, dotted squares represent outliers.

4.4.4 Assessment of cell viability using multiphoton microscopy

Calculation of a live to dead cell ratio proved to be a valid means of assessing tissue viability in this series of perfusion experiments. Cartilage samples could be analysed extremely reliably. The more delicate synovium samples were difficult to harvest and process (e.g. due to slight oedema formation within the tissue) and therefore analysis was not successful in every case, due to poor sample quality.

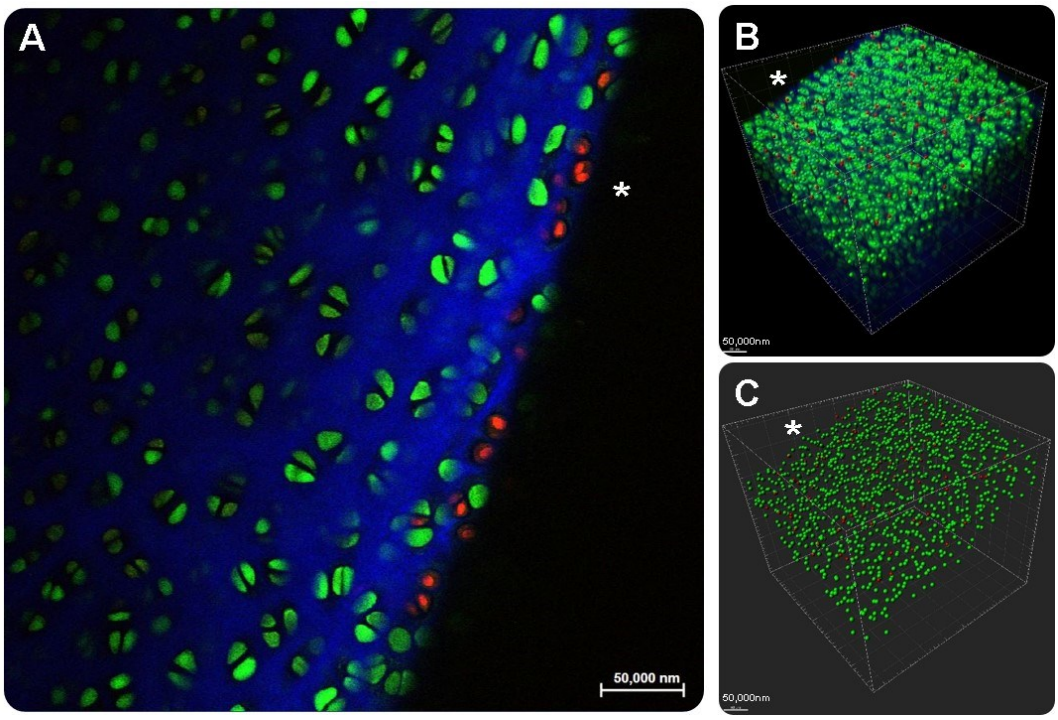

Figure 4-7: Multiphoton and Imaris images of cartilage

Live (green) and dead (red) chondrocytes are shown in their relation to the collagenous fibre grid (blue, **A**). Chondrocytes are stained with CMFDA and PI respectively. Collagen is visualised using the SHG principle. During image acquisition 40 slices were taken and subsequently spanned in a 3D grid. Spheres were assigned to cells (**B**) and the background noise subtracted before computing the live/ dead cell ratio (**C**). Asterisks indicate the

articular surface. Samples were harvested and stained immediately after 6h of ILP and analysed 24h after.

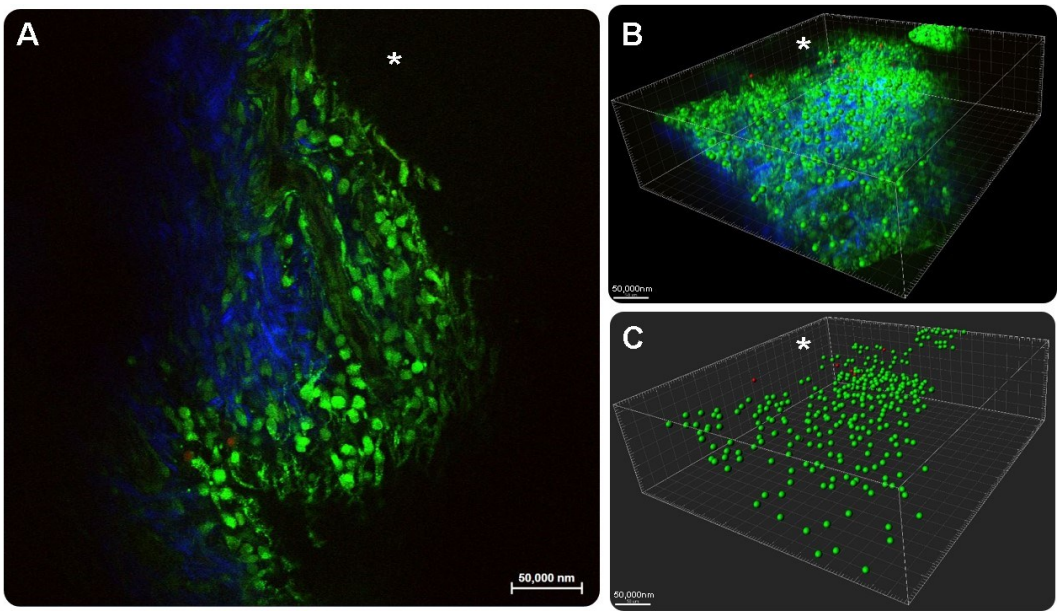

Figure 4-8: Multiphoton and Imaris images of synovium

Synoviocytes are stained in green (CMFDA, live, **A**) and red (PI, dead, **A**). Collagen fibres of the joint capsule show up in the blue channel based on the SHG principle. During image acquisition 40 slices were taken and subsequently spanned in a 3D grid. Spheres were assigned to cells (**B**) and the background noise subtracted before computing the live/ dead cell ratio (**C**). Asterisks indicate the surface area. Samples were harvested and stained immediately after 6h of ILP and analysed 24h after.

Cartilage cell viability in samples collected from non-perfused limbs was 97.19% after six hours (n=4; Q1: 89.86; Q3: 99.10; IQR: 9.24) and 99.65%% after ten hours (n=4; Q1: 98.76; Q3: 99.80; IQR: 1.04). In comparison, cartilage cell viability in samples collected from perfused limbs was 99.34% after six hours (n=31; Q1: 96.45; Q3: 99.76; IQR: 3.31) and 98.18% after ten hours (n=4; Q1: 77.26; Q3: 99.81; IQR: 22.55) perfusion. There was no statistically significant difference in cell viability between non-perfused and perfused samples in all groups. There was also no significant difference in cartilage cell viability between the 6h and 10h time points in perfused

limbs. However, there was a significant reduction in synovium cell viability between the 6h and 10h time points in perfused limbs (p=0.0141).

The calculated ratio of live to dead cells was consistent with a median survival rate of 98.25% (n=4; Q1: 96.16; Q3: 99.33; IQR: 3.16) in non-perfused synovium samples six hours following tissue harvesting. In contrast, samples collected from perfused limbs had a slightly lower median live cell count of 92.36% (n=29; Q1: 69.21; Q3: 97.66; IQR: 28.45). The same trend was observed after an experimental time of ten hours (non-perfused limb: 81.3%; n=4; Q1: 21.2; Q3: 91.9; IQR: 70.7; perfused limb: 53.6%; n=4; Q1: 26.9; Q3: 81.4; IQR: 54.5).

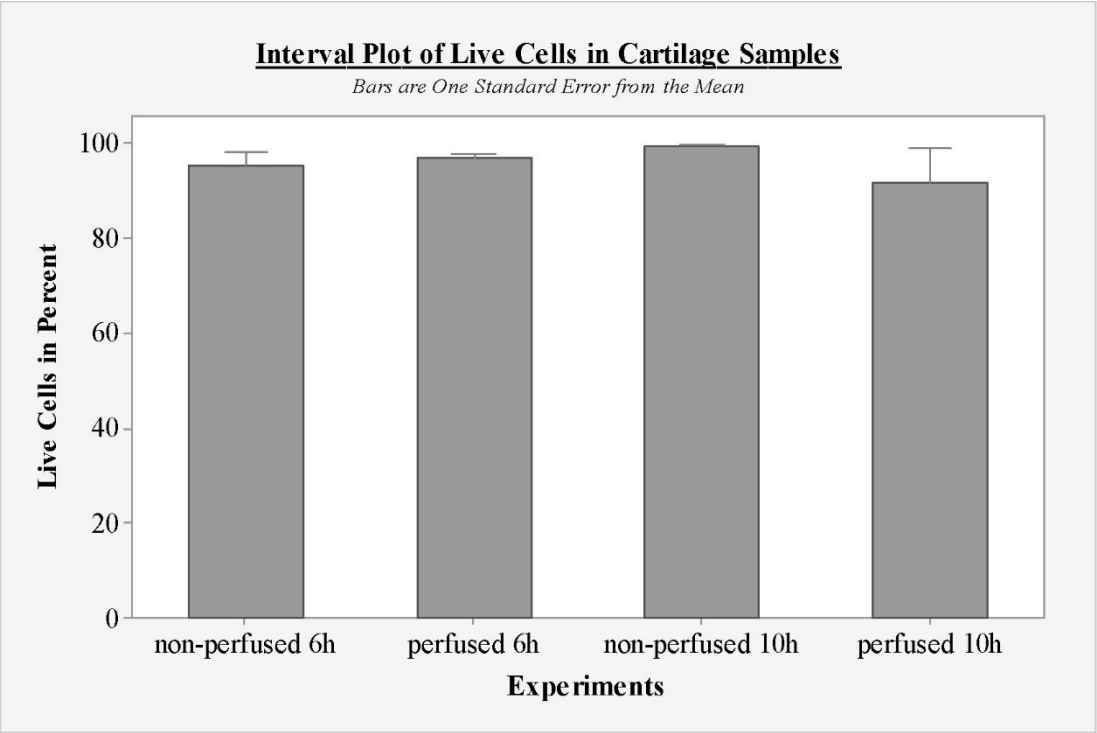

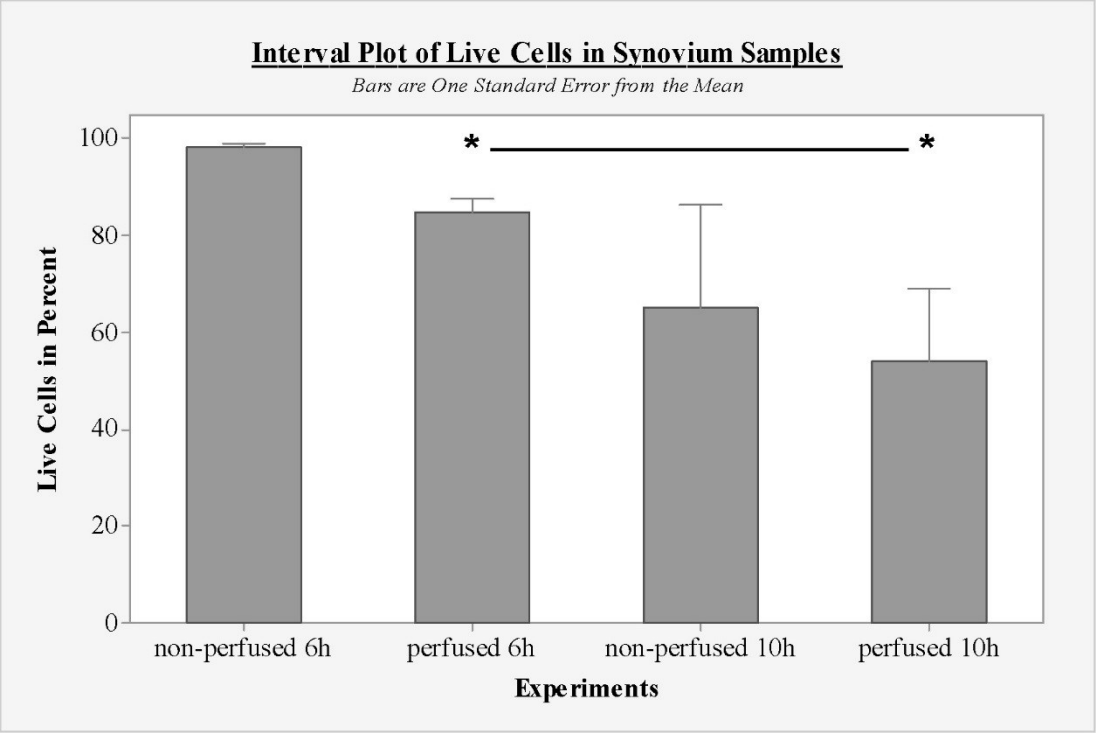

Figure 4-9: Interval plot of live cells in cartilage and synovium samples

Viability of live cells for tissue samples collected after six hours and ten hours of ILP, as well as non-perfused control legs after the same time intervals. In synovium samples, a trend towards lower viability in perfused samples is evident; however, this is not statistically significant, and may be attributable to either a suboptimal nutrient supply during perfusion and/or the difficultly associated with handling and processing the delicate synovial samples. Differences between respective groups were not statistically significant with the exception of a decrease in synovium viability between six and ten hours of perfusion (p=0.0141). Data are reported as mean. Bars represent the standard error of the mean. Asterisks indicate statistically significant different results

4.5 Discussion

4.5.1 Oedema formation and perfusate pressure

Oedema formation is the result of increased vascular permeability which potentially can be attributed to changes in the capillary bed due to prolonged ischemia (Blaisdell 2002). Therefore, an increase in weight of perfused specimens may directly reflect the

integrity of the microvasculature (Mueller, Constantinescu et al. 2013) and thus the extent of ischemia/ reperfusion injury (Petrasek, Homer-Vanniasinkam et al. 1994). Disproportionate oedema formation leads to deterioration of organ function which eventually results in a rapid reduction in the organ's suitability for either transplantation or for research purposes (Verbeke, Roets et al. 1972). With the exception of sporadic reports in which oedema was assessed by histologic examination of tissue samples, measurement of skin fold thickness or tissue's wet to dry weight ratios, the most commonly adopted technique involves the measurement of specimen weight gain over the period of perfusion. Initially, when referring to a perfused caprine mammary gland, Hardwick et al. (1960) defined oedema formation as a greater than 20% increase in specimen weight (Hardwick and Linzell 1960). Subsequently, Kietzmann et al. (1993) substantiated these values, as bovine udders perfused by this group gained an average of 14% of the initial weight during a six hour experiment without any histologically evident changes to the tissue (Kietzmann, Löscher et al. 1993). Overall, the weight gain reported in this series of studies (6h perfusion: median 13.31%) is comparable to data derived from previous published perfusion experiments with artificial perfusates (Hardwick and Linzell 1960, Usui, Sakata et al. 1985, Bristol, Riviere et al. 1991, Domingo-Pech, Garriga et al. 1991, Bäumer, Mertens et al. 2002), suggesting that tissue viability was adequately maintained by the developed perfusion system throughout the duration of perfusion. A stricter limit for intolerable weight gain has however been set in other studies, whereby specimens with more than ten percent increase in specimen weight are excluded from the study (Zeitlin and Eshraghi 2002). In the reported series of studies, the statistically significant increase in oedema formation between six and ten hours of perfusion ($p = 0.0044$) largely informed the decision to limit the experimental time to six hours for subsequent studies (see Chapter 5).

A better relative balance of oncotic pressure between the intra- and extravasal space might be the reason for Friebe et al. (2001) reporting on a weight gain of just 4.5±3.3% in the isolated perfused equine digit (Friebe, Stahl et al. 2001). In that particular report, sodium carboxymethyl cellulose was used to minimise oedema formation. However,

cellulose based materials (Hänsch, Karnaoukhova et al. 1996, Moore, Kaplan et al. 2001, Hernández, Galan et al. 2004, Hernandez, Fuste et al. 2009) and solutions (Bae, Jin et al. 2004, Ewoldt, Anderson et al. 2004) are known to affect neutrophil function and inflammatory processes; therefore, upon consideration of the ultimate objectives of this investigation, it was refrained from the use of cellulose in the current experimental set-up. Starch, a very similar polymer, has also been shown to impair neutrophil migration and its use is similarly contra-indicated in a model of inflammatory cell migration (Handrigan, Burns et al. 2005, Matharu, Butler et al. 2008). Mannitol is widely used in clinical and research settings as a potent agent to control oncotic pressure with very few side effects. Although little is known about its influence on the immune system, recent findings have identified an association between a 24h exposure to mannitol (16,5mM/L) and upregulation of CD 11b in neutrophils (Turina, Mulhall et al. 2008). Given the prolonged exposure time in the study by Turina et al (2008) and the fact that neither TNF-α nor IL-6 were affected by mannitol (Turina, Mulhall et al. 2008), its use was considered appropriate in the proposed study.

Experimental designs which incorporate whole blood as a perfusate generally result in less oedema formation (Constantinescu, Knall et al. 2011, Patan-Zugaj, Gauff et al. 2012), a feature likely attributable to the physiological similarities with the factors which influence *in vivo* oncotic pressure. However, despite the reported drawbacks in terms of oedema formation, relative to whole blood, the use of artificial solutions does facilitate the study of the effects of specific agents. The use of e.g. Tyrode solution enables standardization of the environment, minimizes unwanted interactions and allows the proposed work to focus on migration and behavior of one specific cell type.

As previously mentioned (see Chapter 1.3.4.3), maintenance of hypothermic conditions also constitutes an appropriate means of minimising oedema formation (Constantinescu, Knall et al. 2011). However hypothermic conditions do alter metabolism (Fuller and Lee 2007) and, most importantly with regard to the ultimate aims of this study, they also influence neutrophilic migration behavior and

inflammatory responses (Biggar, Bohn et al. 1984). Hypothermic conditions were therefore considered unsuitable for the proposed work.

In the adopted set-up, a low flow approach was selected; namely one in which the perfusate pressure was set at a level lower than the physiological norm for blood pressure. This approach has been shown to be beneficial in terms of minimising oedema formation (Cypel, Yeung et al. 2008, Constantinescu, Knall et al. 2011, Mueller, Constantinescu et al. 2013), while still allowing a fully functional blood/perfusate supply, as previously demonstrated via the incorporation of dyes within the perfusate (Kietzmann, Löscher et al. 1993). In these reports, the perfusate pressure (mean of 33.73±2,06mmHg) (Constantinescu, Knall et al. 2011) was comparable to the median perfusate pressure of 28mmHg calculated in this current study. However, despite the pressure in the current study being lower than that measured *in vivo*, and slightly lower than that adopted in other porcine ILP set-ups, experiments with added colorants did confirm the presence of a functional perfusate supply to the tissues of interest (see Chapter 0). Technical limitations of the pump precluded experiments with higher flow rates and, as a result, higher perfusate pressures. However, when the data from the coloured dye experiments were considered in combination with the additional viability data, it was concluded that the adopted perfusate pressure levels were suitable.

4.5.2 Metabolic data

Oxygen consumption

Comparison of oxygen consumption between models is challenging, as the uptake of oxygen is dependent on a number of factors; these include the type of tissue being perfused, the mass of the perfused organ and whether the perfusate contains an oxygen carrier such as haemoglobin. When using blood-based perfusates, the rate of oxygen consumption can be calculated by the Fick equation ($(VO_2 = Qx(CaO_2 - CvO_2)$; VO_2: oxygen consumption; Q: cardiac output; CaO_2: arterial oxygen content; CvO_2: venous oxygen content); however the use of artificial solutions, such as that adopted

in the current set-up, precludes the application of such calculations. This is due to the dependency of the arterial and venous oxygen content (CaO_2 and CvO_2) of blood-based perfusates on haemoglobin, as follows: $\frac{1{,}34xHbx(Sa/vO_2)}{100} + (0.003xPa/vO_2)$ (1.34: Hüfner's constant; Hb: haemoglobin; Sa/vO_2: percentage saturation of Hb with oxygen; Pa/vO_2: partial pressure of oxygen).

For isolated organ perfusion, the specimen's weight is also generally considered (Chapman, Goldsworthy et al. 1961, Jensen, Fahrenkrug et al. 1978, Patan, Budras et al. 2009). Partial pressure of oxygen (pO_2), oxygen saturation (SO_2), and pCO_2 in arterial and venous perfusate samples have also been used to determine oxygen consumption (Zeitlin and Eshraghi 2002, Wagner, Nogueira et al. 2003, Polyak, Morton et al. 2008, Constantinescu, Knall et al. 2011). It is however difficult to compare data obtained from perfusion with artificial solutions to the physiological norm, as the latter is based on measurements in blood. Nonetheless, the difference between arterial and venous partial oxygen pressure can be used as an indicator of oxygen consumption (Constantinescu, Knall et al. 2011) and this difference was statistically significant ($p=0.000$) in the data set obtained from the current set-up. The same applies to oxygen saturation. A median uptake of 7.75% of oxygen from the fully oxygenated reservoir was, in combination with other viability data, considered sufficient for future experiments. The reason for outliers, consuming considerably more oxygen at e.g. time point 5h, could not be explained fully, however one reason could be additional oxygen uptake by bacterial overgrowth.

Glucose

Glycolysis is responsible for converting glucose to pyruvate in a living organism. During this process, the excessive energy is used to produce ATP and NAD as the body's energy source. Therefore, in perfusion experiments an uptake of glucose from the perfusate indicates a functioning glycolytic pathway, necessary to keep the specimen viable. However, in most set-ups there exists the potential for bacterial contamination of the system and/or the specimen to contribute towards the overall glucose consumption. According to the literature, a glucose consumption of ≥200mg/h

was considered to be indicative of good tissue viability in the perfused equine digit (Friebe, Stahl et al. 2001). Application of these reported cut off values to other experimental models is however problematic as glucose metabolism is highly organ and tissue specific; furthermore, the mass of the specimen is also a major determinant of the values obtained. Upon consideration of the greater mass and lesser muscle tissue associated with the equine distal digit, compared with the porcine distal limbs used, and the very distinct glucose metabolism within its hoof tissue, direct extrapolation of data to the presented work did not seem appropriate. Nonetheless, fairly constant levels of glucose uptake by the specimen were seen throughout the duration of the perfusion, thus indicating good tissue viability. The initially higher values of glucose consumption, directly after transportation of the specimen, might indicate higher metabolic demands during this equilibration period. A slight decrease in glucose uptake towards the end of the experiment could have been attributable to a temporal decline in tissue viability after five hours of perfusion, thus highlighting a potential limitation of the model. Both, the initially higher value (difference 0h/1h; p=0.475) as well as the later reduction in uptake (difference 5h/ 6h; p=1.00), were not significantly different to their designated comparisons. One explanation for observed outliers could be a potential bacterial contamination using up more glucose, but are not fully understood.

Lactate

Production of lactate is greater during anaerobic glycolysis, compared to aerobic conditions. Lactate is therefore considered a useful indicator of adaequate oxygen delivery. Lactate concentration in porcine blood can range from 0.5 to 5.5 mmol/L, with a median of 1.2mmol/L (IQR: 1.2) (Hofmaier, Dinger et al. 2013). The overall median lactate level from measurements obtained in this study were slightly higher, with a median value of 1.840mmol/L. These values lie within those previously reported. Wagner et al (2003) reported a constant elevation in lactate levels within the VR of perfused porcine limbs (up to 105mg/dL (=5.8mmol/L) (Wagner et al., 2003). Constantinescu et al. (2011) reported a mean maximum lactate value 19.59mmol/L in whole porcine limb perfusions (Constantinescu et al., 2011). In comparison, numerous

studies of the perfused equine digit reported lactate concentrations within physiological limits (Friebe, Stahl et al. 2001, Patan, Budras et al. 2009, Patan-Zugaj, Gauff et al. 2012, Friebe, Schumacher et al. 2013, Patan-Zugaj, Gauff et al. 2014). As previously mentioned, these values are tissue specific and extrapolation from one study to another is not wholly appropriate. For example, it is likely that perfusion of a whole porcine limb as reported by Wagner et al. (2013) and Constantinescu et al. (2011) resulted in higher lactate levels, compared to the equine digit, as a result of increased metabolic demands resulting from the larger amount of soft tissue within the porcine-derived specimens. Overall, most perfusion experiments show elevated lactate levels, usually with a temporal rise, even when physiological values are not ultimately exceeded (Smith, van Alphen et al. 1985, Riviere, Bowman et al. 1989, Adham, Ducerf et al. 1997, Polyak, Morton et al. 2008). This can best be explained by the absence of hepatic clearance. Only a single published study reported a small *decrease* in lactate concentration over time, hypothesising that this phenomenon resulted from lactate utilisation by monocytes (whole porcine leg, (Constantinescu, Knall et al. 2011). In the current study, the initial high lactate value, recorded immediately after connection of the specimen to the system (time point 0h, n=25, 2.411±0,90mmol/L), was considered most likely to reflect the accumulation of lactate during anaerobic transport; such a phenomenon has been reported previously (Kietzmann, Löscher et al. 1993). After initiation of the perfusion, the perfusate subsequently clears the accumulated lactate.

Potassium

Compared with the extracellular space, the intracellular space has a markedly greater potassium content, due to the energy dependent Na^+/K^+ ATPase (active transport system) which maintains an osmotic equilibrium. Thus, upon cellular death, potassium follows its electrochemical gradient resulting in increasing levels of potassium in the extracellular space (Bortner, Hughes et al. 1997, Trimarchi, Liu et al. 2000). Potassium levels, measured in the perfusate, may therefore serve as an indirect indicator of cell death (or cell integrity) (Ward and Buttery 1979, Bortner, Hughes et al. 1997) (Polyak, Morton et al. 2008, Patan, Budras et al. 2009, Constantinescu, Knall et al. 2011).

However, as a reduction in pH may also result in a potassium flux from the intra- to the extracellular space, in an attempt to buffer the acidosis (Oster, Perez et al. 1978), it is advisable also to consider metabolic imbalances when interpreting potassium values. Adequate cell viability can be assumed if the efflux of potassium is below seven percent (Ward and Buttery 1979). Physiological values for potassium concentration in pigs are around 4.3mmol/L (Harris 1974). The median value of potassium concentration measured in the current experiment was 5.200mmol/L (n=176). This is slightly above the physiological range due to the adapted Tyrode recipe. Mean arterial reservoir concentrations of potassium were 5.279±0.28mmol/L (n=29), equating to an overall potassium efflux of 0.0053%; this is clearly below the cited seven percent cut-off value and consistent with good specimen viability.

4.5.3 LDH assays

During glucose synthesis and anaerobic glucose metabolism, LDH interconverts lactate and pyruvate (Berg, Tymoczko et al. 2013). The enzyme is present in almost all of the body's tissues, showing a tissue specific distribution pattern of respective isoenzymes (Markert and Ursprung 1962). With regard to LDH's involvement in anaerobic processes and its release from a broad variety of cells after their death, an elevation of LDH levels can be linked with cell death and injury (Legrand, Bour et al. 1992) and has been used in perfusion experiments as a measure of tissue viability (Ward and Buttery 1979, de Lange, van Eck et al. 1992, Moen, Fosse et al. 1994). Its presence in erythrocytes (Kato, McGowan et al. 2006) also makes it an ideal indicator of haemolysis in perfusion set-ups using a whole blood perfusate as described by Patan et al., 2009. The group measured LDH levels in the range of 12.0±14.7U/h in the isolated perfused equine digit and reported a slight, though statistically insignificant, increase in LDH activity over the ten hour duration of the experiment (Patan, Budras et al. 2009), a result which was considered to be consistent with good tissue viability. In set-ups utilising artificial solutions, such as Tyrode solution, elevations in LDH are considered to reflect cell death resulting from hypoxemia. Due to the absence of any potential contribution of haemolysis, LDH activity in set-ups utilising artificial

solutions tends to be lower (Kietzmann, Löscher et al. 1993, Friebe, Stahl et al. 2001, Friebe, Schumacher et al. 2013). Friebe et al. postulated that adequate tissue viability can be assumed when LDH levels remain below 10U/h. The median LDH activity measured in the current study was 8.581mU/mL (=8.581nmol/min/mL). Attempts to calculate the temporal accumulation of LDH over a set period of time, as conducted in the studies mentioned above, did not seem appropriate in the current study due to the non-re-circulating set-up in which measurements were reflective only of LDH activity at the moment of sampling (e.g. not reflective of accumulation). Nonetheless levels were relatively constant over the whole perfusion period, considered to be a favourable result in terms of cell and specimen viability.

As all cells within the VR would have been lysed in the process of performing LDH activity assays, it was considered feasible that the introduction of neutrophils into the perfusate at 3h might have resulted in a transient increase in LDH levels from 4h, arising from an increased cell number in VR samples due to washed out neutrophils. As this phenomenon was not observed, it was assumed that the neutrophils might have accumulated elsewhere in the system. Alternatively, the sensitivity of the test may have been insufficient to detect subtle elevations arising from the contribution of the injected neutrophils.

4.5.4 Assessment of cell viability using multiphoton microscopy

The presented assessment of cell viability using multiphoton microscopy and 3D imaging software for data analysis was considered a new approach in the context of perfusion experiments and no data for comparison could be found in the relevant literature. The technique was considered ideal as it allows the use of relatively unprocessed samples, thus avoiding any processing-associated cell damage or death. However, this approach will only permit the assessment of viability following conclusion of the experiment, thus limiting the value of the data obtained to inform further refinements of future experiments.

Synovial fluid is derived by ultrafiltration from the blood (Ropes, Bennett et al. 1939) and functions as the main source of cartilage nutrition (Strangeways 1920). In the presented model, blood is substituted by Tyrode solution and very good cartilage survival rates of over 98% may indicate that this perfusate is capable of sufficiently nourishing cartilage over a certain period of time in perfusion experiments. However, cartilage cells derived from samples harvested in non-perfused control limbs also showed a similarly high viability. Therefore, the good overall chondrocyte viability could also be attributable to the aneural, alymphatic and avascular properties of cartilage and the resistance of chondrocytes to short-term metabolic challenges (Brower and Hsu 1969). In comparison, the overall viability of synovium samples was lower than that of chondrocytes and cell viability temporally declined between six and ten hours. Reasons for this could include Tyrode solution as perfusate not being suitable for longer ILP experiments or delicate tissues like synovium being particularly susceptible to challenges associated with ILP experiments in general (e.g. ischemia, oedema). This highlights the constraints of perfusion experiments in the given setting and, following consideration of the results derived from preliminary experiments, resulted in the adoption of a standard perfusion time of six hours for further experiments. As well as maintaining an appropriate level of cell survival, this adopted experimental duration was also considered to allow a sufficient period of time for the assessment of inflammatory cell recruitment in the migration experiments (see Chapter 5). Nonetheless, synovial tissue is considerably more delicate than cartilage; therefore, it remains possible that sample harvesting and processing had disproportionate effects on these different tissues.

4.6 Conclusion

The presented data on viability in the perfused porcine distal limb showed that the designed model is functional and suitable as a basis for further research. As with all models, there are certain limitations to the technique e.g. a restricted experimental time frame and the absence of hepatic metabolism. However, the demonstration of a

functional circulation was considered to be a significant advantage of the model. Such a feature has the potential to facilitate the testing of novel drugs and delivery systems; substances could be administered either systemically (e.g. via the perfusate) or locally (e.g. intra-articular), with subsequent assessment of their distribution and/or elimination.

To date, the viability assessments based on microscopically assessing live/ dead cell ratios has not been used in perfusion experiments. The data generated suggests that the adopted technique could represent a valuable tool for future experiments. In particular, as the measured output is neither tissue nor metabolism dependent, appropriate comparisons and extrapolations can be made between studies.

Chapter 5 Porcine ILP as model for directed cell migration and acute inflammation in the context of arthritis

5.1 Abstract

The use of ILP to study the migration of isolated cells towards an intra-articular chemoattractant represents a novel application of this model. Furthermore, to the author's knowledge, the assessment of inflammatory gene expression following perfusion (treated and untreated) and its comparison to *in vivo* data has not previously been described in the literature. The following chapter reports the results of experiments using porcine ILP as a model for directed cell migration and acute inflammation in the context of arthritis.

The innovative approach of using multiphoton microscopy to assess neutrophil migration in this context appeared feasible. However cell migration towards an intra-articular stimulus needs further refinement. The expression of five genes (COX-1, IFN-γ, TNF-α, IL-1β, IL-6) in response to superparamagnetic iron oxide nanoparticles (SPIONs) was analysed via reverse transcriptase quantitative PCR (qPCR). Samples of six different groups were compared (perfused, SPION injected (PNN); perfused, sham injected (PSN); perfused, non-injected control (PCN); non-perfused (NP); *in vivo*, SPION injected (VN); *in vivo* sham injected (VS)). The expression of COX-1 was significantly ($p= 0.034$) lower (8.16 fold) in PSN specimens, compared with VS specimens ($\Delta\Delta Ct=-3.03$). No statistically significant differences between groups were detected for IFN-γ and TNF-α. The expression of IL-1β was significantly ($p=0.002$) and markedly greater (26.47 fold; $\Delta\Delta Ct=4.72$) in PNN specimens, compared with PSN specimens .The expression of IL-1β expression was significantly ($p=0.02$) lower (11.5 fold, $\Delta\Delta Ct=-3.52$) in PSN specimens, compared with VS specimens. Similar trends could be observed for IL-6, although this was only significant when comparisons were made between PNN and PSN joints. The expression of IL-6 was significantly ($p=0.03$) greater (9.58 fold; $\Delta\Delta Ct=3.26$) in PNN specimens, compared with PSN specimens.

5.2 Introduction

Arthritis is a diseases affecting the quality of life of human and veterinary patients. The two main types of arthritis are rheumatoid arthritis (RA) and osteoarthritis (OA); in both, inflammation plays a pivotal role.

Eicosanoids and leukotrienes

Cyclooxygenase 1 (COX-1; also known as prostaglandin-endoperoxide synthase 1 (PTGS1)) is a constitutively expressed enzyme with homeostatic functions (Griswold and Adams 1996, Crofford 1997). In comparison, cyclooxygenase 2 (COX-2; also known as prostaglandin-endoperoxide synthase 2 (PTGS2)) is a recognised component of the inflammatory process in the synovium of RA joints (Woods, Mogollon et al. 2003), the inhibition of which results in an improvement in clinical symptoms of RA (Lipsky and Isakson 1997). Leukotriene B_4 (LTB_4), a potent neutrophilic chemoattractant, is another important inflammatory mediator in RA, reflected in the fact that RA mouse-models with impaired LTB_4 signalling do not develop any RA-associated signs (Mathis, Jala et al. 2007). In *ex vivo* experiments, COX-2 expression is increased in OA cartilage chondrocytes, resulting in subsequent prostaglandin E_2 (PGE_2) production (Amin, Attur et al. 1997). However, in light of the many inflammatory pathways involved in OA, the relative contribution of increased COX-2 expression in OA is not definitively established (Abramson 1999, Pelletier, Martel-Pelletier et al. 2001). Similar ambiguity also remains with regard to the relative contribution of the entire lipooxygenase pathway in OA; although, the LTB_4 detected in synovial tissue is generally assumed to promote IL-1β production (Atik 1990, Wittenberg, Willburger et al. 1993, Kageyama, Koide et al. 1994).

Cytokines

Despite ongoing difficulties associated with the clinical utility of cytokine data in OA, (Punzi, Oliviero et al. 2005) the involvement of cytokines in OA pathogenesis is well established from a research perspective. In RA, high levels of relevant cytokines can be detected routinely in synovial fluid (Houssiau 1995). Tumor necrosis factor alpha (TNF-α) and interleukin 1 (IL-1) are important cytokines in inflammatory processes;

in RA, the main sources of these cytokines are activated monocytes, macrophages and CD4+ T cells (Szekanecz, Koch et al. 1998).

TNF-α and IL-1β are crucial for the metabolism of cartilage and seem to play a key role in its destruction in both OA (Van De Loo, Joosten et al. 1995, Caron, Fernandes et al. 1996) and RA (Saxne, Palladino et al. 1988, Chikanza, Kingsley et al. 1995). In RA, high concentrations of TNF-α and IL-1β in the synovial fluid induce the production of proteolytic enzymes in chondrocytes (Nawroth, Bank et al. 1986, Haworth, Brennan et al. 1991, Butler, Maini et al. 1994, Pelletier, Martel-Pelletier et al. 2001). In comparison, the low levels detected in OA are thought to inhibit the synthesis of aggrecan and type II collagen (Häuselmann, Flechtenmacher et al. 1996). In other respects, TNF-α is also associated with subchondral bone osteoclastic remodelling in OA (Bertolini, Nedwin et al. 1986). Macrophages located in the synovium of RA affected joints are considered the most relevant source of IL-1 (Arend and Dayer 1995). Despite an associated increase in the IL-1 antagonist (IL-1 receptor antagonist), the magnitude of this elevation appears insufficient to abolish inflammation (Chomarat, Vannier et al. 1995).

Activation of IL-1β is dependent on the protease, caspase 1 (Kronheim, Mumma et al. 1992), the expression of which is also increased in OA cartilage and synovium (Saha, Moldovan et al. 1999). The subsequent activation of cells is precipitated by the surface receptor, IL-1R (Slack, McMahan et al. 1993), the expression of which is elevated in OA cartilage and synovial fibroblasts (Martel-Pelletier, Mccollum et al. 1992, Sadouk, Pelletier et al. 1995).

TNF-α seems to play a key role in promoting synovitis in RA via its ability to induce the expression of other inflammatory cytokines, including IL-1, IL-6, IL-8 and granulocyte-monocyte colony-stimulating factor (Nawroth, Bank et al. 1986, Haworth, Brennan et al. 1991, Butler, Maini et al. 1994). Furthermore, TNF-α also triggers the expression of adhesion molecules on fibroblasts, leading to increased leukocyte recruitment to the affected joints (Chin, Winterrowd et al. 1990). The

importance of TNF-α is supported by the fact that the course of disease can be attenuated by various methods (competitive, monoclonal antibodies) used to inhibit TNF-α–receptor interactions (Williams, Feldmann et al. 1992, Wooley, Dutcher et al. 1993). Additionally, Keffer et al (1991) demonstrated the spontaneous development of an RA like condition in transgenic mice expressing 3'-modified human TNF-α transgene (Keffer, Probert et al. 1991). TNF-α needs to be activated by the TNF-α-converting enzyme (TACE), an up-regulation of which has been reported in OA affected cartilage (Amin 1999). Upon cleavage, the complex binds to two specific TNF receptors (TNFR) (Loetscher, Pan et al. 1990, Schall, Lewis et al. 1990). TNFR55, the receptor mainly responsible for TNF-α-chondrocyte/synovial cell interactions, is increasingly expressed in OA joints (Westacott, Atkins et al. 1994, Alaaeddine, DiBattista et al. 1997). Additionally, a soluble form of TNFR (sTNFR) arises by proteolytic cleavage of TNFR's extracellular domain (Brennan, Gibbons et al. 1995, Alaaeddine, DiBattista et al. 1997). sTNFR operates in a dose-dependent manner; in low concentrations, similar to those found in OA, it is believed that sTNFR stabilizes the bioactive form of TNF-α and therefore facilitates cartilage degeneration (Pelletier, Martel-Pelletier et al. 2001). Indeed, sTNFR is one of the few biomolecular markers used clinically in the detection of OA. Despite this, interpretation of sTNFR data in relation to disease severity remains challenging (Punzi, Oliviero et al. 2005).

Interleukin 6 (IL-6) is the main stimulus for most acute phase proteins and, along with its soluble receptor (sIL6-Rα), is also involved in the shift from acute to chronic inflammation (Gabay 2006). It has been shown to be upregulated in synovial fluid of patients with inflammatory arthritides (Hirano, Matsuda et al. 1988, Houssiau, Devogelaer et al. 1988). This cytokine represents an interesting target for therapeutic agents in the treatment of RA (Nishimoto, Hashimoto et al. 2007, Emery, Keystone et al. 2008).

Enzymes

Relevant cytokines excite the release of matrix metalloproteinases (MMPs) from chondrocytes, synovial fibroblasts and activated T-cells. Due to their proteolytic

activity, MMPs (especially stromelysin and collagenases) play a pivotal role in the turnover and breakdown of the extracellular matrix (Visse and Nagase 2003) and are involved in early stage cartilage remodelling in OA (Martel-Pelletier, Tardif et al. 2000, Martel-Pelletier, Lajeunesse et al. 2005). This degradation is the origin of joint deprivation in RA (Choy and Panayi 2001).

MMP13 has an affinity to type II collagen (Knäuper, López-Otin et al. 1996), the predominant collagen in cartilage (Vachon, Keeley et al. 1990, Gelse, Pöschl et al. 2003), and, together with MMP1 and MMP3, is considered highly important in the pathogenesis of OA. MMPs need to be transformed from their non-active form to the active enzyme. A potent activator for this transformation is the complex of plasminogen activator (PA) and plasminogen (Pelletier, Martel-Pelletier et al. 2001). Expression of PA's urokinase-type receptor (uPAR) on chondrocytes is enhanced by IL-1β. This receptor controls pericellular proteolysis in cartilage degeneration and can be identified in OA, yet not healthy cartilage (Schwab, Gavlik et al. 2001, Schwab, Schulze-Tanzil et al. 2004).

Superparamagnetic iron oxide nanoparticles (SPIONs)

The past decade has seen a significant interest in the potentially varied biomedical applications of superparamagnetic iron oxide nanoparticles (SPIONs). Besides their use in imaging (Estelrich, Sánchez-Martín et al. 2015) and thermoablation therapy (Sawdon, Weydemeyer et al. 2014), their potential as a novel drug delivery system has been at the forefront of relevant research (Estelrich, Escribano et al. 2015). Hereby, SPIONs with a diameter of ≤100nm are most commonly used due to their adjustable shape and size, easy synthesis, high volume to surface ratio and capability to be conjugated to target specific antigens, peptides or antibodies (Malhotra and Prakash 2011, Xu and Sun 2013). In the context of arthritis, SPIONs were often used for cell tracking (Van Buul, Kotek et al. 2011) and imaging (Simon, von Vopelius-Feldt et al. 2006, Labens, Daniel et al. 2017). Although they are known to induce short term inflammation after intra-articular injection (2h to 24h) into healthy murine knee joints,

no aggravation of the condition was observed in diseased joints (Vermeij, Koenders et al. 2015).

Keeping the pivotal role of inflammation in arthritis in mind, targeting inflammation with new agents remains a key objective in the treatment of a complex joint disease and constitutes an interesting field for future research. In this respect, a potentially helpful tool is represented by ILP, an *ex vivo* technique that bridges the gap between *in vitro* and *in vivo* models. Such a system allows mimicking of inflammatory processes and, due to its functional blood supply, facilitates the study of drug delivery systems, and novel drug preparations, in the context of arthritis. The following chapter reports the results derived from a study investigating the application of ILP as model for cell migration and inflammation.

5.3 Materials and methods

5.3.1 Cell migration

Cell isolation and staining for the following perfusion experiments were conducted by Dr. Raphael Labens.

Joint injections relating to, and the harvesting and shipping of synovium samples obtained from, live animals were done by research assistants at North Carolina State University, College of Veterinary Medicine. Tissues were harvested during terminal procedures, in which students practiced their surgical skills. All of these procedures were approved by the Institutional Animal Care and Use Committee (Reference number 09-148-T).

SPIONs were synthesised and characterised by Dr. Xin-Rui Xia (Department of Biological Sciences, North Carolina State University, Raleigh, North Carolina, United States of America).

Histological staining (H&E, Giemsa) was performed by the Veterinary Pathology Unit of the Easter Bush Veterinary Centre.

Details of the following protocols have been described in Chapters 2.2, 2.5 and 2.6.

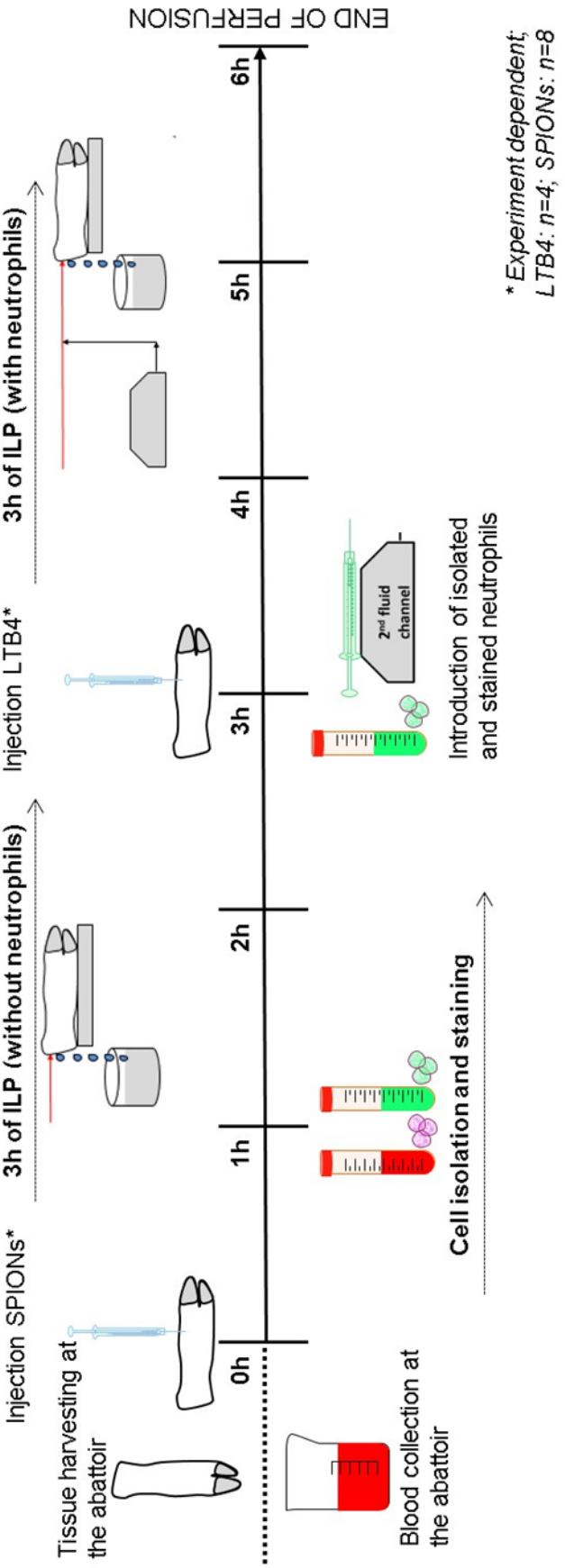
END OF PERFUSION
6h
5h
4h
3h
2h
1h
0h
3h of ILP (with neutrophils)
3h of ILP (without neutrophils)
Injection LTB4*
Injection SPIONs*
2nd fluid channel
Introduction of isolated and stained neutrophils
Cell isolation and staining
Tissue harvesting at the abattoir
Blood collection at the abattoir
* Experiment dependent; LTB4: n=4; SPIONs: n=8

Figure 5-1: Experimental timeline

After sample collection and transport to the laboratory, ILP was initiated. Simultaneously, neutrophils were isolated and stained. After three hours, neutrophils were connected to the system via a second fluid channel. Limbs were either injected with LTB4 (3h; n=4) or SPIONs (0h; n=8). At no time was the same chemoattractant used in the same experiment/joint. Carola Daniel undertook all sample harvesting and processing, the establishment, running and maintenance of the ILP experimental set-up and all injections. Dr. Raphael Labens undertook cell isolation and staining.

5.3.1.1 Cell isolation

Neutrophils were isolated from autologous heparinized (20.000IU/L) porcine blood collected at the time of exsanguination. The blood was aliquoted in 30mL tubes (Sarstedt) and transported back to the abattoir uncooled. After samples had settled for an hour on the bench, neutrophils were isolated by density gradient separation (Ficoll®-Paque, Sigma-Aldrich). The cells were then further suspended in 40ml HBSS without additives (ThermoFisher Scientific). Manual cell counts and cell viability assessments were performed using a haemocytometer. Cells were purified to a defined cell count per milliliter ranging from $5x10^6$ to $20x10^6$ cells/mL, which resulted in a standardised volume of neutrophils solution, sufficient for three hours of ILP. After a further centrifugation step, cells were again re-suspended in HBSS--.

5.3.1.2 Cell staining

Isolated neutrophils were stained with 5-chloromethylfluorescein diacetate (CMFDA) to facilitate their identification in synovium samples after conclusion of the perfusion. Two micrograms of CMFDA powder per milliliter were added to the tubes and the solution was incubated for 30min at room temperature followed by centrifugation at 1000rpm for eight minutes. Cells were subsequently washed twice, re-suspended in 5% porcine serum in HBSS-- and transferred to 20mL syringes (BD DiscarditTM II). The syringes were mounted into syringe pumps (IVAC® P6000 Mk II, Alaris® Medical Systems), which represented a second controlled fluid channel within the

perfusion system (flow rate: 10mL/h). The addition of neutrophils to the perfusate happened after 3h of ILP, which represented half of the experimental time.

5.3.1.3 Chemoattractants

At the same time point, to demonstrate the model's ability for neutrophil migration towards an intra-articular stimulus, the intra-articular injection of LTB_4 (a direct neutrophil chemoattractant) was performed. In a second phase of experiments LTB_4 was exchanged for SPIONs to assess their potential for neutrophil recruitment and to allow for comparison with previously collected tissue samples from live animal experiments (synovium samples provided by the North Carolina State University, College of Veterinary Medicine). In contrast to LTB_4, SPIONs were injected immediately prior to the start of perfusions. Limbs were either injected with LTB_4 (n=4) or SPIONs (n=8); at no time was the same chemoattractant used in the same experiment/joint.

The initially used chemoattractant was LTB_4. The injection was prepared from a 10µM stock solution (Sigma-Aldrich®) in ethanol by diluting respective aliquots with sterile water to 0.1µM. For corresponding sham injections, the same amount of ethanol (without LTB_4) was mixed with sterile water. Joints were injected at the 3h time point. As a second chemoattractant SPIONs were used. They were synthesised and characterised by Dr. Xin-Rui Xia (Department of Biological Sciences, North Carolina State University, Raleigh, North Carolina, United States of America), as described elsewhere (Nigam, Barick et al. 2011, Chang, Zhang et al. 2012, Labens, Daniel et al. 2017). The solution was purified to a concentration of 1mg/mL. Particles were washed with pure water three times during their synthesis. The third wash solution was used for sham injections. Intra-articular SPION-injections and their matched sham injections were performed immediately prior to the commencement of perfusions.

One auxiliary joint of a randomly assigned perfused limb was injected with the respective chemoattractant. The other auxiliary joint of the same limb was injected

with the designated sham fluid. The second hind limb of this animal was perfused under the same conditions with no injections and served as a "perfusion only" control. Joints were injected with a volume of 0.5mL.

Samples obtained from live animals were harvested from the femoropatellar joint 3h following the intra-articular injection of SPIONs.

5.3.1.4 Microscopy and histology

In order to identify stained neutrophils which migrated towards the injected intra-articular stimulus, multiphoton microscopy was used immediately following each perfusion experiment. Synovium was sampled from chemoattractant-injected auxiliary joints as well as from sham injected and non-injected joints for comparison. For orientation purposes during the search for stained cells, collagen fibres were visualised using the SHG principle. Synovium samples from respective joints were also submitted to the university's pathology department for H&E and Giemsa staining. Additionally respective pieces of equipment (e.g. tubing) were checked after use for neutrophil accumulation visible to the naked eye.

5.3.2 Reverse transcriptase quantitative PCR

5.3.2.1 Preparation, validation, and optimisation

Details of the following protocols have been described in chapters 2.5 and 2.6.
Synovium samples were harvested after six hours of ILP. Samples were derived from auxiliary joints of perfused specimens SPION injected (PNN), wash solution injected (PSN), non-injected (PCN)) and non-perfused controls (NP). To allow comparison with *in vivo* changes, tissue samples obtained from live animals under terminal general anaesthesia were also used for qPCR analysis (*in vivo*, SPION injected (VN) and sham injected (VS). These samples were harvested at the North Carolina State University from pigs used for teaching purposes. Samples were submerged in RNAlater, shipped

on dry ice and subsequently stored at -80°C. After the perfusion experiments, synovium samples were harvested for qPCR analysis, put into RNAlater® (ThermoFisher Scientific) and stored at -80°C until further processing.

Approximately 100mg of the frozen sample was minced and transferred to a liquid nitrogen cooled dis-membranator flask containing 500µL guanidinium thiocyanate-phenol (TRIzol, ThermoFisher Scientific). The flask was subsequently mounted into the dis-membranator (Oscillating mill MM200, Retsch) and subjected to a constant oscillation at a frequency of 30.0Hz for 90s. The remaining powder was scraped into an Eppendorf tube containing 500µL of TRIzol and mixed by shaking the tube. Samples were then stored at -80°C.

After thawing, the mixture was incubated for 45min at room temperature prior to centrifugation (11773.44rcf/12000rpm, 4°C; Centrifuge 5415 R, Eppendorf, rotor radius 73mm). The supernatant was then transferred to a clean tube and mixed with 200µL chloroform. The solution was incubated at room temperature for three minutes and centrifuged (4°C, 12000rpm) for a further 15min. The supernatant was decanted into another tube and washed with 400µL of 70% ethanol. All further steps followed the protocol of the commercially available RNeasy® Mini Kit (Qiagen). Purity of the extracted RNA was evaluated using the NandoDrop^{TM} 1000 Spectrophotometer (Thermo Scientific). The extracted RNA was converted to complementary DNA (cDNA) using the Omniscript® RT Kit (Qiagen) and samples were processed according to the suppliers handbook. Two negative controls were created from randomly assigned samples: no RT control (NRTC) and no template control (NTC). The final products were stored at -20°C.

Initial primer validation attempts were conducted on synovium samples of various origins (see Table 5-1); however, this approach yielded disappointing results. Subsequent primer validation attempts were therefore conducted on concanavalin (ConA) stimulated porcine peripheral blood mononuclear cells (PBMCs), as they are

known to sufficiently express most target genes of interest, thus permitting better validation of sequences (Dozois, Oswald et al. 1997).
To identify appropriate housekeeping genes (HKGs) and genes of interest (GOIs), self-designed primers were tested and sequences found in the relevant literature. Self-designed primers were identified using the publicly available Ensemble genome browser (www.ensembl.org). On the basis of these sequences, suitable primers were designed with Primer3web, version 4.1.0 (http://primer3.ut.ee/). Specificity of primers was confirmed with Primer Blast of NCBI (https://blast.ncbi.nlm.nih.gov/Blast.cgi) (Ye, Coulouris et al. 2012). Different thermal profiles and tissues were applied in the process (see Table 5-1).

For HKGs, the geNorm™ Reference Gene Selection Kit (Primerdesign Ltd) was ultimately used. To ensure the best outcome of the kit, samples were sourced from differently treated auxiliary joints (non-perfused limbs, perfused limbs, and perfused SPION injected limbs, n=4 for each group). Generated data was analysed with qbase+ (www.biogazelle.com) using the default M and V analysis tool.

To confirm whether the size of obtained products was consistent with the expected product size, gel electrophoresis was performed (1% agarose gel). Subsequently gels were assessed using Kodak's Gel Logic 200 Imaging System.

Table 5-1: Genes/ sequences tested unsuccessfully for qPCR experiments

Various primers were tested in the process of validation and optimisation of qPCR experiments. Sequences were found in the literature (numbers one to three), self-designed (number five) or commercially designed by Primerdesign Ltd (number four). For the geNorm kit used to identify the most appropriate HKG, sequences were not provided by the manufacturer. The validation process included the testing of different thermal profiles to increase primer efficiency (asteriks) and different tissues (letters a to d). The table shows sequences of primers which proved to be unsuitable for planned experiments for various reasons, including too low/high efficiency or suboptimal dissociation curves.

1) Sequence derived from the literature (Nygard, Jørgensen et al. 2007)

2) Sequence derived from the literature (Dozois, Oswald et al. 1997)

3) Sequence derived from the literature (Blitek, Waclawik et al. 2006)

4) Commercially designed primer (Primerdesign Ltd)

5) Self-designed primer

a) Tested on synovium from a with neutrophils perfused limb, joint LTB_4 injected

b) Tested on synovium from a freshly slaughtered pig, no further processing

c) Tested on pooled synovium samples from perfused and non-perfused limbs

d) Tested on ConA stimulated PBMCs

*) Tested with various thermal profiles

Gene	Sequence (left)	Sequence (right)
Housekeeping Genes		
HPRT1	GGACTTGAATCATGTTTGTG[1a*]	CAGATGTTTCCAAACTCAAC[1a*]
ACTB	CACGCCATCCTGCGTCTGGA[1a*]	AGCACCGTGTTGGCGTAGAG[1a*]
	GGACTTCGAGCAGGAGATGG[2cd]	GCACCGTGTTGGCGTAGAGG[2cd]
	geNorm™ Reference Gene Selection Kit [4]	geNorm™ Reference Gene Selection Kit [4]
B2M	CAAGATAGTTAAGTGGGATCGAGAC[1a]	TGGTAACATCAATACGATTTCTGA[1a]
	geNorm™ Reference Gene Selection Kit [4]	geNorm™ Reference Gene Selection Kit [4]
Cyclo-phillin	TAACCCCACCGTCTTCTT[2cd]	TGCCATCCAACCACTCAG[2cd]
	AGAAGGCCTGGACGTCTTG[d*]	CGTACTCCCCACAGTCAGAG[d*]
	TGGCTCCCAGTTCTTCCTG[d*]	ATGATCACCTTCTGCTTGGG[d*]
GPI	geNorm™ Reference Gene Selection Kit [4]	geNorm™ Reference Gene Selection Kit [4]
UBC	geNorm™ Reference Gene Selection Kit [4]	geNorm™ Reference Gene Selection Kit [4]
GAPDH	ACACTCACTCTTCTACCTTTG[1a*]	CAAATTCATTGTCGTACCAG[1a*]
	TTCCACTTTTGATGCTGGGG[d*]	CCACCACCCTGTTGCTGTA[d*]
Genes of Interest		
TNF-α	GATCATCGTCTCAAACCTCAGA[b*]	CAGGAGGGCATTGGCATA[b*]
	ATCGGCCCCCAGAAGGAAGAG[2cd]	GATGGCAGAGAGGAGGTTGAC[2cd]
	AACCTCAGATAAGCCCGTCG[d*]	GCATACCCACTCTGCCATTG[d*]
IL-1β	TGACAACAATAATGACCTGTTATTTG[b*]	TCCAGGTTTTGGGTGCAG[b*]
	AAAGGGGACTTGAAGAGAG[2cd]	CTGCTTGAGAGGTGCTGATGT[2cd]
IL-6	ATGAACTCCCTCTCCACAAGC[2cd]	TGGCTTTGTCTGGATTCTTTC[2cd]
	TGTCGAGGCTGTGCAGATTA[d*]	GCATTTGTGGTGGGGTTAGG[d*]
IFN-γ	GTTTTTCTGGCTCTTACTGC[2cd]	CTTCCGCTTTCTTAGGTTAG[2cd]
	TGGTAGCTCTGGGAAACTGA[d*]	TGATGAGTTCACTGATGGCTT[d*]
COX-1	GGGAGTCCTTCTCCAATGTG[3cd]	CATAAATGTGGCCGAGGTCT[3cd]
	CTGAAGCCCTACACCTCCTT[d*]	CTGGGTAGAACTCCAAGGCA[d*]
	CAGCCCTTCAATGAGTACCG[d*]	AACTCAGCTGCCATCTCCTT[d*]
COX-2	ATGATCTACCCGCCTCACAC[3cd]	AAAAGCAGCTCTGGGTCAAA[3cd]
	CTGCTGAGTTTAACACACTCTACC[4d]	GATGCCATGTTCCAGTAAGATAGAG[4d]
MMP1	TGTTCAGCTGTCCCAAGATG[b*]	GAACGGGGTTTTCGGAAG[b*]
MMP3	CCTGCCCAAGTGGAGAAA[b*]	AATGGTAGAATCAATAACACTTCTTGG[b*]

Table 5-2: Final oligonucleotides

Primers used in qPCR with an annealing temperature of 60°C. The first four rows show the left and right sequences of housekeeping genes respectively. Sequences of the GOI primers are displayed below. Commercially designed primers were designed by Primerdesign Ltd and are marked with an asterisk.

Primer	Sequence (5'-3')	Product size (bp)
Left GAPDH*	geNorm™ Reference Gene Selection Kit	/
Right GAPDH*	geNorm™ Reference Gene Selection Kit	
Left ATP5G1*	geNorm™ Reference Gene Selection Kit	/
Right ATP5G1*	geNorm™ Reference Gene Selection Kit	
Left TNF-α	CTCAAACCTCAGATAAGCCCG	124
Right TNF-α	TGGTTGTCTTTCAGCTTCACG	
Left IL-1β*	CCTCTCCAGCCAGTCTTCAT	126
Right IL-1β*	GCCATCAGCCTCAAATAACAG	
Left IL-6	ACCGGTCTTGTGGAGTTTCA	149
Right IL-6	GTGGTGGCTTTGTCTGGATT	
Left IFN-γ	GGTAGCTCTGGGAAACTGAATG	150
Right IFN-γ	CTGACTTCTCTTCCGCTTTCT	
Left COX-1*	GGAAGAAGCAGTTGCCAGATG	142
Right COX-1*	CCAGAAGTCTTGAAGAACTGGTG	

Table 5-3: Standardised thermal profile

Number of cycles	Stage	Temperature in °C	Time in seconds
1	**Activation**	95	120
	Amplification		
40	Denaturation	95	10
	Data collection	60	60
	Dissociation	95	60
1		55	30
		95	30

5.3.2.2 Data processing

For the purpose of qPCR analysis, samples were limited to the six potentially most interesting groups and to four to five samples per group, to allow a single 96-well plate to accommodate all samples per GOI (see Table 5-4). Plates were run in duplicates.

The qPCR data obtained were processed with an adapted 2-ΔΔ method described by Livak et al. (Livak and Schmittgen 2001).

Table 5-4: Experimental groups for qPCR analysis

For qPCR analysis, samples have been divided into six experimental groups. For all perfused groups, neutrophils were added to the perfusate after three hours of perfusion time. Auxiliary joints were either injected with a SPION solution as chemoattractant (PNN) or with the wash solution used in the process of SPION synthesis as sham injection (PSN). In a third perfused group, serving as control, no joints were injected at all (PCN). These perfused groups are to be compared to a non-perfused limb resting at room temperature for the duration of the experiments (NP) and to tissues from injected joints (SPION or wash solution) of live animals under general anaesthesia (VN and VS respectively).

Experimental Groups		Sample size n
PNN	**P**erfused, **N**anoparticles injection, **N**eutrophils	5
PSN	**P**erfused, **S**ham injection, **N**eutrophils	5
PCN	**P**erfused, **C**ontrol (no injection), **N**eutrophils	5
NP	**N**on-**P**erfused	5
VN	*In **V**ivo*, **N**anoparticles injection	4
VS	*In **V**ivo*, **S**ham injection	4

5.3.3 Statistical analysis

All data were statistically analysed using commercially available (Minitab17, Statistical Software). An analysis of variance was performed (one-way ANOVA) and as *post-hoc* test a Fisher pairwise comparison was applied.

5.4 Results

5.4.1 Cell migration

No difference in cell migration could be detected amongst groups with different concentration of neutrophils. No obvious accumulation of neutrophils within the perfusion system (e.g. tubing) could be observed. In the venous return samples LDH activity was not increased after introduction of neutrophils into the system. This would have been considered indicative for a large amount of neutrophils being flushed out of the limb (see Chapter 4.3.3).

Multiphoton microscopy failed to identify the presence of large number of neutrophils in synovium samples. A few sporadic neutrophils could be seen in selected synovium samples from SPIONs injected joints. No neutrophils were visible in samples of LTB_4-, sham- and non-injected joints. Similarly, histologic assessment of samples (H&E, Giemsa) failed to identify large numbers of inflammatory cells. Random microscopical assessment of blood vessels and connective tissue of selected limbs further substantiated these findings.

Presented images are exemplary and are all derived from a SPION injected joint of one perfused porcine limb. However due to processing requirements, images are obtained from different pieces of the harvested synovium. It was not possible to perform histological examination on the same piece of synovium that was used for multiphoton microscopy.

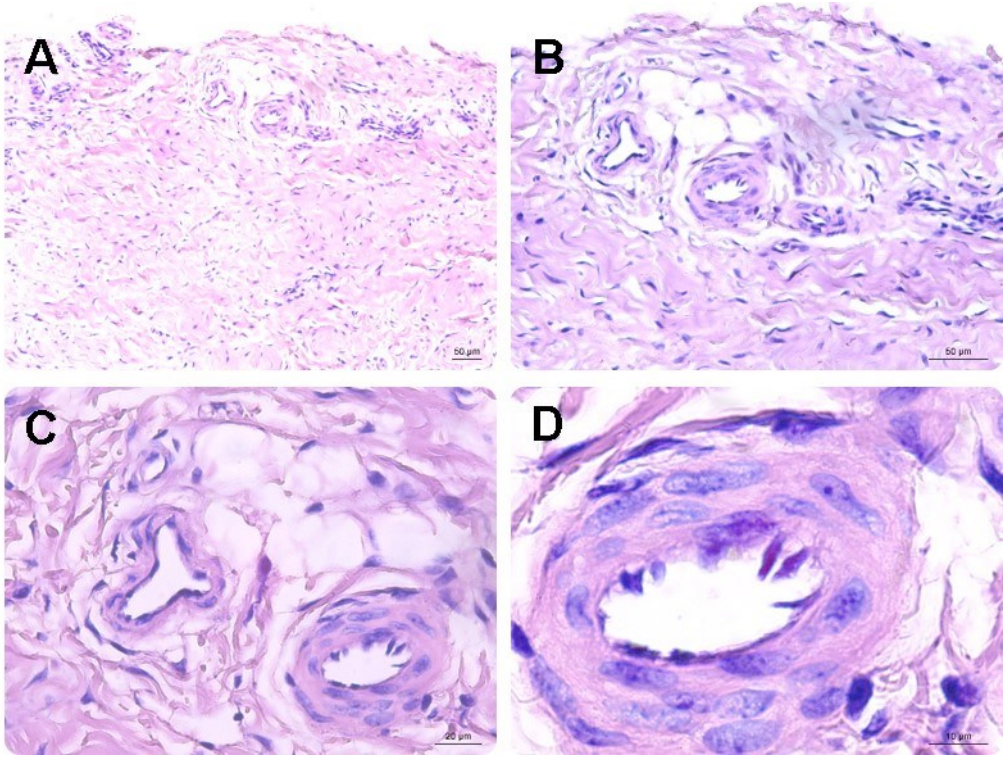

Figure 5-2: Synovium; SPION injected joint; H&E staining

Cells with a characteristic neutrophil appearance could not be detected in the H&E stained samples, neither in the tissue (**A** and **B**) nor within the blood vessels (**C** and **D**). This may have been attributable to technical problems in cell migration experiments. In addition, handling of delicate synovium samples made histological processing difficult, which could lead to suboptimal results. H&E staining; Nikon E600; magnification 10x, 20x, 40x and 100x respectively.

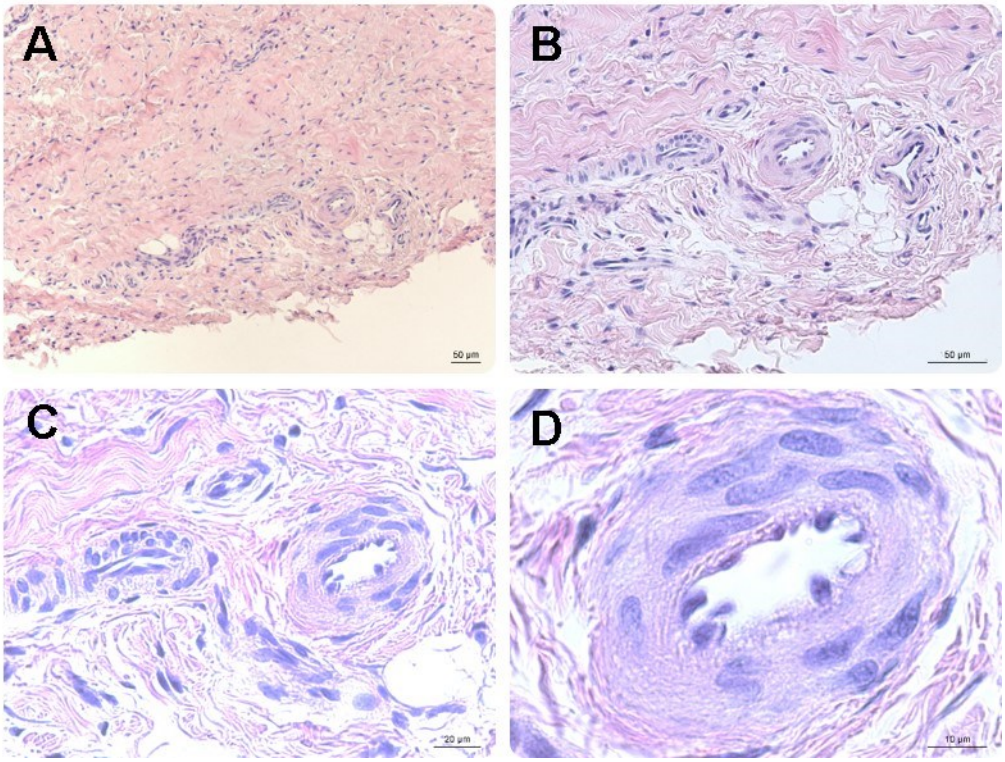

Figure 5-3: Synovium; SPION injected joint; Giemsa staining

Cells with a characteristic neutrophil appearance could not be detected in the Giemsa stained samples, neither in the tissue (**A** and **B**) nor within the blood vessels (**C** and **D**). However, synoviocytes seemed to be slightly more macrophage shaped rather than displaying a clear fibroblast phenotype, a finding potentially consistent with the presence of early inflammation (Davies 1946, Barland, Novikoff et al. 1962). Giemsa staining; Nikon E600; magnification 10x, 20x, 40x and 100x respectively.

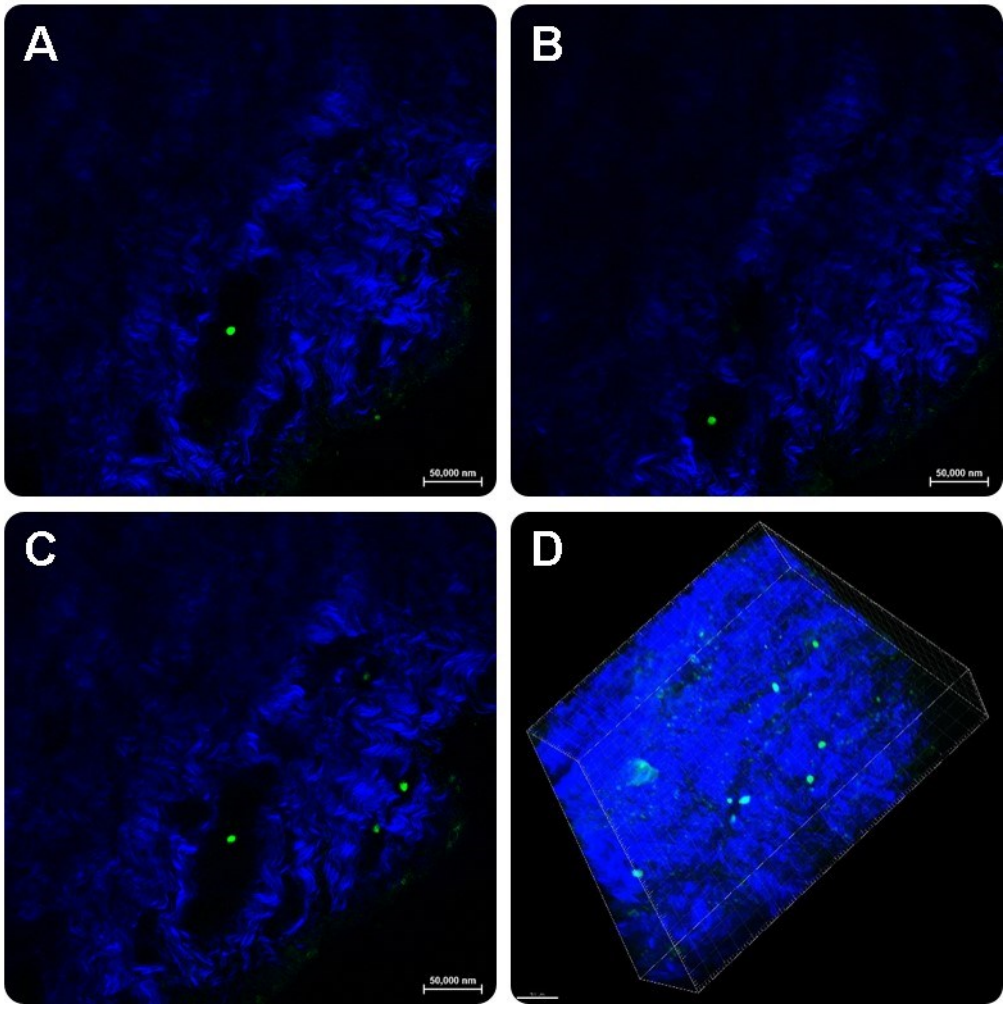

Figure 5-4: Synovium; SPION injected joint; multiphoton and Imaris (1)

In selected synovium samples from SPION injected joints, few neutrophils (green) could be detected in 2D (**A**, **B** and **C**) and 3D (**D**) samples. Collagen fibres (blue) were visualised using the SHG principle and served as a first reference point for orientation and focusing within the sample. Green background noise is attributed to SPIONs' autofluorescent properties. Neutrophils: CMFDA stained, green; collagen: SHG principle, blue, multiphoton microscope, Imaris (Bitplane, Switzerland).

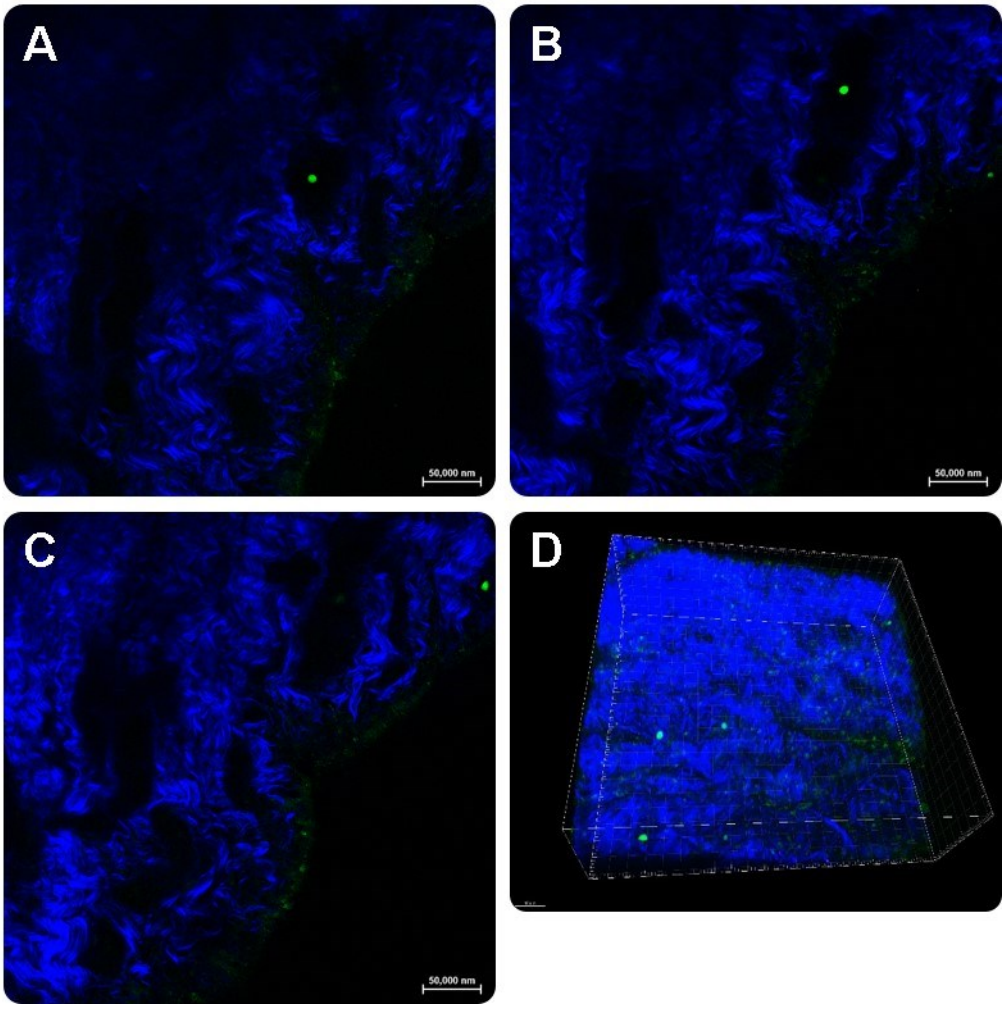

Figure 5-5: Synovium; SPION injected joint; multiphoton and Imaris (2)

In selected synovium samples from SPION injected joints, few neutrophils (green) could be detected in 2D (**A**, **B** and **C**) and 3D (**D**) samples. No neutrophils were detected in any of the other groups (LTB_4 injected, sham injected, non-injected). However, in the context of expected cell migration and the amount of neutrophils, which were introduced into the system, cell migration experiments did not work as hypothesised. Neutrophils: CMFDA stained, green; collagen: SHG principle, blue, Multiphoton microscope, Imaris (Bitplane, Switzerland).

5.4.2 Reverse transcriptase quantitative PCR

Primer efficiency for GOIs was reasonable for sample cDNA concentrations ranging between 10 to 2.5ng per reaction (COX-1: 78.8%; IFN-γ: 82%; TNF-α: 84.7%; IL-1β: 83.7%; IL-6: 98.6%). Therefore, 5ng per reaction were used in main experiments, which matches the manufacturer's recommendations. Sufficient primer quality could not be achieved for COX-2, MMP1 and MMP3.

To ensure the use of optimal HKGs, a commercial kit was ultimately used. Variability of samples proved to be comparatively high, which necessitated the use of two HKGs. GAPDH and ATP5G1, the two most stably expressed HKGs, were picked and obtained data normalised against the geometric mean of both.

Up- or downregulations by more than two fold and hence ΔΔCt values of more than one were considered to represent genuine differences in gene expression. These values were interpreted in light of the accompanying p-values obtained from the one-way-ANOVAs. An overview over groups can be found in Table 5-4: Experimental groups for qPCR analysisTable 5-4.

Table 5-5: Results of ANOVA and *post-hoc* tests

A one-way ANOVA was performed to inform on differences between groups (p=0.047). Hypothetically, groups PNN and VN should display a significantly higher inflammatory gene expression than their respective controls (PSN, VS). The functionality of the ILP model and its suitability to provide translational data to live animals would be supported by the absence of any significant difference in inflammatory gene expression between groups PNN and VN, indicating similar in vivo- and ex vivo-derived results. Sham injected, non-injected and non-perfused limbs should not be different from their respective controls (PSN/PCN, PCN/NP), as this shows that neither perfusion nor sham injection alters the inflammatory pattern in synovium samples.

PNN: perfused, nanoparticle; **PSN**: perfused, sham; **PCN**: perfused, control; **NP**: non-perfused; **VN**: in vivo, nanoparticle; **VS**: in vivo, sham

Research question	Groups compared	Statistically significant difference Y/N and p-value				
		COX-1	IFN-γ	TNF-α	IL-1β	IL-6
Does a SPION injection have a pro inflammatory effect in perfusion experiments?	PNN vs. PSN	N p=0.294	N p=0.286	N p=0.078	Y p=0.002	Y p=0.030
Does a sham injection have a pro inflammatory effect in perfusion experiments?	PSN vs. PCN	N p=0.662	N p=0.697	N p=0.340	N p=0.156	N p=0.264
Does perfusion itself cause an inflammatory gene profile in the specimen?	PCN vs. NP	N p=0.848	N p=0.971	N p=0.585	N p=0.553	N p=0.652
Does a SPION injection have a pro inflammatory effect *in vivo*?	VN vs. VS	N p=0.779	N p=0.155	N p=0.963	N p=0.747	N p=0.523
Is there a difference between the inflammatory profiles following SPION injection in perfusion experiments and *in vivo*?	PNN vs. VN	N p=0.350	N p=1.00	N p=0.146	N p=0.582	N p=0.223
Is there a difference between the inflammatory profiles following sham injection in perfusion experiments and *in vivo*?	PSN vs. VS	Y p=0.034	N p=0.396	N p=0.854	Y p=0.020	Y p=0.011

Table 5-6: ΔΔCt, up/ down regulation and fold change for all GOIs and their respective experimental groups

To answer the research questions of interest, various groups have been compared. Comparisons were made per GOI. The ΔΔCt value represents the difference between the ΔCt value of an experimental group and a respective control group. A value of zero therefore stands for no difference between groups. To calculate the fold change in gene expression log2(ΔΔCt). In case of ΔΔCt being zero, log2(0) would have a value of one. Hence a fold change of one represents no difference between compared groups.

The terms up/ down regulation refer to an in-/ decreased expression in the experimental group relative to its control group.

PNN: perfused, nanoparticle; **PSN**: perfused, sham; **PCN**: perfused, control; **NP**: non-perfused; **VN**: *in vivo*, nanoparticle; **VS**: *in vivo*, sham

Gene	Control Group	Experimental Group	ΔΔCt Value	Up/Down Regulation	Fold Change	P Value
COX-1	PSN	PNN	1.35	**up**	**2.56**	0.294
	PCN	PSN	-0.56	down	1.47	0.662
	NP	PCN	-0.24	down	1.18	0.848
	VS	VN	-0.40	down	1.31	0.779
	VN	PNN	-1.28	**down**	**2.42**	0.350
	VS	PSN	-3.03	**down**	**8.16**	**0.034**
IFN-γ	PSN	PNN	0.62	up	1.54	0.286
	PCN	PSN	0.23	up	1.17	0.697
	NP	PCN	0.99	up	1.01	0.971
	VS	VN	-0.94	down	1.92	0.155
	VN	PNN	1.04	**up**	**2.06**	1.00
	VS	PSN	-0.52	down	1.44	0.396
TNF-α	PSN	PNN	2.19	**up**	**4.56**	0.078
	PCN	PSN	0.80	up	1.74	0.340
	NP	PCN	1.01	**up**	**2.01**	0.585
	VS	VN	0.06	up	1.04	0.963
	VN	PNN	1.90	**up**	**3.70**	0.146
	VS	PSN	-0.23	down	1.17	0.854
IL-1β	PSN	PNN	4.72	**up**	**26.47**	**0.002**
	PCN	PSN	1.96	**up**	**3.89**	0.156
	NP	PCN	-0.76	down	1.69	0.553
	VS	VN	0.46	up	1.37	0.747
	VN	PNN	0.74	up	1.67	0.582
	VS	PSN	-3.52	**down**	**11.50**	**0.020**
IL-6	PSN	PNN	3.26	**up**	**9.58**	**0.030**
	PCN	PSN	1.61	**up**	**3.04**	0.264
	NP	PCN	0.64	up	1.56	0.652
	VS	VN	1.02	**up**	**2.02**	0.523
	VN	PNN	-1.86	**down**	**3.64**	0.223
	VS	PSN	-4.11	**down**	**17.23**	**0.011**

COX-1

A comparison between PNN and PSN showed an apparent, although non-significantly (p=0.294) greater (2.56 fold; ΔΔCt=1.35) COX-1 gene expression in treated limbs. A comparison between PNN and an *in vivo* SPION-injection showed an apparent, although non-significantly (P=0.350) lower (2.42 fold; ΔΔCt=-1.28) COX-1 gene expression in the PNN specimen. In comparison, there was a significantly (p=0.034) lower (8.16 fold; ΔΔCt=-3.03) COX-1 gene expression in the perfused sham injected joints (PSN) compared with the *in vivo* sham injected joints (VS).

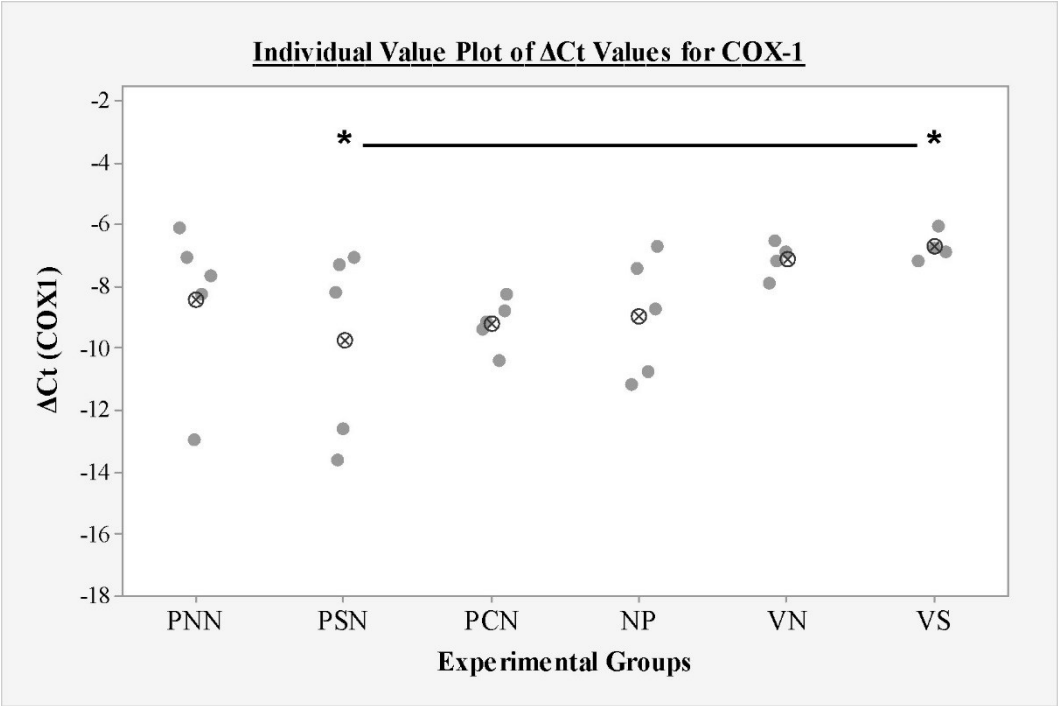

Figure 5-6: Individual value plot of ΔCt values for COX-1

Analysis of COX-1 gene expression failed to indicate upregulation of this GOI in SPION injected joints. However the statistical analysis did reveal a statistically significant difference (p=0.034) between perfused and *in vivo* sham injected joints (VS vs. PSN). This may have been attributable to the use of a cell free perfusate and the associated lack of opportunity for neutrophil migration which may have negatively influenced inflammatory gene expression in the synovial samples. Alternatively, pre-existing joint inflammation, contaminated wash solution or technical problems during intra-articular injection in the *in vivo* specimens may also have contributed to the differences noted. It should be noted that variability of *in vivo* data is low and derived from four different pigs. Graph shows results of

post-hoc test (Fisher pairwise comparison). Crossed circles indicate mean values. Asterisks indicate statistically significant differences.

IFN-γ

The expression of IFN-γ was relatively similar in all groups, with no statistically significant difference between groups.

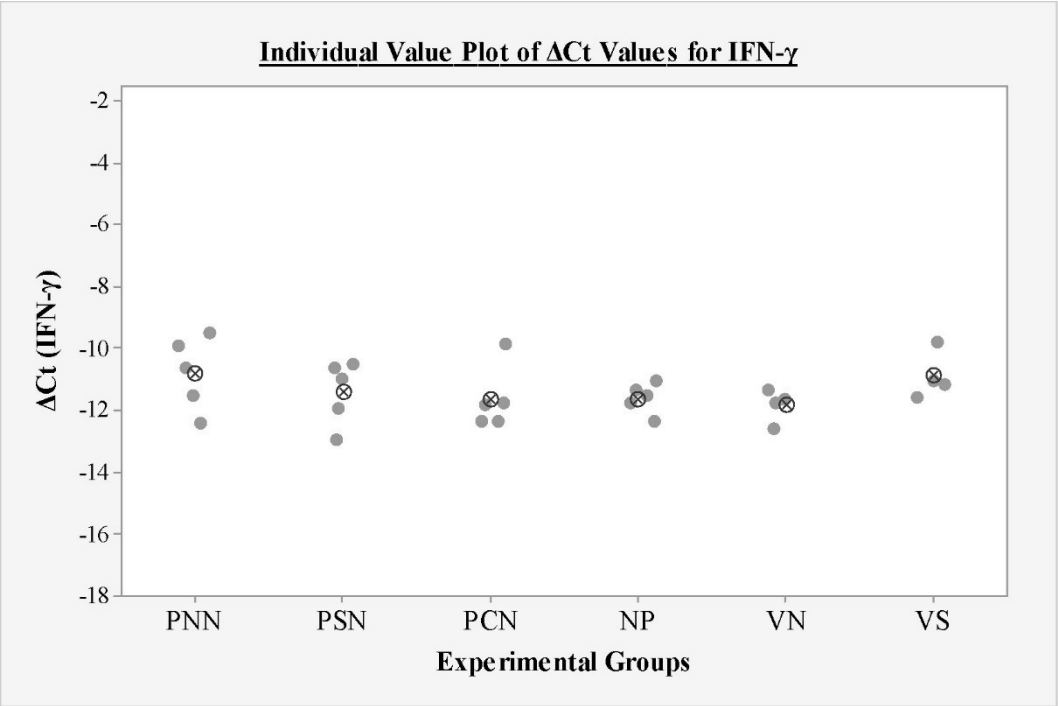

Figure 5-7: Individual value plot of ΔCt values for IFN-γ

No statistically significant differences could be detected between any of the tested groups for IFN-γ expression. Crossed circles indicate mean values. Graph shows results of *post-hoc* test (Fisher pairwise comparison).

TNF-α

Despite an apparently greater (4.56 fold, ΔΔCt=2.19) TNF-α expression in PNN joints, compared with the PSN joints; although not statistically significant, it did approach significance (p=0.078). The apparently greater (3.7 fold, ΔΔCt=1.90) TNF-α expression in the PNN joints, compared with the VN joints was not statistically significant (p=0.146). There was no significant difference (p=0.585) in TNF-α expression between control perfused joints (PCN) and non-perfused limbs (NP).

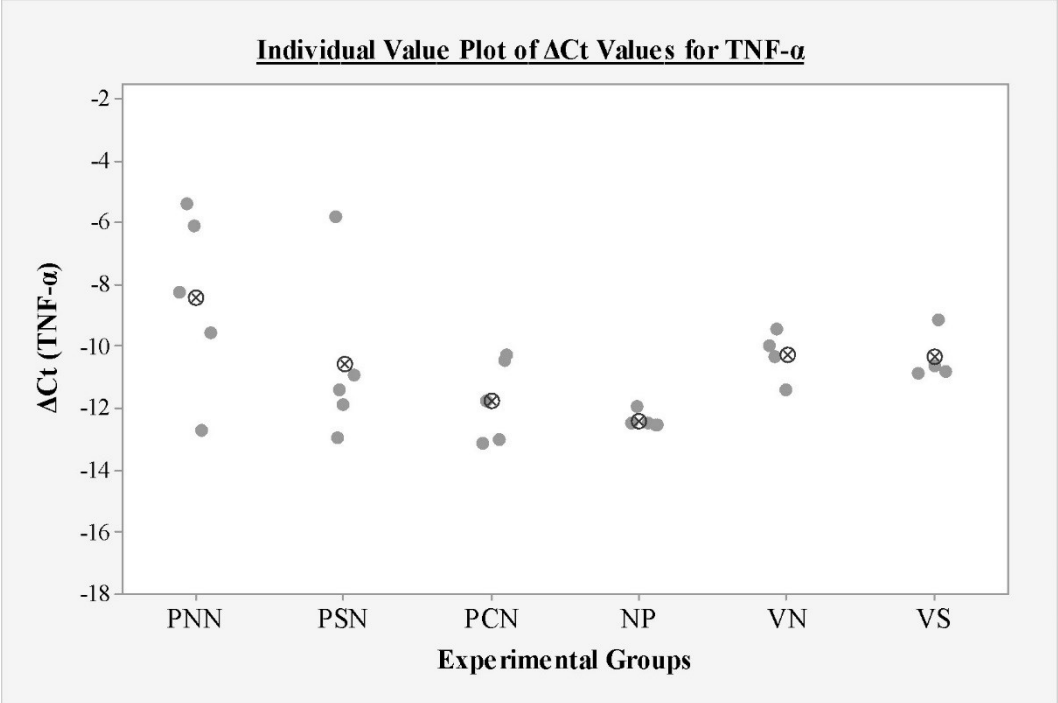

Figure 5-8: Individual value plot of ΔCt values for TNF-α

Analysis of variance failed to produce statistically significant differences between selected groups. However a trend towards upregulation of TNF-α in perfused limbs injected with SPIONs, compared to sham injected limbs (i.e. PNN vs. PSN) could be appreciated (p=0.078). Graph shows results of *post-hoc* test (Fisher pairwise comparison). Crossed circles indicate mean values.

IL-1β

Perfused and SPION injected joints (PNN) had a markedly (26.47 fold; ΔΔCt=4.72) and significantly (p=0.002) greater IL-1β expression, compared with sham injected perfused joints (PSN). Sham injected perfused joints (PSN) had a significantly (p=0.02) lower (11.5 fold; ΔΔCt=-3.52) IL-1β expression compared with *in vivo* sham injected joints (VS).

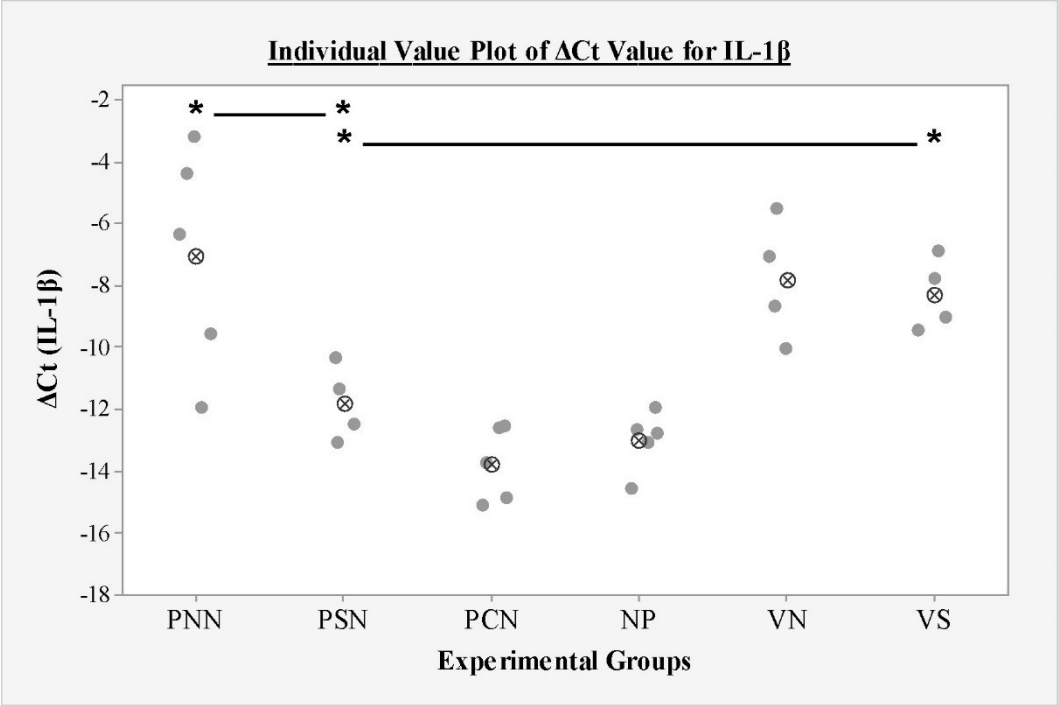

Figure 5-9: Individual value plot of ΔCt values for IL-1β

SPION injected perfused joints (PNN) had a significantly greater (p=0.002) IL-1β expression than sham injected (PSN) perfused joints, indicating a pro inflammatory effect. There was no significant difference between (p=0.747) sham injected (VS) and SPION injected (VN) *in vivo* samples, with sham injected *in vivo* samples (VS) having a significantly (p=0.020) greater IL-1β expression than perfused sham injected (PSN) joints. The differences (VS vs PSN) and lack of differences (VN vs VS) noted may could be attributable to the use of a cell free perfusate and failed neutrophil migration. These circumstances might have led to a lack of opportunity for changes in the inflammatory gene expression in PSN synovial samples. Additional factors which resulted in inflammation in the joints of live animals may also have contributed to the results obtained. Graph shows results of *post-hoc* test (Fisher pairwise

comparison). Crossed circles indicate mean values. Asterisks indicate statistically significant differences.

IL-6

IL-6 analyses showed similar trends to the IL-1β analyses. Perfused SPION injected joints (PNN) had a significantly (P=0.03) greater (9.58 fold, ΔΔCt=3.26) IL-6 expression compared with perfused sham injected joints (PSN). There was no significant difference (p=0.223) in IL-6 expression between perfused SPION injected joints (PNN) joints and *in vivo* SPION injected joints (VN). As with the IL-1β expression, perfused sham injected joints (PSN) had a significantly (p=0.011) lower (17.23 fold; ΔΔCt=-4.11) IL-6 expression than *in vivo* sham injected joints (VS).

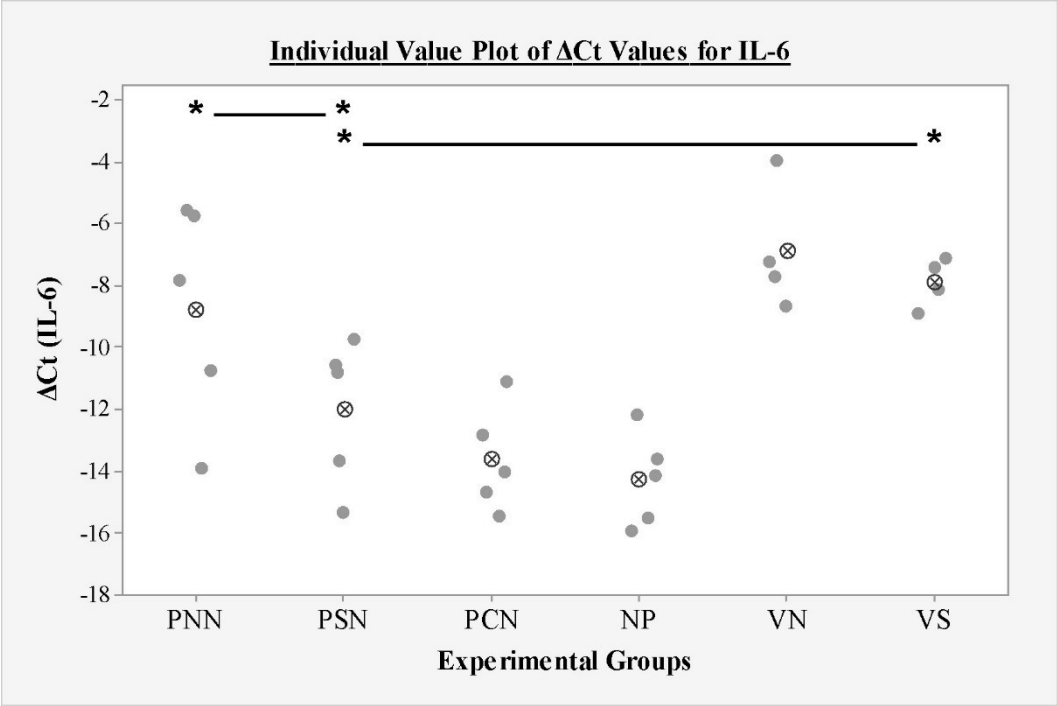

Figure 5-10: Individual value plots of ΔCt values for IL-6

For IL-6 the same statistically significant differences could be observed as for IL-1β. Increased IL-6 expression in PNN, compared with PSN was significant (p=0.030). *In vivo* sham-injected joints (VS) had a significantly greater (p=0.011) IL-6 expression than perfused sham-injected limbs (PSN). The differences (VS vs PSN) and lack of differences

(VN vs VS) noted may could be attributable to the use of a cell free perfusate and failed neutrophil migration. These circumstances might have led to a lack of opportunity for changes in the inflammatory gene expression in PSN synovial samples. Additional factors which resulted in inflammation in the joints of live animals may also have contributed to the results obtained. Graph shows results of *post-hoc* test (Fisher pairwise comparison). Crossed circles indicate mean values. Asterisks indicate statistically significant different results.

5.5 Discussion

5.5.1 Cell migration

Multiphoton and histology

When the study was conducted, the use of multiphoton microscopy in the given context has not been described elsewhere. It could therefore be hypothesised that flaws in the technique may have prohibited detection of neutrophils in synovium samples. To make sure that the sample could be detected under the multiphoton microscope and to allow orientation within the sample, collagen fibres were visualized using the SHG principle (Fine and Hansen 1971, Han, Giese et al. 2005, Su, Chen et al. 2011). Collagen could be detected without difficulties in all samples, which indicates functionality of the technique. Autofluorescence of used nanoparticles was also visible, further supporting the suitability of the method. Moreover, few genuine neutrophils were detected in selected samples, thus confirming that, following perfusion, their presence in the synovium can be visualised with multiphoton microscopy and that the cell staining worked as intended. These points strongly support the applicability of the adopted method of neutrophil detection. Furthermore, no neutrophils were visible by histopathological examination (H&E, Giemsa). Histology is a very well established technique and has been used to successfully to show neutrophil aggregation within the vessels of an LPS-challenged perfused equine limb (Patan-Zugaj, Gauff et al. 2012).

Perfusion system

The failure to detect neutrophils in synovium samples raises a question regarding their fate within the system. It is possible that the injected neutrophils adhered to parts of the perfusion system, thus not reaching the synovial capillaries. In early preliminary experiments, such a phenomenon could be observed; namely, the adherence of neutrophils to a rubber cap in used syringes. Following awareness of this occurrence, respective pieces of equipment were exchanged for better suited options (e.g. syringes of a different material). Although there was no grossly visible adherence of cellular debris to the hardware in the present study, additional microscopic assessment of used equipment could have provided further retrospective confirmation of whether neutrophils were lost throughout the length of the perfusion system. In contrast, preliminary experiments did reveal evidence (including macroscopic evidence) of neutrophil accumulation in syringes and connection pieces (3-way-tap). Initial attempts to minimize this occurrence by positioning syringe pumps on rocker plates was found to be technically unfeasible. Therefore the final perfusion system relied on regular manual shaking of the syringes and gentle flushing of the 3-way-taps to minimize cellular accumulation at these locations. At the time neutrophils and perfusate met within the 3-way-tap the perfusate had body temperature (see Chapter 3). An impairment of neutrophil function due to exposure to hyperthermia can therefore be ruled out.

In early experiments neutrophils were re-suspended in HBSS++, containing magnesium and calcium. As these components are known to activate neutrophils (Simchowitz and Spilberg 1979, Grzesiak and Pierschbacher 1995) and increase their tendency to adhere to equipment, subsequent experiments used HBSS--devoid of these electrolytes. Consequently, neutrophils were only exposed to magnesium and calcium at the point where they entered the limb, when they were exposed to the perfusate. While this alteration in the neutrophil suspension fluid likely minimized the chance of adherence within the system, even the short-term exposure to calcium and magnesium within the perfusate might have compromised the responsiveness of neutrophils to the chemoattractant. This responsiveness may have been further compromised by the fact

that the open circuit experimental set-up only permits a single exposure of circulating neutrophils to the inflammatory stimulus. Although a closed system would potentially yield better results in terms of cell migration, this would necessitate the design of a new perfusate to meet the metabolic demands of the neutrophils and maintain their viability and functionality for several hours. Furthermore, neutrophils which are activated through repeated exposures to an inflammatory stimulus, resulting from the continuous circulation of perfusate, are more likely to adhere to the tubing, thus presenting additional technical challenges.

Limb

It is also possible that the failure to detect neutrophils within the synovial samples may be partly attributable to random migration into tissues or accumulation within the vasculature of the perfused limb. Despite Patan et al. (2014) observing marked margination and accumulation of calprotectin-positive cells within the lumen of laminar blood vessels in an endotoxin challenged perfused equine distal limb, there was limited cellular extravasation into tissues, even after ten hours perfusion in a closed system (Patan-Zugaj, Gauff et al. 2014). Although a similar phenomenon might theoretically explain the dearth of tissue neutrophils identified in the current study, histological and multiphoton microscopy based examination also failed to identify neutrophil accumulation within blood vessels in tissue samples obtained from randomly assigned limbs. Skin and connective tissue from the injection site as well as very distal areas of the limb were also assessed microscopically in randomly assigned specimens to shed light on the neutrophil's fate. However no neutrophils could be identified. In hindsight, a more targeted and extensive histological assessment of the vasculature and other tissues may have provided more information on the fate of the infused neutrophils. A further refinement to the methodology might have involved the use of immunohistochemistry when analysing synovium samples, using neutrophil markers such as myeloperoxidase (MPO) (Patan-Zugaj, Gauff et al. 2014), an enzyme found in neutrophils granulocytes which plays an important antimicrobial role (Pinkus and Pinkus 1991).

Venous return

The use of MPO assays was considered a feasible means of detecting the presence of neutrophils in the venous return (VR) samples. As previously mentioned, LDH assays were used to provide information on tissue viability (see Chapter 4.3.3) therefore it was hypothesized that an abundance of flushed out neutrophils in the VR samples would have resulted in a significant increase in LDH activity. As the failure to identify such an elevation in LDH activity was consistent with the absence of a significant number of neutrophils, it was decided to refrain from MPO assays, which effectively rely on the same principal; namely, indirect evidence of neutrophilic presence via the detection of a neutrophil-derived enzyme. It is however possible that the LDH assay was insufficiently sensitive to detect low numbers of neutrophils.

Chemoattractants

Non-efficient chemoattraction was considered to be another potential reason underlying the absence of large numbers of neutrophils in the synovium samples. LTB_4 has been described in the literature as a potent neutrophil chemoattractant (Chou, Kim et al. 2010). Why it failed to recruit neutrophils in sufficient numbers in the presented work is not fully understood; although, potential reasons include an insufficient intra-articular concentration of the chemoattractant or diffusion of LTB_4 out of the joint shortly after intra-articular injection. However, as mentioned earlier, multiphoton microscopic examination of exemplary tissue samples obtained from the injection site failed to reveal a neutrophil accumulation in tissues surrounding the joint. A further explanation might be an insufficient duration of exposure of the neutrophils to the LTB_4, a factor directly related to the use of an open system.

Following failure of the LTB_4 experiments to reveal a detectable level of neutrophilic attraction, SPIONs were used as alternative chemoattractant. Reports within the scientific literature confirm histological evidence of inflammatory cell influx 24h following intra-articular SPION injection (Vermeij, Koenders et al. 2015). Moreover the potential of SPIONs to act as a chemoattractant within an hour of exposure has been demonstrated in transwell migration assays (Labens, Daniel et al. 2017). Overall,

the interactions of SPIONs with healthy cells are not yet fully understood (Singh and Nalwa 2007, Patil, Adireddy et al. 2015). A more conservative approach may have been to use intra-articular LPS injections as a means of recruiting neutrophils (Tanaka, Kagari et al. 2006). This approach is very well established in a broad variety of research applications and may have been more applicable to the validation of a new model. However, in light of the limited number of pigs, the available published and unpublished data generated by the research group, the overarching area of research activity of the group, and the unique possibility of a comparison to *in vivo* data, it was agreed to maintain focus on the effect of intra-articular SPION injections as a stimulus for neutrophilic attraction.

5.5.2 Reverse transcriptase quantitative PCR

Ideally, for qPCR experiments, primer efficiency should be as close as possible to 100%, with efficiencies between 90 and 110% commonly considered appropriate (Bustin, Benes et al. 2009). Although primers used in the presented work did not always meet this criterion (COX-1: 78.8%; IFN-γ: 82%; TNF-α: 84.7%; IL-1β: 83.7%; IL-6: 98.6%), dissociation and melting curves of the primers used appeared to be very clean. Within the financial limits of the project an extensive assessment of RNA integrity numbers (RIN) for all samples was not possible. However, exemplary RNA samples were tested for quality using the Agilent TapeStation, and the RIN values obtained were within acceptable limits. It was therefore decided that the slightly lower primer efficiencies were acceptable. Nonetheless, when interpreting qPCR results this lower than optimal primer efficiency could potentially lead to a failure to recognize valid results (Bustin, Benes et al. 2009). Functional primers for COX-2, MMP1 and MMP3 could not be found, neither by commercial nor self-designed means. Given the complications encountered in qPCR preparations, post-transcriptional cytokine assessment might represent an appropriate alternative approach (Anderson 2008).

Assessment of inflammatory genes in perfusion models represents a novelty in this particular field of research. Comparison of perfused and non-perfused specimens

enabled the assessment of whether or not perfusion *per se* causes inflammation, thus providing valuable and relevant information with respect to the future application of such models. The unique opportunity to compare data derived from ILP with *in vivo*-derived data was not only in accordance with the 3R principle, but also demonstrated the model's ability to react to an inflammatory stimulus in an almost physiological manner. However the inflammatory gene expression data has to be interpreted in the context of the failed cell migration experiments. It is likely that the significance of the gene expression results would have been more apparent and simpler to interpret had successful cell migration been achieved. Observed changes could therefore be more due to resident granulocytes, rather than cells derived from the perfusate. However, in light of the many potential reasons which may underlie the failure to achieve neutrophilic migration in this group of experiments (see above), it remains possible that significant changes may be detected regarding inflammatory gene expression in the absence of inflammatory cell influx. Therefore, despite the failure to induce detectable cell migration, the results of the qPCR analyses could still reveal trends in relative gene expression and provide a basic overview of inflammatory events in joints of the isolated perfused distal porcine limb.

Other articular tissues, namely cartilage, was not evaluated as no changes were expected given the short experimental time (6h).

PNN vs PSN

Comparing gene expression in synovium samples from perfused, SPIONs injected limbs (PNN) with that from their sham-injected counterparts (PSN) provided information on the inflammatory potential of SPIONs' and revealed the model's functionality for researching events in the context of acute inflammation. The failure to identify a statistically significant increase in COX-1 expression was to be expected as it plays a minor role in inflammation compared to its isoenzyme COX-2 (Griswold and Adams 1996). An assessment of the relationship between the isoenzymes would have been of interest; however, no working primer could be designed for COX-2. All analysed cytokines, except IFN-γ, showed an increased expression in SPION injected joints. This was statistically significant for IL-1β and IL-6 and approached significance

for TNF-α (p=0.078). The literature reports on SPIONs' capability to induce oxidative stress, which leads to activation of Activator protein 1 (AP-1) and nuclear factor kappa-light-chain-enhancer of activated B cells (NF-κB) and subsequently to an enhanced gene expression of pro-inflammatory cytokines (Naqvi, Samim et al. 2010). An upregulation of interleukins was also observed after two hours of SPION injection into healthy murine knee joints (Vermeij, Koenders et al. 2015); this effect lasted 24h. In the current study, intra-articular SPIONs injection caused a similar effect in the ILP experiments as previously described for *in vitro* and *in vivo* experiments, indicating functionality of the developed model.

No inter-group differences were identified which were consistent with either the wash solution (used for sham injections) inducing, or the SPIONs failing to induce inflammation. The SPION induced inflammatory gene response could potentially be attributable to endotoxin contamination of the SPIONs during their synthesis (Vermeij, Koenders et al. 2015). In light of the potential contributory role of recruited inflammatory cells to the inflammatory gene profile of the synovial samples, it is possible that the lack of an inflammatory cell influx may have resulted in an under-estimate of the inflammatory gene expression.

PSN vs PCN

A lack of a pro-inflammatory effect of sham injection should be reflected in the failure to identify a difference in GOI expression between perfused, sham-injected specimens (PSN) and control perfusions (PCN; without injection). This was true for all analysed genes. This lack of a sham injection-associated effect (e.g. via a mechanical stimulus or non-sterile injection procedure) suggests that any pro-inflammatory effect associated with SPION injection was attributable to the SPIONs *per se*, not the method of administration. However as previously mentioned, potential reasons for the failure of the sham injection to induce inflammatory gene expression include the cell free nature of the perfusate and the failure to induce neutrophil migration, whereby the absence of an inflammatory cell influx may have negatively influenced the overall inflammatory gene expression in the synovial samples obtained.

PCN vs NP

Comparison of the inflammatory gene expression in control perfusions (PCN) with non-perfused limbs (NP) provided information on the potential pro-inflammatory effects of perfusion *per se*. As data derived from cardiopulmonary bypass surgeries has demonstrated that extracorporeal blood circuits can cause inflammation (Paparella, Yau et al. 2002), inflammatory changes may also be expected in perfusion experiments. Provided that non-perfused specimens (NP) were healthy and that the perfusion conditions were able to permit the detection of inflammatory changes, the absence of any differences in GOI expression between the non-perfused (NP) and control perfused (PCN) groups is consistent with a lack of any perfusion-associated pro-inflammatory effects and supports the use of the model for studying short term events and interventions in the context of arthritis.

Perfusion failed to result in a statistically significant increased expression of the GOIs, compared with the non-perfused samples. These results therefore substantiate the idea that ILP is well suited for studying short term changes related to inflammation. Nonetheless, in light of the absence of sufficient cell migration, the gene expression data should to be interpreted with a level of caution. Had it occurred, any relative upregulation in inflammatory gene expression in the perfused samples would have been attributable to the technique; for example, via contamination of the perfusate or the hardware.

VN vs VS

The rationale behind comparing *in vivo* SPION injected joints (VN) with their control (*in vivo*, sham injected; VS) is similar to that behind the PNN *versus* PSN comparison, as described earlier. Furthermore, this comparison permits the detection of the pro-inflammatory effects of SPION injection without the requirement to consider the potential additional effects of extracorporeal perfusion *per se*. Whereas in perfused limbs SPIONs significantly increased the expression of IL-1β and IL-6 (and non-significantly increased the expression of TNF-α and COX-1), the same intervention *in vivo* failed to result in a significant increase in expression of any of the GOIs, relative

to sham injected joints. As previously mentioned, and in light of the relatively greater GOI expression in the sham injected *in vivo* specimens (relative to the sham injected perfused specimens; see below), this could be attributable to a non-sterile joint injection procedure or endotoxin contamination of the wash fluid used for sham injection (Vermeij, Koenders et al. 2015).

PNN vs VN

To find out whether SPION injection has the same effect *ex vivo* (PNN) as *in vivo* (VN), the PNN and VN groups were compared. Failure to identify any inter-group differences could be considered as being consistent with the perfused limbs displaying a physiological response, thus supporting the use of ILP to bridge the gap between *in vitro* and *in vivo* experiments. No statistically significant difference in the expression of any of the GOIs was observed when comparing perfused (PNN) and *in vivo* (VN). Although comparison of the perfused SPION injected group (PNN) with the *in vivo* group (VN) did reveal some minor trends, potentially reflecting very subtle relative up/down regulations, the overall analysis failed to reveal any significant differences between groups, indicating the same response in the ILP set up as the *in vivo* experiment.

PSN vs VS

Similarly, comparison of both sham injected groups (perfused PSN; *in vivo* VS) is justified from the viewpoint of supporting ILP as a suitable model to bridge the gap between *in vitro* and *in vivo* experiments. Although no significant inter-group difference was observed with respect to IFN-γ and TNF-α expression, a significantly greater expression of COX-1, IL-1 beta and IL-6 was detected in the *in vivo* sham injected joints, compared with the perfused joints. These findings are consistent with a level of inflammation in the *in vivo* joints which was absent in the perfused joints. Potential reasons for this include contamination of the solution used for the *in vivo* sham injections and/or a non-sterile injection technique and/or an increased level of trauma associated with the joint injections.

Combining results from qPCR experiments, it seems likely that ILP is suited for its intended use. It demonstrates the potential for the model to react to an inflammatory stimulus in the same manner as that observed in both *in vitro* (Naqvi, Samim et al. 2010) and *in vivo* (Vermeij, Koenders et al. 2015) experiments. However, consideration of the data derived from the sham injected *in vivo* experiments does suggest technical complications associated with these sham injections. Firstly, SPION injection resulted in comparable results in both the *in vivo* and perfused joint models, indicating a functional ILP model and leading to the assumption that comparable results between groups would also be seen following the sham injections. However, sham injected *in vivo* experiments revealed significantly greater expression of three GOIs, compared with the sham injected perfused limbs. It was considered unlikely that the different models inherently responded differently to the respective challenges (SPION versus sham); therefore, the different responses observed were considered most likely attributable to an issue with the sham injected *in vivo* joints. As the same wash fluid was used for sham injections in all experiments (*ex vivo* and *in vivo*), any effects attributable to endotoxin contamination of the fluid should have been observed in both models. Therefore, it is likely that the inflammatory responses observed in the *in vivo* joints was attributable to differences in sham injection technique, especially as SPION injection resulted in a similar level of GOI expression in both models.

5.6 Conclusion

Multiphoton microscopy, including the SHG principle, seems suited for imaging synovium samples, even though it failed to reveal evidence of neutrophil influx in the cell migration experiments. In light of the fact that histological analysis also failed to identify significant neutrophilic infiltration, it seems more likely that cell migration did not occur as hypothesised. The reasons for this remain unclear; however, potential explanations include non-efficient chemoattraction or loss of neutrophils within the system. The ultimate fate of the injected neutrophils remains undetermined and

requires further investigation before any refinements to the experimental set-up and/or methodology can be implemented.

The inflammatory gene expression data suggests that ILP itself does not induce a direct pro-inflammatory effect in joint-associated tissues, thus supporting the use of this approach to study the inflammatory potential of certain reagents and drugs. The intra-articular administration of SPIONs led to an increase in inflammatory cytokine gene expression within a 6h time frame, during 3h of which, the limb was perfused with neutrophils. However, SPIONs failed to induce a significant level of neutrophil recruitment. Whether this was attributable to technical problems impeding adequate cell migration or insufficient chemoattractant activity of SPIONs remains to be established.

Although continued investigation is warranted to further optimise this novel approach to arthritis research, overall, the data does highlight the potential value of the ILP model in studies aimed at investigating cell migration and inflammation.

Chapter 6 Future perspectives

6.1 Research field

As a way of preserving (donor) organs for re-/ transplantation isolated perfusion systems have always been of interest. Especially in organ preservation (e.g. kidney) the technique is well established. For use in the context of transplantation surgery often more sophisticated are used, as optimal preservation of the perfused specimen is of utmost importance. Therefore the use is of true pulsatile flow is more common in models used for transplantation surgery and has recently, once again, been shown to be superior for perfusion experiments (von Horn and Minor 2018).
Due to various tissues being involved, perfusion of isolated extremities proves to be particularly challenging. Although *ex vivo* perfusion seems to compare favourably to other means of preservation (e.g. cold storage) data on the subject is still limited (Kruit, Winters et al. 2018). However Ozer et al. (2015) were able to show that twelve hours of warm perfusion of an amputated porcine limb with autologous blood did result in a near normal contractility of muscle fibres during ex vivo perfusion and after re-plantation. He also observed no significant increase in specimen weight durin perfusion (Ozer, Rojas-Pena et al. 2015). The group was later able to successfully extend the perfusion period to 24h, when using autologous blood as perfusate (Ozer, Rojas-Pena et al. 2015). These results are promising that preservation of extremities via perfusion systems will become more and more feasible in the future and eventually draw nearer to the good results already being achieved in organ preservation.

Research models using isolated organ/ limb perfusion were extensively used in the 1970s. Thereafter their use subsided, which might be due to a long optimisation process being required before perfusion models are ready to use and due to the final set-up usually being very labour intensive. Additionally, at the time, perfusion was widely used to investigate research questions of physiological nature (e.g. milk synthesis), which might not be in the centre of interest today. However, ILP's great potential in research was rediscovered in the 1990s and 2000s, mainly by research

groups based in Hanover (Kietzmann and Friebe) and Vienna (Licka and Patan). Additionally, keeping the growing importance of the 3R principle in mind, availability of a model that bridges the gap between *in vitro* and *in vivo* research becomes increasingly interesting.

More recently Markgraf et al. (2018) used the isolated perfused porcine kidney as tool to effectively validate the technique of hyper spectral imaging (HSI) as a non-invasive, optical method to assess tissue parameters (e.g. distribution maps of oxygen saturation, tissue water content, (Markgraf, Janssen et al. 2018)). While this is of interest for the clinical use of HSI, the method might also be an interesting tool to measure viability in, for research purposes, perfused specimens. However, the costs involved might limit its practicability in this context.

Progress was also made in developing an *ex vivo* heart perfusion system, which is capable to operate in three different ways, namely allowing perfusion of the specimen in the traditional Langendorff mode, as well as a pump supported working mode and a passive afterload working-mode (Xin, Gellner et al. 2018).

Lately Chung et al. (2018) used *ex vivo* perfusion of a porcine spleen as model of bacterial sepsis (Chung, Wanford et al. 2018). Connecting the organ to a closed, pressure-controlled, extracorporeal circuit, as used in CPB surgery, the group perfused the organ successfully for six hours with a blood-based perfusate. Metabolic parameters and confocal microscopy of tissue samples confirmed viability and integrity of the micro organ structure. The gram-positive bacterium *Streptococcus pneumonia* was added to the perfusate after an hour to mimic bacterial sepsis. Cluster of bacteria could be identified after perfusion and interestingly neutrophils seemed to have migrated towards the infection site, co-localising with the clusters (as shown by confocal microscopy and immunohistochemistry). Furthermore enzyme-linked immunosorbent assays (ELISA) were able to show increased levels of TNF-α in serum samples of infected specimens, whereas IL-6 levels were similar in experimental and control groups. These results not only showcase that extracorporeal perfusion

rightfully deserves to play a role in modern research, but also that the technique has great potential for modelling cell migration.

6.2 ILP model

6.2.1 Perfusion set-up

In light of the problems associated with neutrophil migration, a closed, re-circulating perfusion system, which allows repeated exposure of neutrophils to the chemoattractant throughout the period of perfusion, could be a potential future refinement of the set-up adopted in this current study. Although the simplest option would be to pump the VR, which dripped freely into a beaker, back into the AR, various technical challenges would have to be addressed. Besides the necessary purchase of additional equipment, maintaining the temperature at physiological levels would represent a significant challenge. Ensuring that the perfusate is at body temperature at the point of entry into the perfused limb necessitates heating the AR to 59°C. The addition of cooler VR fluid to the AR reservoir would clearly reduce the temperature of the AR and subsequently, the temperature of the perfusate as it enters the limb. Although this temperature reduction could be minimised by the heating the VR fluid (e.g. passage of the tubing leading from the VR through a heated water bath), this would likely have a detrimental effect on the neutrophils. Therefore, a different heating and insulating system, which maintains a constant physiological temperature within the system, would have to be designed if it was necessary to adopt a closed, re-circulating system.

In the presented work, adapted Tyrode solution was used as the perfusate. Although this solution was designed to meet the nutritional requirements of the perfused specimen, it was not optimised to meet the requirements of the infused neutrophil. It is likely that methodological adaptions would be necessary in order to maintain the viability and functionality of the neutrophils within a re-circulating system. Patan et al. (2012) reported on neutrophil migration within the laminar tissue of a perfused

equine forelimb stimulated with endotoxins. In this report, a closed perfusion system was used in which the AR was completely replaced every two hours in an attempt to combat any cell damage which may have resulted from the perfusion. With a view to maintaining neutrophil viability, such an approach could also be considered as an appropriate option for future experiments on the perfused porcine limb. However, due to the laborious processing necessary, the limited availability of isolated and stained cells would remain a challenge which would need to be addressed.

6.2.2 Viability

Different viability parameters (namely, weight gain, blood pressure, oxygen uptake, glucose consumption and lactate and potassium levels) were measured during the duration of the perfusion. However, in the presented model, this data was only recorded for future analysis and did not result in any corrective interventions during the perfusion. Adaptation of the model to permit the implementation of "live adjustments" based on real time viability data could be considered as a progressive refinement. If a closed system was developed (as previously discussed), potential adjustments might include responsive interventions to decreasing glucose levels resulting from glucose uptake by the system. The addition of insulin to the perfusate has been described in the literature as a means of controlling potassium levels (Constantinescu, Knall et al. 2011). Insulin increases the activity of the Na+/K+ ATPase pump, resulting in removal of excess potassium from the extracellular space.

Additionally, the epoc® analyser (Woodley Equipment) permits the measurement of more analytes than those recorded in the present study (e.g. pH or partial pressure of carbon dioxide). Incorporating such additional data into the overall viability analysis and making necessary adjustments to maintain values within physiological liomits could also offer supplementary benefits.

6.2.3 Cell migration and inflammation

6.2.3.1 Neutrophil shape change assays

To assess the neutrophil's functionality, which is a requirement for chemotaxis, neutrophil shape change assays can be performed. The change in shape which occurs with neutrophil stimulation can be detected by flow cytometry (Cole, Garlick et al. 1995). Preliminary experiments have been performed within the scope of this project according to the following protocol.

The neutrophilic response to the chemoattractant LTB_4 (Palmblad, Malmsten et al. 1981) was determined by a shape change assay. Neutrophils were isolated as described in Chapter 2.2. except Tyrode solution was used to re-suspend the cells, thus mimicking perfusion conditions. This adaptation was adopted because it was hypothesised that any positive results would not only demonstrate functionality of the neutrophils, but also the capacity of the perfusate to provide sufficient magnesium and calcium to activate the isolated neutrophils.

One hundred and eighty microlitres of isolated neutrophil solution was augmented with 20µL 1µM LTB_4 in adapted Tyrode solution (final concentration of 0.1µM). Neutrophils were stimulated for ten minutes at 37°C in a shaking heat block. To terminate the reaction, 2.5% glutaraldehyde was added and the tubes were placed on ice. Samples were immediately analysed in triplicate by flow cytometry. The low-angle forward scatter was assessed as an indicator of cell diameter. Samples were gated on the control group (no exposure to a chemoattractant). To ensure the analysis was limited to the neutrophil population, side scatter measurements, based on the cellular granularity, were also applied (Cole, Garlick et al. 1995, Kitchen, Rossi et al. 1996).

Flow cytometric assessment revealed a shift to the right, indicating a shape change and accordingly an activation of neutrophils.

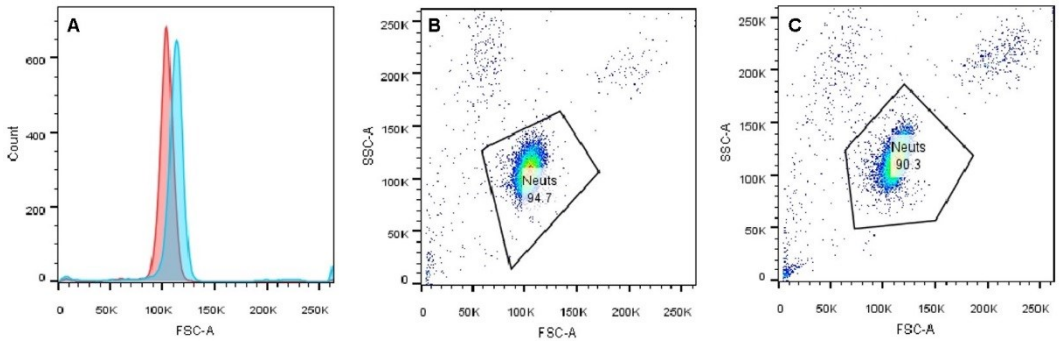

Figure 6-1: Shape change assays - flow cytometry

A shift to the right can be seen in LTB_4 exposed cells (**A**, blue) compared to their untreated controls (**A**, red). This represents an increase in size and can therefore be considered a sign of activation.

As the sample size was small (n=4) and neutrophils were not analysed after passing through the perfusion system, caution must be exercised when making conclusions based on this data. Nevertheless, the results are promising as neutrophils seemed to be viable and functional, even after prolonged transportation. However these preliminary studies only tested LTB_4 as a chemoattractant. Results derived from studies using SPIONs as a chemoattractant would have been of great interest. Similarly, in light of the intended use of the neutrophils within the ILP model presented, it would have been interesting to conduct the shape change assays in neutrophils exposed to the conditions associated with perfusion of the model. This would have involved the following approach. Neutrophils would have been prepared as for the perfusion experiments (diluted in HBSS--, CMFDA stained). Following transfer to 20mL syringes mounted on a syringe pump. The neutrophil-containing solution would then meet the warmed Tyrode solution (containing Ca^{2+} and Mg_2) via a 3-way-tap and the mixture of both fluids would flow through a 21G venous catheter. At the end of the catheter, and before the Tyrode/ neutrophil mixture enters the limb, samples would be obtained at the following time points: t_1: 0min, t_2: 90min and t_3: 180min; each respectively representing the beginning, middle and end of the neutrophil perfusion experiment.

6.2.3.2 LPS

In the light of the failure to demonstrate successful cell migration, it would have been interesting to test the chemoattractant properties of other injected substances. This may have helped to determine whether the lack of cell migration was solely attributable to technical issues, or whether the chemo-attractive properties of the intra-articular LTB_4 were non-functional, despite its recognition as a classic potent reagent for neutrophils recruitment (Chou, Kim et al. 2010). In comparison, the chemoattractant properties of SPIONs are less well established, thus impacting on any efforts to attribute the lack of cell migration to a particular factor. This is especially the case in light of the relative novelty of the experimental set-up associated with the perfused model. It would therefore be of interest to further validate the model using other established inflammatory stimuli which are likely to induce a measurable level of neutrophil migration. Lipopolysaccharide (LPS) would appear to be a suitable candidate (Tanaka, Kagari et al. 2006).

6.2.3.3 Joint fluid

In the majority of perfusion experiments, joint fluid samples were collected after the conclusion of the experiment and immediately placed in dry ice prior to storage at -80°C. The following preliminary experiments were conducted on freshly harvested joint; attempts to collect cell pellets following centrifugation (no pellet present); cytologic assessment of smears prepared from synovial fluid (H&E staining, no cells were identified); assessment of fluorescence in synovial fluid samples harvested from LTB4 injected joint using a plate reader (1420 Multilabel Counter, VICTOR³ TM, Perkin Elmer precisely, no difference in fluorescence between control and experimental groups). Although these preliminary experiments were unsuccessful, this must be interpreted in light of the subsequent confirmation of absent cell migration.

Conducting a manual or automated white blood cell count would have been a relatively simple method of assessing fresh synovial fluid samples. White blood cells (WBCs; basophils, eosinophils, T and B lymphocytes, monocytes/macrophages, neutrophils)

are crucial in the acute inflammatory response and consistent with this, an inflammatory arthropathy is generally characterised by a WBC count of >2000/mm^3 in synovial fluid. Values ranging between 1000 and 2000/mm^3 may be associated with mild inflammation and such results should be interpreted in light of the clinical appearance of the patient (Punzi, Oliviero et al. 2005). In RA, synovial macrophages are involved in the initial inflammatory response , followed by lymphocytes and CD4+ T cells (Firestein 2003, Cope, Schulze-Koops et al. 2007). Neutrophils can also be found in synovial fluid samples from RA patients , where a prolongation of their life span (via reduced apoptosis) results in persistently elevated numbers (Ottonello, Cutolo et al. 2002). Despite inflammation being a recognised component in the pathogenesis of OA, the synovial fluid WBC count is usually below 2000/mm^3 with the proportion of polymorphonuclear cells (PMNs) generally lying between 2 and 10% (Punzi, Oliviero et al. 2005).

Another potentially interesting option, which may have complemented the existing data set, would have been to perform MPO assays on frozen synovial fluid samples. As this enzyme is most amply found in neutrophil granulocytes (Pinkus and Pinkus 1991), a positive result would have been consistent with the presence of neutrophils, thus confirming functional cell migration.

Chapter 7 Conclusion

The presented model represents an interesting and potentially valuable tool in the field of arthritis related research. It has the potential to bridge the gap between *in vitro* and *in vivo* research, which is of great importance, not only but especially, in large animal research. Additionally, when using abattoir derived specimens or limbs derived from other terminal research experiments, the technique is in accordance with the 3Rs principle. Its main advantage is a functional perfusate supply, which permits the testing of novel therapeutic agents and different routes of delivery, both locally (e.g. intra-articular) and systemically (e.g. via the perfusate).

Suitable specimen viability was demonstrated, via the assessment of established perfusion parameters. Furthermore, the study demonstrated the applicability of live to dead cell ratio calculations as a novel method of assessing specimen viability; one not previously reported in the literature in the context of perfusion experiments.

The model's ability to mimic cell migration requires further assessment and likely necessitates further modification to the adopted methodologies. With the appropriate modification, it is believed that the technique has the potential to serve this intended purpose.

Proof of concept was achieved for using multiphoton microscopy combined with the SHG principle as technique for assessing neutrophil recruitment towards an intra-articular stimulus.

The qPCR data was novel within the field of research which incorporates similar perfusion-based studies. Although the results of qPCR analysis should be interpreted in light of the absence of significant cell migration the findings indicate a failure of specimen perfusion *per se* to cause excessive inflammation *per se*, yet demonstrate the capacity for the model to react to an inflammatory stimulus in a manner which approximates the "live animal situation", as evidenced by the unique direct comparison

between the *ex vivo*- and *in vivo*-derived data. The generated results can therefore be considered to represent a preliminary point of reference for future studies.

Overall, the presented work represented the adoption of an old technique which, when combined with new adaptations, resulted in the development of a remarkable platform for testing novel drugs and varied delivery systems in the context of arthritis.

Chapter 8 References

Abramson, S. (1999). "The role of COX-2 produced by cartilage in arthritis." Osteoarthritis and Cartilage **7**(4): 380-381.

Adham, M., et al. (1997). "The isolated perfused porcine liver: assessment of viability during and after six hours of perfusion." Transplant International **10**(4): 299-311.

Alaaeddine, N., et al. (1997). "Osteoarthritic synovial fibroblasts possess an increased level of tumor necrosis factor-receptor 55 (TNF-R55) that mediates biological activation by TNF-alpha." Journal of Rheumatology **24**(10): 1985-1994.

Amin, A. (1999). "Regulation of tumor necrosis factor-α and tumor necrosis factor converting enzyme in human osteoarthritis." Osteoarthritis and Cartilage **7**(4): 392-394.

Amin, A. R., et al. (1997). "Superinduction of cyclooxygenase-2 activity in human osteoarthritis-affected cartilage. Influence of nitric oxide." Journal of Clinical Investigation **99**(6): 1231.

Anderson, K. O., et al. (1985). "Rheumatoid arthritis: review of psychological factors related to etiology, effects, and treatment." Psychological Bulletin **98**(2): 358.

Anderson, P. (2008). "Post-transcriptional control of cytokine production." Nature Immunology **9**(4): 353.

Araki, Y., et al. (2005). "Pressure–volume relationship in isolated working heart with crystalloid perfusate in swine and imaging the valve motion." European Journal of Cardio-Thoracic Surgery **28**(3): 435-442.

Arend, W. P. and J. M. Dayer (1995). "Inhibition of the production and effects of interleukins-1 and tumor necrosis factor α in rheumatoid arthritis." Arthritis and Rheumatism **38**(2): 151-160.

Atik, O. S. (1990). "Leukotriene B 4 and prostaglandin E 2-like activity in synovial fluid in osteoarthritis." Prostaglandins, Leukotrienes and Essential Fatty Acids **39**(4): 253-254.

Bae, J.-s., et al. (2004). "The effect of polysaccharides and carboxymethylcellulose combination to prevent intraperitoneal adhesion and abscess formation in a rat peritonitis model." Journal of Veterinary Medical Science **66**(10): 1205-1211.

Barland, P., et al. (1962). "Electron microscopy of the human synovial membrane." Journal of Cell Biology **14**(2): 207-220.

Barlow, G. and D. H. Knott (1964). "Hemodynamic alterations after 30 minutes of pentobarbital sodium anesthesia in dogs." American Journal of Physiology - Legacy Content **207**(4): 764-766.

Barthel, M., et al. (1989). "The perfused porcine pancreas as a model for testing organ protective solutions." Research in Experimental Medicine **189**(5): 303-311.

Bäumer, W. and M. Kietzmann (1999). "The isolated perfused bovine udder as a model of dermal eicosanoid release." Alternatives to Laboratory Animals - ATLA **28**(5): 643-649.

Bäumer, W. and M. Kietzmann (2001). "Effects of steroidal and non-steroidal antiphlogistic drugs on eicosanoid synthesis in irritated skin: studies with the isolated perfused bovine udder." Journal of Pharmacy and Pharmacology **53**(5): 743-747.

Bäumer, W., et al. (2002). "The Isolated Perfused Bovine Uterus as a Model for Mucous Membrane Irritation and Inflammation." Alternatives to Animal Experimentation - ALTEX **19**(2): 57-63.

Bell, R. M., et al. (2011). "Retrograde heart perfusion: the Langendorff technique of isolated heart perfusion." Journal of Molecular and Cellular Cardiology **50**(6): 940-950.

Bendele, A. (2001). "Animal models of osteoarthritis." Journal of Musculoskeletal and Neuronal Interactions **1**(4): 363-376.

Bentley, G. (1975). "Articular cartilage studies and osteoarthrosis." Annals of the Royal College of Surgeons of England **57**(2): 86.

Berg, J., et al. (2013). Stryer Biochemie. Berlin Heidelberg, Springer-Verlag Berlin Heidelberg.

Berhane, Y., et al. (2006). "Assessment of endothelium-dependent vasodilation in equine digital resistance vessels." Journal of Veterinary Pharmacology and Therapeutics **29**(5): 387-395.

Bertolini, D. R., et al. (1986). "Stimulation of bone resorption and inhibition of bone formation in vitro by human tumour necrosis factors." Nature **319**(6053): 516-518.

Bhattacharya, J. and N. Staub (1980). "Direct measurement of microvascular pressures in the isolated perfused dog lung." Science **210**(4467): 327-328.

Biggar, W., et al. (1984). "Neutrophil Migration In Vitro and In Vivo During Hypothermia." Infection and Immunity **46**(3).

Blaisdell, F. (2002). "The pathophysiology of skeletal muscle ischemia and the reperfusion syndrome: a review." Cardiovascular Surgery **10**(6): 620-630.

Blitek, A., et al. (2006). "Expression of cyclooxygenase-1 and-2 in the porcine endometrium during the oestrous cycle and early pregnancy." Reproduction in Domestic Animals **41**(3): 251-257.

Bortner, C. D., et al. (1997). "A primary role for K+ and Na+ efflux in the activation of apoptosis." Journal of Biological Chemistry **272**(51): 32436-32442.

Braun, M. and M. Kietzmann (2004). "Ischemia reperfusion injury in the isolated hemoperfused bovine uterus-a model for the investigation of anti-inflammatory substances." Alternatives to Animal Experimentation - ALTEX **21**(Suppl 3): 49-56.

Brennan, F., et al. (1995). "TNF inhibitors are produced spontaneously by rheumatoid and osteoarthritic synovial joint cell cultures: evidence of feedback control of TNF action." Scandinavian Journal of Immunology **42**(1): 158-165.

Bristol, D., et al. (1991). "The isolated Perfused Equine Skin Flap Preparation and Metabolic Parameters." Veterinary Surgery **20**(6): 424-433.

Brower, T. D. and W.-Y. Hsu (1969). "2 Normal Articular Cartilage." Clinical Orthopaedics and Related Research **64**: 9-17.

Brunicardi, F. C., et al. (2001). "Immunoneutralization of somatostatin, insulin, and glucagon causes alterations in islet cell secretion in the isolated perfused human pancreas." Pancreas **23**(3): 302-308.

Bustin, S. A., et al. (2009). "The MIQE guidelines: minimum information for publication of quantitative real-time PCR experiments." Clinical Chemistry **55**(4): 611-622.

Butler, A., et al. (2002). "Successful extracorporeal porcine liver perfusion for 72hr." Transplantation **73**(8): 1212-1218.

Butler, D., et al. (1994). "Modulation of proinflammatory cytokine release in rheumatoid synovial membrane cell cultures. Comparison of monoclonal anti TNF-alpha antibody with the interleukin-1 receptor antagonist." European Cytokine Network **6**(4): 225-230.

Butler, J., et al. (1993). "Inflammatory response to cardiopulmonary bypass." Annals of Thoracic Surgery **55**(2): 552-559.

Cameron, D. P., et al. (1972). "Metabolic clearance of human growth hormone in patients with hepatic and renal failure, and in the isolated perfused pig liver." Metabolism **21**(10): 895-904.

Caron, J. P., et al. (1996). "Chondroprotective effect of intraarticular injections of interleukin-1 receptor antagonist in experimental osteoarthritis. Suppression of collagenase-1 expression." Arthritis and Rheumatism **39**(9): 1535-1544.

Caron, M., et al. (2012). "Redifferentiation of dedifferentiated human articular chondrocytes: comparison of 2D and 3D cultures." Osteoarthritis and Cartilage **20**(10): 1170-1178.

Chan, R. K., et al. (2004). "IgM binding to injured tissue precedes complement activation during skeletal muscle ischemia-reperfusion." Journal of Surgical Research **122**(1): 29-35.

Chang, B., et al. (2012). "General one-pot strategy to prepare multifunctional nanocomposites with hydrophilic colloidal nanoparticles core/mesoporous silica shell structure." Journal of Colloid and Interface Science **377**(1): 64-75.

Chapman, N., et al. (1961). "The Isolated Perfused Bovine Liver." Journal of Experimental Medicine **113**(6): 981-996.

Chikanza, I., et al. (1995). "Peripheral blood and synovial fluid monocyte expression of interleukin 1 alpha and 1 beta during active rheumatoid arthritis." Journal of Rheumatology **22**(4): 600-606.

Chin, J. E., et al. (1990). "Role of cytokines in inflammatory synovitis." Arthritis and Rheumatism **33**(12): 1776-1786.

Chinchoy, E., et al. (2000). "Isolated four-chamber working swine heart model." Annals of Thoracic Surgery **70**(5): 1607-1614.

Chomarat, P., et al. (1995). "Balance of IL-1 receptor antagonist/IL-1 beta in rheumatoid synovium and its regulation by IL-4 and IL-10." Journal of Immunology **154**(3): 1432-1439.

Chou, R. C., et al. (2010). "Lipid-cytokine-chemokine cascade drives neutrophil recruitment in a murine model of inflammatory arthritis." Immunity **33**(2): 266-278.

Choy, E. H. S. and G. S. Panayi (2001). "Cytokine Pathways and Joint Inflammation in Rheumatoid Arthritis." New England Journal of Medicine **344**(12): 907-916.

Chung, W. Y., et al. (2018). "An ex vivo porcine spleen perfusion as a model of bacterial sepsis." Alternatives to Animal Experimentation - ALTEX.

Cole, A., et al. (1995). "A flow cytometric method to measure shape change of human neutrophils." Clinical Science **89**(5): 549-554.

Colombo, C., et al. (1983). "A new model of osteoarthritis in rabbits." Arthritis and Rheumatism **26**(7): 875-886.

Constantinescu, M., et al. (2011). "Preservation of Amputed Extremities by Extracorporeal Blood Perfusion; a Feasibility Study in a Porcine Model." Journal of Surgical Research **171**(1): 291-299.

Cope, A., et al. (2007). "The central role of T cells in rheumatoid arthritis." Clinical and Experimental Rheumatology **25**(5): S4.

Crofford, L. J. (1997). "COX-1 and COX-2 tissue expression: implications and predictions." Journal of Rheumatology. Supplement **49**: 15-19.

Cypel, M., et al. (2008). "Technique for Prolonged Normothermic Ex Vivo Lung Perfusion." Journal of Heart and Lung Transplantation **27**(12): 1319-1325.

Daniel, C. R., et al. (2018). "Extracorporeal perfusion of isolated organs of large animals–Bridging the gap between in vitro and in vivo studies." Alternatives to Animal Experimentation - ALTEX **35**(1): 77-98.

Davies, D. (1946). "Synovial membrane and synovial fluid of joints." Lancet **248**(6432): 815-819.

De Groot, H. and U. Rauen (2007). "Ischemia-reperfusion injury: processes in pathogenetic networks: a review." Transplantation Proceedings (Conference) **39**(2): 481-484.

de Lange, J., et al. (1992). "The isolated blood-perfused pig ear: an inexpensive and animal-saving model for skin penetration studies." Journal of Pharmacological and Toxicological Methods **27**(2): 71-77.

De Raucourt, E., et al. (1998). "Anticoagulant activity of dextran derivatives." Journal of Biomedical Materials Research **41**(1): 49-57.

Demmy, T. L., et al. (1992). "Isolated biventricular working rat heart preparation." Annals of Thoracic Surgery **54**(5): 915-920.

Dittrich, S., et al. (2000). "Haemodilution improves organ function during normothermic cardiopulmonary bypass: investigations in isolated perfused pig kidneys." Perfusion **15**(3): 225-229.

Domingo-Pech, J., et al. (1991). "Preservation of the amputed canince hind limb by extrcorporeal perfusion." International Orthopaedics **15**(4): 289-291.

Dozois, C. M., et al. (1997). "A reverse transcription-polymerase chain reaction method to analyze porcine cytokine gene expression." Veterinary Immunology and Immunopathology **58**(3): 287-300.

Dragu, A., et al. (2011). "Extracorporeal perfusion of free muscle flaps in a porcine model using a miniaturized perfusion system." Archives of Orthopaedic Trauma Surgery **131**(6): 849-855.

Drapanas, T., et al. (1966). "Hemodynamics of the isolated perfused pig liver: metabolism according to routes of perfusion and rates of flow." Annals of Surgery **164**(3): 522.

Eggli, P. S., et al. (1988). "Quantitation of structural features characterizing weight- and less-weight-bearing regions in articular cartilage: A stereological analysis of medical femoral condyles in young adult rabbits." Anatomical Record **222**(3): 217-227.

Ehinger, A., et al. (2006). "Tissue distribution of cefquinome after intramammary and "systemic" administration in the isolated perfused bovine udder." Veterinary Journal **172**(1): 147-153.

Eichholtz, F. and E. Verney (1924). "On some conditions affecting the perfusion of isolated mammalian organs." Journal of Physiology **59**(4-5): 340-344.

Emery, P., et al. (2008). "IL-6 receptor inhibition with tocilizumab improves treatment outcomes in patients with rheumatoid arthritis refractory to anti-tumour necrosis factor biologicals: results from a 24-week multicentre randomised placebo-controlled trial." Annals of the Rheumatic Diseases **67**(11): 1516-1523.

Erasmus, M., et al. (2006). "Normothermic ex vivo lung perfusion of non-heart-beating donor lungs in pigs: from pretransplant function analysis towards a 6-h machine preservation." Transplant International **19**(7): 589-593.

Estelrich, J., et al. (2015). "Iron oxide nanoparticles for magnetically-guided and magnetically-responsive drug delivery." International Journal of Molecular Sciences **16**(4): 8070-8101.

Estelrich, J., et al. (2015). "Nanoparticles in magnetic resonance imaging: from simple to dual contrast agents." International Journal of Nanomedicine **10**: 1727.

Ewoldt, J. M., et al. (2004). "Evaluation of a sheep laparoscopic uterine trauma model and repeat laparoscopy for evaluation of adhesion formation and prevention with sodium carboxymethylcellulose." Veterinary Surgery **33**(6): 668-672.

Fine, S. and W. Hansen (1971). "Optical second harmonic generation in biological systems." Applied Optics **10**(10): 2350-2353.

Finn, A., et al. (1993). "Interleukin-8 release and neutrophil degranulation after pediatric cardiopulmonary bypass." Journal of Thoracic and Cardiovascular Surgery **105**(2): 234-241.

Firestein, G. S. (2003). "Evolving concepts of rheumatoid arthritis." Nature **423**(6937): 356-361.

Fischer, A., et al. (1985). "Anticoagulant activity of dextran derivatives. Part II: Mechanism of thrombin inactivation." Biomaterials **6**(3): 198-202.

Forman, M., et al. (1992). "Pharmacologic perturbation of neutrophils by Fluosol results in a sustained reduction in infarct size in the canine model of reperfusion." Journal of the American College of Cardiology **19**(1): 205-216.

Friebe, M., et al. (2013). "Synovial distribution of "systemically" administered acetylsalicylic acid in the isolated perfused equine distal limb." BMC Veterinary Research **9**(56).

Friebe, M., et al. (2001). "The isolated perfused equine distal limb as an ex vivo model for pharmacokinetic studies." Journal of Veterinary Pharmacology and Therapeutics **36**(3): 292-297.

Fuller, B. J. and C. Y. Lee (2007). "Hypothermic perfusion preservation: the future of organ preservation revisited?" Cryobiology **54**(2): 129-145.

Gabay, C. (2006). "Interleukin-6 and chronic inflammation." Arthritis Research and Therapy **8**(2): S3.

Gauff, F., et al. (2013). "Hyperinsulinaemia increases vascular resistance and endothelin-1 expression in the equine digit." Equine Veterinary Journal **45**(5): 613-618.

Gauff, F. C., et al. (2014). "Effect of short-term hyperinsulinemia on the localization and expression of endothelin receptors A and B in lamellar tissue of the forelimbs of horses." American Journal of Veterinary Research **75**(4): 367-374.

Gelse, K., et al. (2003). "Collagens—structure, function, and biosynthesis." Advanced Drug Delivery Reviews **55**(12): 1531-1546.

Gentry, P. and W. Black (1976). "Influence of pentobarbital sodium anesthesia on hematologic values in the dog." American Journal of Veterinary Research **37**(11): 1349-1352.

Goodrich, L. R. and A. J. Nixon (2006). "Medical treatment of osteoarthritis in the horse–a review." Veterinary Journal **171**(1): 51-69.

Griswold, D. E. and J. L. Adams (1996). "Constitutive cyclooxygenase (COX-1) and inducible cyclooxygenase (COX-2): rationale for selective inhibition and progress to date." Medicinal Research Reviews **16**(2): 181-206.

Grosse-Siestrup, C., et al. (2002). "Isolated Hemoperfused Slaughterhouse Livers as a Valid Model to Study Hepatotoxicity." Toxicologic Pathology **30**(6): 749-754.

Gruber, J., et al. (2004). "Induction of interleukin-1 in articular cartilage by explantation and cutting." Arthritis and Rheumatism **50**(8): 2539-2546.

Grzesiak, J. J. and M. D. Pierschbacher (1995). "Shifts in the concentrations of magnesium and calcium in early porcine and rat wound fluids activate the cell migratory response." Journal of Clinical Investigation **95**(1): 227-233.

Guarrera, J., et al. (2004). "Pushing the envelope in renal preservation: improved results with novel perfusate modifications for pulsatile machine perfusion of cadaver kidneys." Transplantation Proceedings (Conference) **36**(5): 1257-1260.

Guarrera, J. V., et al. (2004). "Pulsatile machine perfusion with Vasosol solution improves early graft function after cadaveric renal transplantation." Transplantation **77**(8): 1264-1268.

Guingamp, C., et al. (1997). "Mono-iodoacetate-induced experimental osteoarthritis. A dose-response study of loss of mobility, morphology, and biochemistry." Arthritis and Rheumatism **40**(9): 1670-1679.

Hamilton, R., et al. (1974). "A simple and inexpensive membrane "lung" for small organ perfusion." Journal of Lipid Research **15**: 182-186.

Han, M., et al. (2005). "Second harmonic generation imaging of collagen fibrils in cornea and sclera." Optics Express **13**(15): 5791-5797.

Handrigan, M., et al. (2005). "Hydroxyethyl starch inhibits neutrophil adhesion and transendothelial migration." Shock **24**(5): 434-439.

Hänsch, G., et al. (1996). "Activation of human neutrophils after contact with cellulose-based haemodialysis membranes: intracellular calcium signalling in single cells." Nephrology Dialysis Transplantation **11**(12): 2453-2460.

Hansen, L., et al. (2000). "Somatostatin restrains the secretion of glucagon-like peptide-1 and-2 from isolated perfused porcine ileum." American Journal of Physiology - Endocrinology and Metabolism **278**(6): E1010-E1018.

Hansen, L., et al. (2004). "Glucagon-like peptide-1 secretion is influenced by perfusate glucose concentration and by a feedback mechanism involving somatostatin in isolated perfused porcine ileum." Regulatory Peptides **118**(1): 11-18.

Hardwick, D. (1965). "The incorporation of carbon dioxide into milk citrate in the isolated perfused goat udder." Biochemical Journal **95**: 233-237.

Hardwick, D. (1966). "The fate of acetyl groups derived from glucose in the isolated perfused goat udder." Biochemical Journal **99**: 228-231.

Hardwick, D. and J. Linzell (1960). "Some factors affecting milk secretion by the isolated perfused mammary gland." Journal of Physiology **154**(3): 547-571.

Hardwick, D., et al. (1963). "The metabolism of acetate and glucose by the isolated perfused udder. 2. The contribution of acetate and glucose to carbon dioxide and milk constituents." Biochemical Journal **88**(2): 213.

Hardwick, D., et al. (1961). "The effect of glucose and acetate on milk secretion by the perfused goat udder." Biochemical Journal **80**(1): 37.

Harris, W. (1974). "Hemoglobin, blood gases and serum electrolyte values in swine." Canadian Veterinary Journal **15**(10): 282.

Häuselmann, H., et al. (1996). "The superficial layer of human articular cartilage is more susceptible to interleukin-1–induced damage than the deeper layers." Arthritis and Rheumatism **39**(3): 478-488.

Haworth, C., et al. (1991). "Expression of granulocyte-macrophage colony-stimulating factor in rheumatoid arthritis: Regulation by tumor necrosis factor-α." European Journal of Immunology **21**(10): 2575-2579.

Hebb, C. O. and J. Linzell (1951). "Some conditions affecting the blood flow through the perfused mammary gland, with special reference to the action of adrenaline." Quarterly Journal of Experimental Physiology and Cognate Medical Sciences **36**(3): 159-175.

Hellewell, P. G. and J. D. Pearson (1983). "Metabolism of circulating adenosine by the porcine isolated perfused lung." Circulation Research **53**(1): 1-7.

Helminen, H. J., et al. (1993). "An inbred line of transgenic mice expressing an internally deleted gene for type II procollagen (COL2A1). Young mice have a variable phenotype of a chondrodysplasia and older mice have osteoarthritic changes in joints." Journal of Clinical Investigation **92**(2): 582.

Hernandez, M., et al. (2009). "Haemodialysis through a cellulose membrane induces dephosphorylation of CD11b and promotes leukocyte adhesion to endothelial cells." Clinical and Investigative Medicine. Medecine clinique et experimentale **32**(1): E48-56.

Hernández, M. R., et al. (2004). "Biocompatibility of cellulosic and synthetic membranes assessed by leukocyte activation." American Journal of Nephrology **24**(2): 235-241.

Hicks, M., et al. (2006). Organ Preservation. Methods in Molecular Biology. R. M. Hornick P. Totowa, New Jersey, Humana Press.

Hirano, T., et al. (1988). "Excessive production of interleukin 6/B cell stimulatory factor-2 in rheumatoid arthritis." European Journal of Immunology **18**(11): 1797-1802.

Hirsh, J., et al. (1995). "Heparin: mechanism of action, pharmacokinetics, dosing considerations, monitoring, efficacy, and safety." Chest Journal **108**(4_Supplement): 258S-275S.

Hoechel, J., et al. (2003). "Effects of different perfusates on functional parameters of isolated perfused dog kidneys." Nephrology Dialysis Transplantation **18**(9): 1748-1754.

Hofmaier, F., et al. (2013). "Range of blood lactate values in farm pigs prior to experimental surgery." Laboratory Animals **47**(2): 130-132.

Honkanen, R. A., et al. (1995). "Barbiturates inhibit hexose transport in cultured mammalian cells and human erythrocytes and interact directly with purified GLUT-1." Biochemistry **34**(2): 535-544.

Houssiau, F. (1995). "Cytokines in rheumatoid arthritis." Clinical Rheumatology **14**(2): 10-13.

Houssiau, F. A., et al. (1988). "Interleukin-6 in synovial fluid and serum of patients with rheumatoid arthritis and other inflammatory arthritides." Arthritis and Rheumatology **31**(6): 784-788.

Huber, M., et al. (2000). "Anatomy, biochemistry, and physiology of articular cartilage." Investigative Radiology **35**(10): 573-580.

James, A., et al. (1956). "The metabolism of propionic acid." Biochemical Journal **64**(4): 726.

Jensen, S. L., et al. (1978). "Secretory effects of secretin on isolated perfused porcine pancreas." American Journal of Physiology-Endocrinology and Metabolism **235**(4): E381.

Jensen, S. L., et al. (1978). "Secretory effects of VIP on isolated perfused porcine pancreas." American Journal of Physiology-Gastrointestinal and Liver Physiology **235**(4): G387-G391.

Jensen, S. L., et al. (1975). "Isolation and perfusion of the porcine pancreas." Scandinavian Journal of Gastroenterology. Supplement **37**: 57-61.

Kageyama, Y., et al. (1994). "Short Paper: Leukotrien B4-induced lnterleukin-1β in Synovial Cells from Patients with Rheumatoid Arthritis." Scandinavian Journal of Rheumatology **23**(3): 148-150.

Kato, G. J., et al. (2006). "Lactate dehydrogenase as a biomarker of hemolysis-associated nitric oxide resistance, priapism, leg ulceration, pulmonary hypertension, and death in patients with sickle cell disease." Blood **107**(6): 2279-2285.

Keffer, J., et al. (1991). "Transgenic mice expressing human tumour necrosis factor: a predictive genetic model of arthritis." EMBO Journal **10**(13): 4025.

Kietzmann, M., et al. (1993). "The isolated perfused bovine udder as an in vitro model of percutaneous drug absorption skin viability and percutaneous absorption of dexamethasone, benzoyl peroxide, and etofenamate." Journal of Pharmacological and Toxicological Methods **30**(2): 75-84.

Kietzmann, M., et al. (2010). "Tissue distribution of cloxacillin after intramammary administration in the isolated perfused bovine udder." BMC Veterinary Research **6**(1): 46.

Kitchen, E., et al. (1996). "Demonstration of reversible priming of human neutrophils using platelet-activating factor." Blood **88**(11): 4330-4337.

Knäuper, V., et al. (1996). "Biochemical characterization of human collagenase-3." Journal of Biological Chemistry **271**(3): 1544-1550.

Kobayashi, E., et al. (2012). "The pig as a model for translational research: overview of porcine animal models at Jichi Medical University." Transplantation Research **1**(1): 8.

Köhrmann, K. U., et al. (1994). "The isolated perfused kidney of the pig: new model to evaluate shock wave-induced lesions." Journal of Endourology **8**(2): 105-110.

Kronheim, S. R., et al. (1992). "Purification of interleukin-1β converting enzyme, the protease that cleaves the interleukin-1β precursor." Archives of Biochemistry and Biophysics **296**(2): 698-703.

Kruit, A. S., et al. (2018). "Current insights into extracorporeal perfusion of free tissue flaps and extremities: a systematic review and data synthesis." Journal of Surgical Research **227**: 7-16.

Kumar, V., et al. (2010). Robbins and Cotran, Pathologic Basis of Disease, Saunders Elsevier.

Labens, R., et al. (2017). "Effect of intra-articular administration of superparamagnetic iron oxide nanoparticles (SPIONs) for MRI assessment of the cartilage barrier in a large animal model." PloS one **12**(12): e0190216.

Labens, R., et al. (2013). "Ex vivo effect of gold nanoparticles on porcine synovial membrane." Tissue Barriers **1**(2): e24314.

Lampen, P., et al. (2003). "Penetration studies of vitamin E acetate applied from." Journal of Cosmetic Science **54**: 119-131.

Lampropoulou-Adamidou, K., et al. (2014). "Useful animal models for the research of osteoarthritis." European Journal of Orthopaedic Surgery and Traumatology **24**(3): 263-271.

Lauryssens, M., et al. (1961). "Metabolism of stearate-l-C14 in the isolated cow's udder." Journal of Lipid Research **2**(4): 383-388.

Lauryssens, M., et al. (1960). "Incorporation of [1-14C] and [3-14C] butyrate into milk constituents by the perfused cow's udder." Journal of Dairy Research **27**(02): 151-160.

Lee, S. S., et al. (2007). "Strain hardening of red blood cells by accumulated cyclic supraphysiological stress." Artificial Organs **31**(1): 80-86.

Legrand, C., et al. (1992). "Lactate dehydrogenase (LDH) activity of the number of dead cells in the medium of cultured eukaryotic cells as marker." Journal of Biotechnology **25**(3): 231-243.

Linhorst, E., et al. (2000). "Longitudinal characterization of synovial fluid biomarkers in the canine meniscectomy model of osteoarthritis." Journal of Orthopaedic Research **18**(2): 269.

Linzell, J., et al. (1967). "The incorporation of acetate, stearate and D (-)-beta-hydroxybutyrate into milk fat by the isolated perfused mammary gland of the goat." Biochemical Journal **104**: 34-42.

Lipsky, P. E. and P. C. Isakson (1997). "Outcome of specific COX-2 inhibition in rheumatoid arthritis." Journal of Rheumatology. Supplement **49**: 9-14.

Livak, K. J. and T. D. Schmittgen (2001). "Analysis of relative gene expression data using real-time quantitative PCR and the 2− ΔΔCT method." Methods **25**(4): 402-408.

Loetscher, H., et al. (1990). "Molecular cloning and expression of the human 55 kd tumor necrosis factor receptor." Cell **61**(2): 351-359.

Lotz, M. and R. F. Loeser (2012). "Effects of aging on articular cartilage homeostasis." Bone **51**(2): 241-248.

Malhotra, M. and S. Prakash (2011). "Targeted drug delivery across blood-brain-barrier using cell penetrating peptides tagged nanoparticles." Current Nanoscience **7**(1): 81-93.

Mancina, E., et al. (2015). "Determination of the Preferred Conditions for the Isolated Perfusion of Porcine Kidneys." European Surgical Research **54**(1-2): 44-54.

Markert, C. L. and H. Ursprung (1962). "The ontogeny of isozyme patterns of lactate dehydrogenase in the mouse." Developmental Biology **5**(3): 363-381.

Markgraf, W., et al. (2018). "Hyperspectral imaging for ex-vivo organ characterization during normothermic machine perfusion." European Urology Supplements **17**(2): e767.

Martel-Pelletier, J., et al. (2005). "Etiopathogenesis of osteoarthritis." Arthritis and Allied Conditions: a Textbook of Rheumatology **15**: 2199-2226.

Martel-Pelletier, J., et al. (2000). Metalloproteases and their modulation as treatment in osteoarthritis. Principles of Molecular Rheumatology, Springer**:** 499-513.

Martel-Pelletier, J., et al. (1992). "The interleukin-1 receptor in normal and osteoarthritic human articular chondrocytes. Identification as the type I receptor and analysis of binding kinetics and biologic function." Arthritis and Rheumatism **35**(5): 530-540.

Matharu, N., et al. (2008). "Mechanisms of the anti-inflammatory effects of hydroxyethyl starch demonstrated in a flow-based model of neutrophil recruitment by endothelial cells." Critical Care Medicine **36**(5): 1536-1542.

Mathis, S., et al. (2007). "Role of leukotriene B 4 receptors in rheumatoid arthritis." Autoimmunity Reviews **7**(1): 12-17.

McCoy, A. (2015). "Animal Models of Osteoarthritis Comparisons and Key Considerations." Veterinary Pathology: 0300985815588611.

Messell, T., et al. (1992). "Extrinsic control of the release of galanin and VIP from intrinsic nerves of isolated, perfused, porcine ileum." Regulatory Peptides **38**(3): 179-198.

Moen, O., et al. (1994). "Roller and centrifugal pumps compared in vitro with regard to haemolysis, granulocyte and complement activation." Perfusion **9**(2): 109-117.

Mold, C. and C. Morris (2001). "Complement activation by apoptotic endothelial cells following hypoxia/reoxygenation." Immunology **102**(3): 359-364.

Moore, M. A., et al. (2001). "Effect of cellulose acetate materials on the oxidative burst of human neutrophils." Journal of Biomedical Materials Research **55**(3): 257-265.

Mueller, S., et al. (2013). "Ischemia/ reperfusion injury of porcine limbs after extracorporeal perfusion. ." Journal of Surgical Research **181**(1): 170-182.

Naqvi, S., et al. (2010). "Concentration-dependent toxicity of iron oxide nanoparticles mediated by increased oxidative stress." International Journal of Nanomedicine **5**: 983.

Nawroth, P., et al. (1986). "Tumor necrosis factor/cachectin interacts with endothelial cell receptors to induce release of interleukin 1." Journal of Experimental Medicine **163**(6): 1363-1375.

Newton, W. (1933). "The normal behaviour of the isolated uterus of the guinea-pig, and its reactions to œstrin and oxytocin." Journal of Physiology **79**(3): 301-316.

Nickel, R., Schummer, A., Seiferle, E. (2005). Lehrbuch der Anatomie der Haustiere, Band 3 Kreislaufsystem, Haut und Hautorgane. Stuttgart, Germany, Parey Verlag, Habermehl KH, Vollmerhaus B, Wilkens H, Waibl H.

Nigam, S., et al. (2011). "Development of citrate-stabilized Fe3O4 nanoparticles: conjugation and release of doxorubicin for therapeutic applications." Journal of Magnetism and Magnetic Materials **323**(2): 237-243.

Nishimoto, N., et al. (2007). "Study of active controlled monotherapy used for rheumatoid arthritis, an IL-6 inhibitor (SAMURAI): evidence of clinical and radiographic benefit from an x ray reader-blinded randomised controlled trial of tocilizumab." Annals of the Rheumatic Diseases **66**(9): 1162-1167.

Nygard, A.-B., et al. (2007). "Selection of reference genes for gene expression studies in pig tissues using SYBR green qPCR." BMC Molecular Biology **8**(1): 67.

Oster, J., et al. (1978). "Relationship between blood pH and potassium and phosphorus during acute metabolic acidosis." American Journal of Physiology - Renal Physiology **235**(4): F345-F351.

Oswald, I., et al. (1992). "IL-10 synergizes with IL-4 and transforming growth factor-beta to inhibit macrophage cytotoxic activity." The Journal of Immunology **148**(11): 3578-3582.

Ottonello, L., et al. (2002). "Synovial fluid from patients with rheumatoid arthritis inhibits neutrophil apoptosis: role of adenosine and proinflammatory cytokines." Rheumatology **41**(11): 1249-1260.

Ozer, K., et al. (2015). "Ex situ limb perfusion system to extend vascularized composite tissue allograft survival in swine." Transplantation **99**(10): 2095-2101.

Palmblad, J., et al. (1981). "Leukotriene B4 is a potent and stereospecific stimulator of neutrophil chemotaxis and adherence." Blood **58**(3): 658-661.

Paparella, D., et al. (2002). "Cardiopulmonary bypass induced inflammation: pathophysiology and treatment. An update." European Journal of Cardio-Thoracic Surgery **21**(2): 232-244.

Patan-Zugaj, B., et al. (2012). "Effects of the addition of endotoxin during perfusion of isolated forelimbs of equine cadavers." American Journal of Veterinary Research **73**(9): 1462-1468.

Patan-Zugaj, B., et al. (2014). "Effect of endotoxin on leukocyte activation and migration into laminar tissue of isolated perfused equine limbs." American Journal of Veterinary Research **75**(9): 842-850.

Patan, B., et al. (2009). "Effects of long-term extracorporeal blood perfusion of the distal portion of isolated equine forelimbs on metabolic variables and morphology of laminar tissue." American Journal of Veterinary Research **70**(5): 669-677.

Patil, U. S., et al. (2015). "In vitro/in vivo toxicity evaluation and quantification of iron oxide nanoparticles." International Journal of Molecular Sciences **16**(10): 24417-24450.

Pavy, F. W., et al. (1903). "On the mechanism of phloridzin glycosuria." Journal of Physiology **29**(6): 467-491.

Peeters, G. and L. Massart (1952). "Fat synthesis in the perfused lactating cow's udder." Archives Internationales de Pharmacodynamie et de Therapie **91**(3-4): 389-398.

Pegg, D. and C. Green (1976). "Renal preservation by hypothermic perfusion. III. The lack of influence of pulsatile flow." Cryobiology **13**(2): 161-167.

Pelletier, J. P., et al. (2001). "Osteoarthritis, an inflammatory disease: potential implication for the selection of new therapeutic targets." Arthritis and Rheumatism **44**(6): 1237-1247.

Persson, S. (1967). "On blood volume and working capacity in horses. Studies of methodology and physiological and pathological variations." Acta Veterinaria Scandinavica: Suppl 19: 19.

Peter, S., et al. (2002). "Liver and kidney preservation by perfusion." Lancet **359**(9306): 604-613.

Petrasek, P. F., et al. (1994). "Determinants of ischemic injury to skeletal muscle." Journal of Vascular Surgery **19**(4): 623-631.

Pinkus, G. S. and J. L. Pinkus (1991). "Myeloperoxidase: a specific marker for myeloid cells in paraffin sections." Modern Pathology **4**(6): 733-741.

Polyak, M., et al. (2008). "Effect of a novel solution for organ preservation on equine large colon in an isolated pulsatile perfusion system." Equine Veterinary Journal **40**(4): 306-312.

Punzi, L., et al. (2005). "New biochemical insights into the pathogenesis of osteoarthritis and the role of laboratory investigations in clinical assessment." Critical Reviews in Clinical Laboratory Sciences **42**(4): 279-309.

Rehfeld, J., et al. (1982). "The molecular nature of vascularly released cholecystokinin from the isolated perfused porcine duodenum." Regulatory Peptides **3**(1): 15-28.

Riviere, J., et al. (1989). "The isolated perfused porcine skin flap (IPPSF): I. A novel in vitro model for percutaneous absorption and cutaneous toxicology studies." Fundamental and Applied Toxicology **7**(3): 444-453.

Roets, E., et al. (1979). "Metabolism of [U-14C; 2, 3-3H]-L-valine by the isolated perfused goat udder." Journal of Dairy Research **46**(01): 47-57.

Roets, E., et al. (1974). "Metabolism of [14 C] citrulline in the perfused sheep and goat udder." Biochemical Journal **144**: 435-446.

Roets, E., et al. (1979). "Metabolism of ornithine in perfused goat udder." Journal of Dairy Science **62**(2): 259-269.

Ropes, M. W., et al. (1939). "The origin and nature of normal synovial fluid." Journal of Clinical Investigation **18**(3): 351.

Sadouk, M. B., et al. (1995). "Human synovial fibroblasts coexpress IL-1 receptor type I and type II mRNA. The increased level of the IL-1 receptor in osteoarthritic cells is related to an increased level of the type I receptor." Laboratory Investigation **73**(3): 347-355.

Saha, N., et al. (1999). "Interleukin-1ß-converting enzyme/capase1 in human osteoarthritic tissues." Arthritis and Rheumatology **42**: 1577-1587.

Sawdon, A., et al. (2014). "Antitumor therapy using nanomaterial-mediated thermolysis." Journal of Biomedical Nanotechnology **10**(9): 1894-1917.

Saxne, T., et al. (1988). "Detection of tumor necrosis factor α but not tumor necrosis factor β in rheumatoid arthritis synovial fluid and serum." Arthritis and Rheumatism **31**(8): 1041-1045.

Schall, T. J., et al. (1990). "Molecular cloning and expression of a receptor for human tumor necrosis factor." Cell **61**(2): 361-370.

Schmitt, K. R. L., et al. (2007). "Hypothermia suppresses inflammation via ERK signaling pathway in stimulated microglial cells." Journal of Neuroimmunology **189**(1): 7-16.

Schumacher, S., et al. (2011). "Ex vivo examination of the biocompatibility of biodegradable magnesium via microdialysis in the isolated perfused bovine udder model." International Journal of Artificial Organs **34**(1): 34-43.

Schwab, W., et al. (2001). "Expression of the urokinase-type plasminogen activator receptor in human articular chondrocytes: association with caveolin and β1-integrin." Histochemistry and Cell Biology **115**(4): 317-323.

Schwab, W., et al. (2004). "Interleukin-1ß-induced expression of the urokinase-type plasminogen activator receptor and its co-localization with MMPs in human articular chondrocytes." Histology and Histopathology **19**(1): 105-112.

Sezai, A., et al. (1999). "Major organ function under mechanical support: comparative studies of pulsatile and nonpulsatile circulation." Artificial Organs **23**(3): 280-285.

Shah, A., et al. (2008). "Comparison of Pulsatile Perfusion and Cold Storage for Paired Kidney Allografts." Transplantation **86**(7): 1006-1009.

Silbernagl, S. (2012). Taschenatlas Physiologie, Georg Thieme Verlag.

Simchowitz, L. and I. Spilberg (1979). "Generation of superoxide radicals by human peripheral neutrophils activated by chemotactic factor. Evidence for the role of calcium." Journal of Laboratory and Clinical Medicine **93**(4): 583-593.

Simon, G. H., et al. (2006). "MRI of arthritis: Comparison of ultrasmall superparamagnetic iron oxide vs. Gd-DTPA." Journal of Magnetic Resonance Imaging **23**(5): 720-727.

Singh, S. and H. S. Nalwa (2007). "Nanotechnology and health safety–toxicity and risk assessments of nanostructured materials on human health." Journal of Nanoscience and Nanotechnology **7**(9): 3048-3070.

Skrzypiec-Spring, M., et al. (2007). "Isolated heart perfusion according to Langendorff—still viable in the new millennium." Journal of Pharmacological and Toxicological Methods **55**(2): 113-126.

Slack, J., et al. (1993). "Independent binding of interleukin-1 alpha and interleukin-1 beta to type I and type II interleukin-1 receptors." Journal of Biological Chemistry **268**(4): 2513-2524.

Smith, A., et al. (1985). "Limb preservation in replantation surgery." Plastic and Reconstructive Surgery **75**(2): 227-237.

Steinau, H.-U. (2013). Major limb replantation and postischemia syndrome: investigation of acute ischemia-induced myopathy and reperfusion injury, Springer Science & Business Media.

Strangeways, T. (1920). "Observations on the nutrition of articular cartilage." British Medical Journal **1**(3098): 661.

Su, P.-J., et al. (2011). "Determination of collagen nanostructure from second-order susceptibility tensor analysis." Biophysical Journal **100**(8): 2053-2062.

Szekanecz, Z., et al. (1998). "Cytokines in rheumatoid arthritis." Drugs and Aging **12**(5): 377-390.

Tanaka, D., et al. (2006). "Essential role of neutrophils in anti-type II collagen antibody and lipopolysaccharide-induced arthritis." Immunology **119**(2): 195-202.

Tindal, J. (1957). "Blood flow in the isolated perfused bovine udder." American Journal of Physiology - Legacy Content **191**(2): 287-292.

Trimarchi, J. R., et al. (2000). "Noninvasive measurement of potassium efflux as an early indicator of cell death in mouse embryos." Biology of Reproduction **63**(3): 851-857.

Tsuchida, T., et al. (2001). "Effect of Perfusion during Ischemia on Skeletal Muscle." Journal of Surgical Research **101**(2): 238-241.

Tsuchida, T., et al. (2003). "The Effect of Perfusion with UW Solution on the Skeletal Muscle and Vascular Endothelial Exocrine Function in Rat Hindlimbs." Journal of Surgical Research **110**(1): 266-271.

Turina, M., et al. (2008). "Mannitol upregulates monocyte HLA-DR, monocyte and neutrophil CD11b, and inhibits neutrophil apoptosis." Inflammation **31**(2): 74-83.

Ündar, A., et al. (2002). "Pediatric physiologic pulsatile pump enhances cerebral and renal blood flow during and after cardiopulmonary bypass." Artificial Organs **26**(11): 919-923.

Usui, M., et al. (1985). "Effect of Fluorocarbon Perfusion upon the Preservation of Amputed Limbs." Bone and Joint Journal **67-B**(3): 473-477.

Vachon, A., et al. (1990). "Biochemical analysis of normal articular cartilage in horses." American Journal of Veterinary Research **51**(12): 1905-1911.

Van Buul, G. M., et al. (2011). "Clinically translatable cell tracking and quantification by MRI in cartilage repair using superparamagnetic iron oxides." PloS one **6**(2): e17001.

Van De Loo, F. A., et al. (1995). "Role of interleukin-1, tumor necrosis factor α, and interleukin-6 in cartilage proteoglycan metabolism and destruction effect of in situ blocking in murine antigen-and zymosan-induced arthritis." Arthritis and Rheumatism **38**(2): 164-172.

Vang, J. O. and T. Drapanas (1966). "Metabolism of lactic acid and keto acids by the isolated perfused calf liver: evaluation of perfusion via portal vein and hepatic artery." Annals of Surgery **163**(4): 545.

VanGiesen, P., et al. (1983). "Storage of amputed parts prior to replantation - An experimental study with rabbit ears." Journal of Hand Surgery **8**(1): 60-65.

Varan, B., et al. (2002). "Systemic inflammatory response related to cardiopulmonary bypass and its modification by methyl prednisolone: high dose versus low dose." Pediatric Cardiology **23**(4): 437-441.

Verbeke, R., et al. (1959). "Incorporation of dl-[1-14C] leucine and [1-14C] isovaleric acid into milk constituents by the perfused cow's udder." Biochemical Journal **73**(1): 24.

Verbeke, R., et al. (1968). "Incorporation of DL-[2-14 C] ornithine and DL-[5-14 C] arginine in milk constituents by the isolated lactating sheep udder." Biochemical Journal **106**: 719-724.

Verbeke, R., et al. (1972). "Metabolism of [U-14C]-L-threonine and [U-14C]-L-phenylalanine by the isolated perfused udder." Journal of Dairy Research **39**(02): 239-250.

Vermeij, E. A., et al. (2015). "The in-vivo use of superparamagnetic iron oxide nanoparticles to detect inflammation elicits a cytokine response but does not aggravate experimental arthritis." PloS one **10**(5): e0126687.

Villeneuve, J., et al. (1996). "The hepatic microcirculation in the isolated perfused human liver." Hepatology **23**(1): 24-31.

Visse, R. and H. Nagase (2003). "Matrix metalloproteinases and tissue inhibitors of metalloproteinases structure, function, and biochemistry." Circulation Research **92**(8): 827-839.

von Horn, C. and T. Minor (2018). "Isolated kidney perfusion: the influence of pulsatile flow." Scandinavian Journal of Clinical and Laboratory Investigation **78**(1-2): 131-135.

Wagner, S., et al. (2003). "The isolated normothermic hemoperfused porcine forelimb as a test system for transdermal absorption studies." Journal of Artifical Organs **6**(3): 183-191.

Ward, L. and P. Buttery (1979). "The patho-physiological basis for tests of viability in isolated perfused organs." Biomedicine **30**(4): 181-186.

Watanabe, N., et al. (2007). "Deformability of red blood cells and its relation to blood trauma in rotary blood pumps." Artificial Organs **31**(5): 352-358.

Waugh, W. H. and T. Kubo (1969). "Development of an isolated perfused dog kidney with improved function." American Journal of Physiology - Legacy Content **217**(1): 277-290.

Weiss, E. and R. Jurmain (2007). "Osteoarthritis revisited: a contemporary review of aetiology." International Journal of Osteoarchaeology **17**(5): 437-450.

Westacott, C., et al. (1994). "Tumor necrosis factor-alpha receptor expression on chondrocytes isolated from human articular cartilage." Journal of Rheumatology **21**(9): 1710-1715.

Williams, R. O., et al. (1992). "Anti-tumor necrosis factor ameliorates joint disease in murine collagen-induced arthritis." Proceedings of the National Academy of Sciences **89**(20): 9784-9788.

Wittenberg, R. H., et al. (1993). "In vitro release of prostaglandins and leukotrienes from synovial tissue, cartilage, and bone in degenerative joint diseases." Arthritis and Rheumatism **36**(10): 1444-1450.

Woods, J. M., et al. (2003). "The role of COX-2 in angiogenesis and rheumatoid arthritis." Experimental and Molecular Pathology **74**(3): 282-290.

Wooley, P. H., et al. (1993). "Influence of a recombinant human soluble tumor necrosis factor receptor FC fusion protein on type II collagen-induced arthritis in mice." Journal of Immunology **151**(11): 6602-6607.

Wüstenberg, R.-Y. (2006). Modell der isoliert hämoperfundierten distalen Rindergliedmaßen für experimentelle Untersuchungen zur Pathogenese der Klauenrehe, Freie Universität Berlin.

Xin, L., et al. (2018). "A New Multi-Mode Perfusion System for Ex Vivo Heart Perfusion Study." Journal of Medical Systems **42**(2): 25.

Xu, C. and S. Sun (2013). "New forms of superparamagnetic nanoparticles for biomedical applications." Advanced Drug Delivery Reviews **65**(5): 732-743.

Ye, J., et al. (2012). "Primer-BLAST: a tool to design target-specific primers for polymerase chain reaction." BMC Bioinformatics **13**(1): 134.

Zeitlin, I. and H. Eshraghi (2002). "The release and vascular action of bradykinin in the isolated perfused bovine udder." Journal of Physiology **543**(1): 221-231.